To the Graduate Council:

I am submitting herewith a dissertation written by Te-Hua Lin entitled "Heat Transfer in Iron Titanium Hydride Beds." I recommend that it be accepted in partial fulfillment of the requirements for the degree of Doctor of Philosophy, with a major in Chemical Engineering.

Jack A. Watson

Jack S. Watson, Major Professor

We have read this dissertation
and recommend its acceptance:

W. H. Johnson

S. Y. Shieh

George C. Frazier

Joseph J. Cuoma

Accepted for the Council:

L. Evans Roth

Vice Chancellor
Graduate Studies and Research

4

HEAT TRANSFER IN IRON TITANIUM HYDRIDE BEDS

A Dissertation

Presented for the

Doctor of Philosophy

Degree

The University of Tennessee, Knoxville

Te-Hua Lin

June 1981

ACKNOWLEDGEMENT

The author wishes to acknowledge his major professor, Dr. J. S. Watson, whose constant assistance and numerous helpful suggestions make this work possible.

The author also wishes to thank P. W. Fisher of the Oak Ridge National Labortory for providing his computing results and some useful mathematical expressions which are inevitably needed in this study.

The experimental part of this research was done at Chemical Technology Division, Oak Ridge National Laboratory. The author is indebted to the members of the division, especially Frank L. Rogers who constructed the experimental equipment and performed the measurements.

The author also wishes to thank Brookhaven National Laboratory for providing the testing material for experiments, J. M. Morgan of the Plant and Equipment Division, Oak Ridge National Laboratory for cutting aluminum foam, and the members of the Drafting Department of the Chemical Technology Division, Oak Ridge National Laboratory for preparing some drawings in this report.

ABSTRACT

New data on the thermal conductivity of FeTi hydride at pressure of hydrogen were obtained. They were found to be inverse related to absolute temperature. Comparing with the previous results, their dependence on hydrogen pressure is considered more reliable and should be used in modeling study to predict the behavior of the hydride beds.

The experimental results show that before a practical reaction is obtained, activation (conditioning) of the FeTi hydride is necessary. Since even at the pressure of 500 psig hydrogen, there is no indication of reaction between hydrogen and FeTi hydride not previously activated.

According to the mathematical model study, the addition of aluminum in the form of reticulated open-cell does benefit the reaction in the hydride bed. The heat transfer improvement is a strong function of the form of the aluminum. The smaller the cell size, the faster the hydrogen charging/discharging rate.

The aluminum content and the cell size in the Al-enhanced hydride bed are determined by at least two factors: (1) the expected rate, and (2) the amount of hydrogen to be charged/ discharged. For more detailed design purpose, the model developed in the report can be used to assess the bed performance.

For the Al-enhanced FeTi hydride bed with very small cells, the heat transfer resistance may not be the controlling step. In these case, an accurate knowledge of kinetics is needed for predictions.

TABLE OF CONTENTS

LIST OF TABLES

LIST OF FIGURES

FIGURE PAGE

FIGURE PAGE

CHAPTER 1

BACKGROUND

A major problem of distributed electrical energy is that the demand varies throughout the day and week, and there is no universal and cost effective method of storing large amount of excess energy for later use. A new and promising load leveling concept now under development is based on the storage of energy as hydrogen in the form of decomposable metal hydrides. This could also prove to be an attractive way to store energy for use in remote and mobile locations. Hydride may compete with batteries for energy for transportation (automobiles, etc) when hydrocarbon fuels are unavailable.

Hydrogen is highly recommended as a possible fuel substitute for fossil fuels in the not too distant future when they are no longer available at economic price. The present methods of storing hydrogen are suitable and safe for the present industrial uses of hydrogen, but they are not suitable for moving vehicles or for special applications where compactness is required. For example, hydrogen stored as a compressed gas calls for large and heavy vessels; while liquid storage consumes significant energy in the process of liquefaction and in refrigeration to compensate for heat losses. Morever, liquid hydrogen could present serious safety problem if it were to be considered as a common fuel for use in a motor use. Metal hydrides, in contrast, store hydrogen compactly and safely at ambient temperature and moderate pressures.

The use of hydrogen as a fuel for automobiles, trucks and buses has attracted considerable interest for years. The main incentive is that hydrogen and oxygen combine to form water with energy liberation, and this eliminates many of the pollutant problems associated with hydrocarbon fuels. Since certain hydrides, e.g., iron titanium hydride, can sustain thousands of storing cycles using the high purity hydrogen, the substitution of hydride reservoir for gas tanks in future vehicle has become an interesting topic in the energy community.

The use of hydrides in chemical heat pump is also promising (1-2). In principle, the heat pump effect can be achieved by decomposing a metal hydride bed at a given temperature, transferring the evolved hydrogen to a second bed and reacting it there at a higher temperature, with a metal that forms a more stable hydride (stable at a higher temperature). The decomposition requires heat, which can be of low grade; it can be obtained from the surroundings, from a solar collector or from a waste source. The reaction of hydrogen with the metal in the second bed gives off higher grade heat (at a higher temperature). Depending on the selection of hydrides, the difference between low grade and high grade heat can be from 50 to 100 centigrade.

The hydride can be formed by reaction of various metal or intermetallic compounds with hydrogen. Hydrogen is readily delivered or recovered by heating the hydride to an elevated temperature and maintaining the hydrogen pressure below the equilibrium dissociation pressure. The hydride will dissociate until the equilibrium pressure is restored.

The factors involved in the selection of hydride as the energy storage media are as follow:

1. High hydrogen pressure at reasonable temperature (low absolute stability).
2. Low or moderate exothermic heat of formation.
3. High hydrogen capacity per unit volume.
4. High hydrogen capacity per unit mass.
5. Low cost.
6. Ease of fabrication.
7. Rapid kinetics of formation and dissociation.
8. Resistance to extensive particulation.

Although numerous decomposable hydrides have been discovered, only a few are practical for energy storage. Many hydrides are unsuitable because of their high unit cost(cost per lb. of available hydrogen), unsuitable stability, or scarcity of components (3-8). Iron titanium hydride, $FeTiH_y$ ($y<2$), has received the most attention and shown the most potential for many applications thus far.

1.1 IRON TITANIUM HYDRIDE BEHAVIOR

The reaction between FeTi and H_2 is exothermic during hydriding (or charging), and endothermic during dehydrating (or discharging). The hydride forms(or decomposes) readily and has a pressure depending upon the composition and temperature. This behavior is illustrated in Figure 1 for charging and discharging H_2 at 40 °C under equilibrium conditions. The abscissa is the hydrogen loading expressed in terms of atom ratio, H/(Fe+Ti)or H/M, in the hydride (9). The lower curve in Figure 1 is the dissociation pressure for dehydrating, and the higher

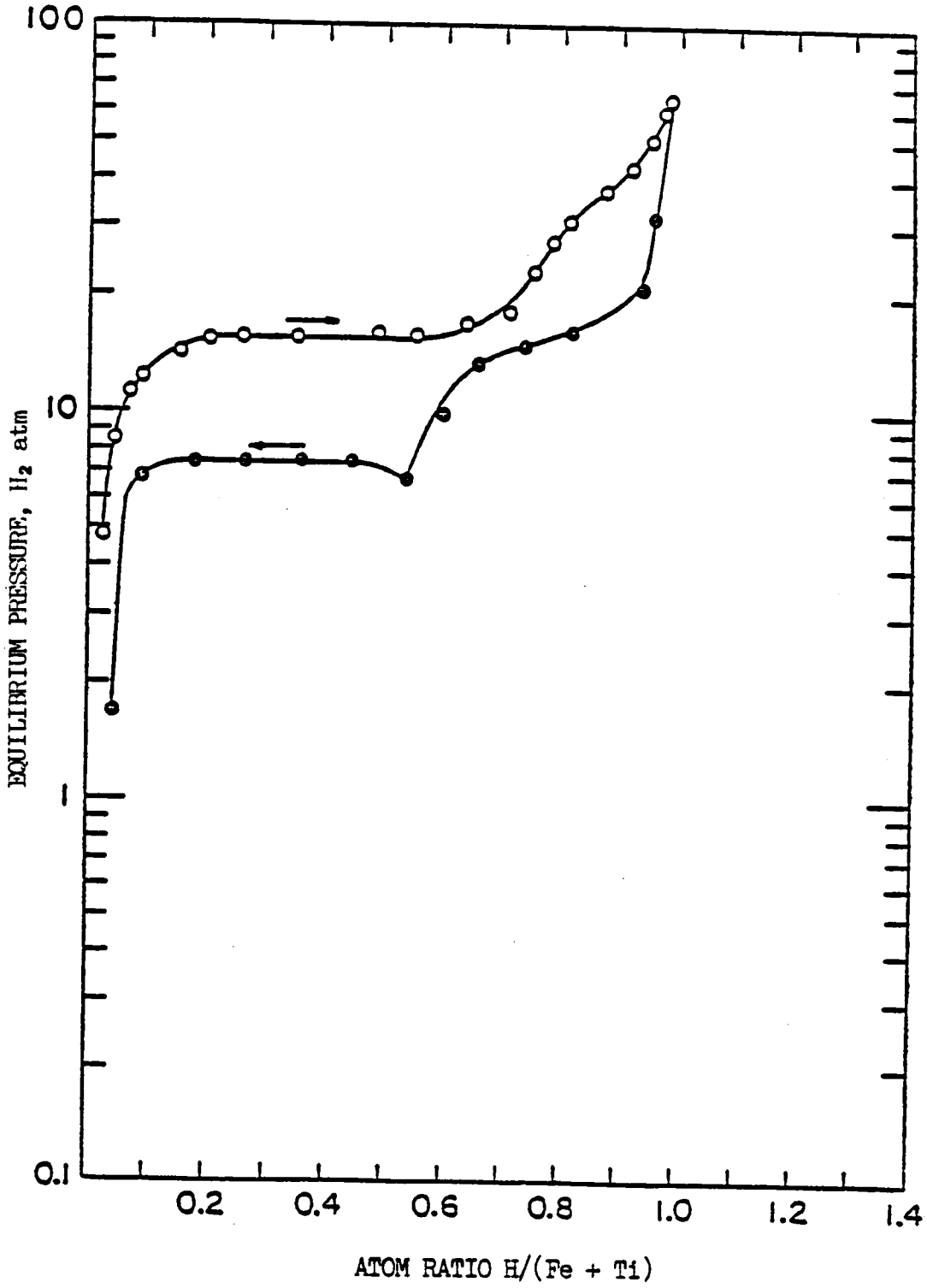

Figure 1. Hysteresis in the system FeTi-H at 40°C.

curve is the pressure observed during hydriding. The difference between these curves, a phenomenon called hystersis, has been noticed over a period of about 68 years, and was first recognized in 1913 by Holt, et al. (10). They attributed the differential pressure to an adsorbed condensed surface film of hydrogen formed during hydriding which disappeared on desorption. There have been several other explanations for the hystersis proposed since then; the latest one was given by C. E. Lundin, et al. (11). Their proposal was based on a model of induced lattice strains occurring during hydrogen absorption and the relief of the strains on desorption. This strain and its reversal cause a hystersis in the interstitial hole size during cyclic hydrogen occupancy.

The steep initial rise in pressure is the region of solid solution of hydrogen in the metal lattice, designated as the α-phase of the FeTi-H system. The equlibrium pressure remains constant and forms a plateau as the hydrogen content is increased further. The composition at which the plateau begins marks the point at which a new phase appears and also marks the maximum solubility of hydrogen in the α-phase. At room temperature, the composition corresponds to $FeTiH_{0.1}$ (H/M=0.05). The new phase called as the β-phase is the monohydride. Both the α- and β-phases coexist until the solid composition corresponds to $FeTiH_{1.04}$ where the isotherms begin a steep ascent. At this point the α-phase had disappeared. Beyond this, formation of the γ- or dihydride phase begins. The exact point of inception is temperature dependent and is somewhat difficult to determine since the breaks in the isotherms occurs gradually. As shown

in Figure 2 (9), the 55 °C isotherm shows only a vestigial plateau structure, and this temperature appears quite similar to a critical temperature. Above this two discrete solid hydride phases do not coexist, and the monohydride is transformed continuously into the dehydride phase.

As indicated in Figures 2 and 3 (12), the effect of increasing temperature is to increase the equilibrium pressure. Thus for a fixed charging pressure, the driving force for the reaction is increased by operating at a lower temperature.

The dip occurring at the beginning of the γ-phase in the lower temperature desorption isotherms at H/M=0.5 does not occur in the absorption isotherm. And as shown in Figure 2, the dip is less pronounced at higher temperatures and finally disappears altogether in the 70 °C isotherm. Wicke and Otto (13) have suggested that the dip phenomenon is due to the supersaturation of hydrogen vacancies in the hydride phase and the fact that the dip is encountered only in desorption isotherms lends support to this explanation.

The reaction taking place in the lower plateau region, H/M from 0.05 to 0.52, may be written as

$$2.13FeTiH_{0.1} + H_2 \rightleftharpoons 2.13FeTiH_{1.04} \qquad (1)$$

which is followed by

$$2.20FeTiH_{1.04} + H_2 \rightleftharpoons 2.20FeTiH_{1.95} \qquad (2)$$

The kinetic and thermodynamic properties relevant to this study are described in the following sections.

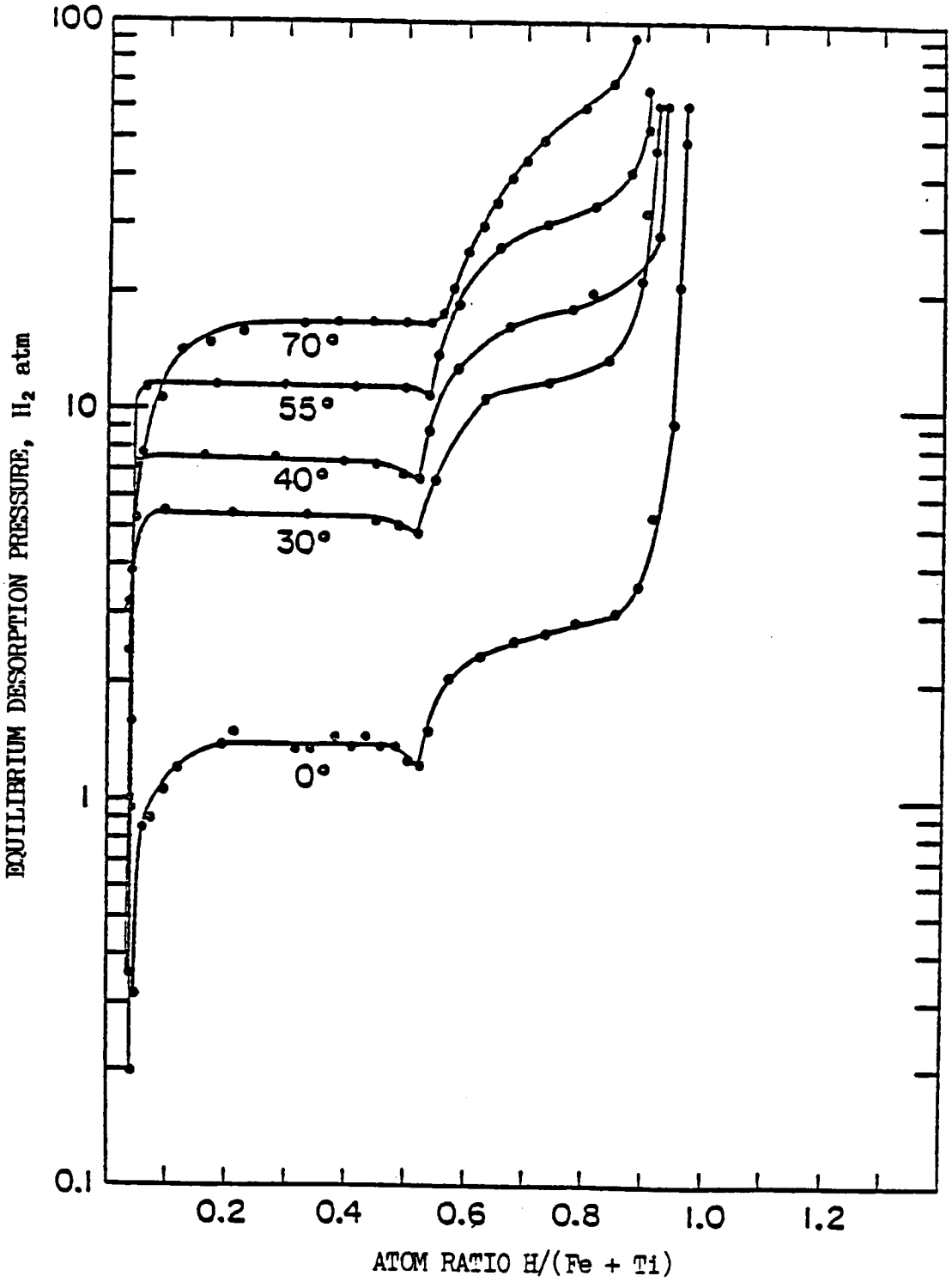

Figure 2. Equilibrium desorption isotherms for the system FeTi-H.

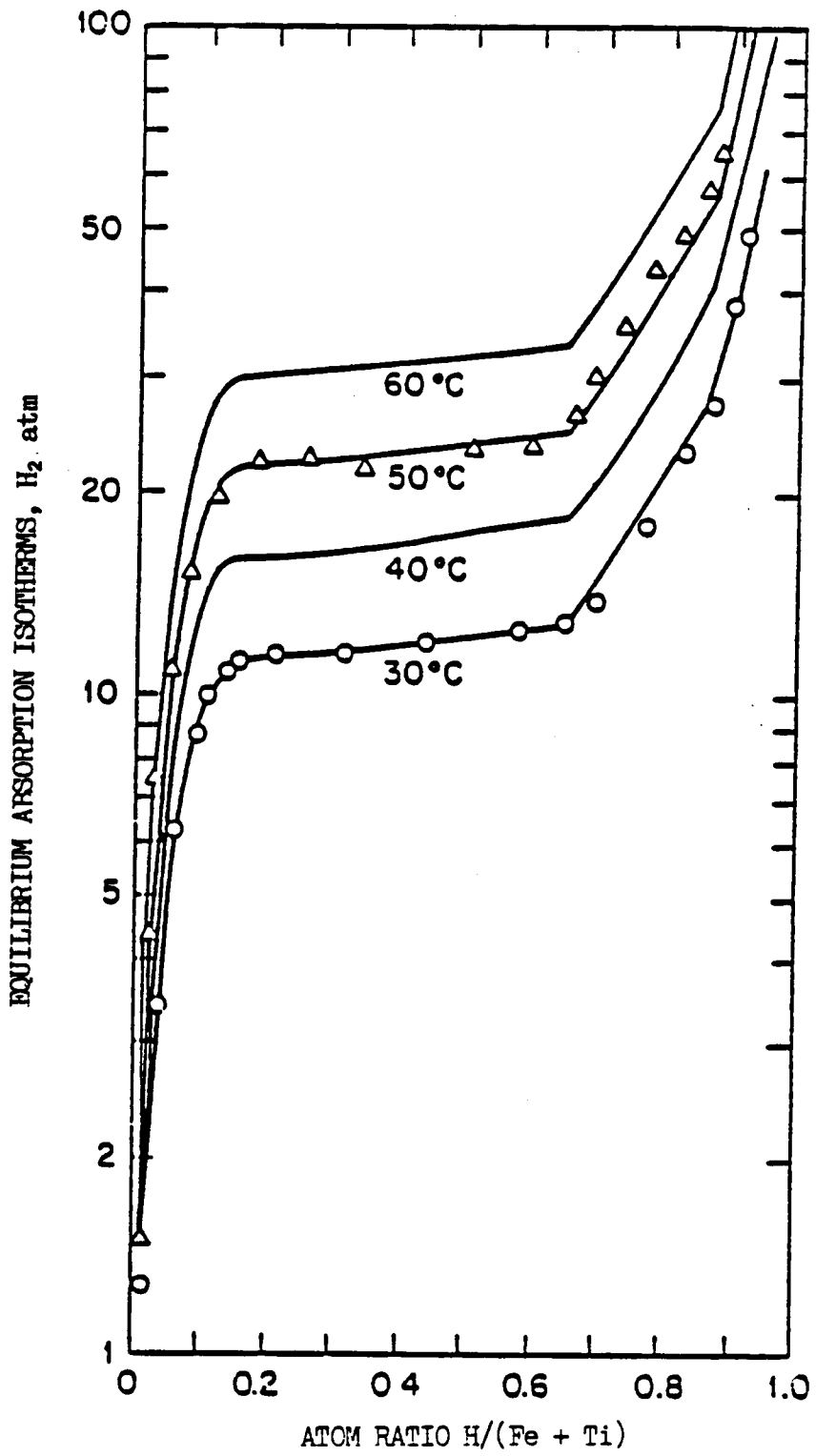

Figure 3. Equilibrium absorption isotherms for the system FeTi-H.

1.2 KINETICS

The ultimate success of this study depends on knowledge of the hydride formation and decomposition. Earlier work has shown that the rate of decomposition is adequate for many practical purposes; that is, local compositions and pressures will be approximately in equilibrium. The rate will often be limited only by the rate at which the heat of reaction can be supplied.

On the other hand, the rate of hydriding is generally quite slow and limited by heat transfer as well as other factors. These factors include specific surface area of the solid, impurities in the gas, presence of catalyst, etc.

(A). Hydriding

The most reliable kinetic data available are believed to be those shown in Figure 4 (9). The experiments from which the data were taken attempted to hold the system at constant temperature. To keep the system isothermal, large amount of 1/8-in. diameter steel balls was mixed with small FeTi alloy particles, where the steel balls served to increase the thermal inertia of the system. The heat generated during the reaction could then be conducted into the large mass of steel balls and thus cause less (perhaps negligible) rise of the system temperature.

No conclusions about reaction kinetics have been reached from these data although attempts have been made to analyze them. In the temperature and pressure range examined, the rate of hydriding seems to be more sensitive to temperature than to pressure.

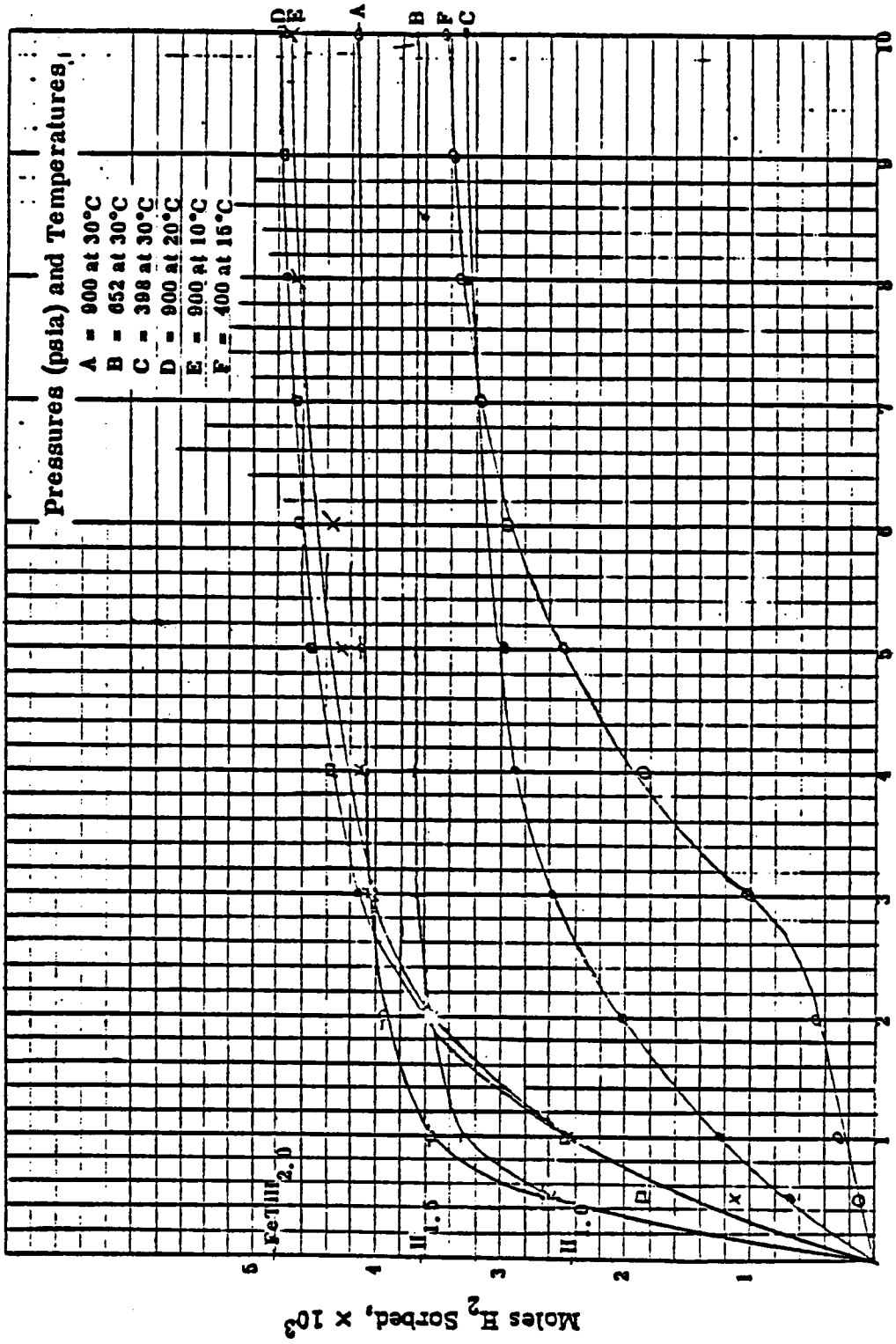

Figure 4. Rate of formation of iron titanium hydride.

Another set of kinetic results obtained by P. D. Goodell, et al. (14) is thought to be inadequate (15) probably because they used the dynamic pressure instead of static one. This could not help much the modeling study.

(B). Dehydriding

The dehydriding data shown in Figure 5 (9) were taken from experiments in which the particles were sufficiently small, that internal particle mass transfer resistance was negligible. The iron titanium hydride was decomposed isothermally under vacuum. As in the hydriding case, large masses of steel balls were used.

It was found that the kinetics of the isothermal decomposition reaction appeared to be first order; this is demonstrated by the long linear sections of the curves in Figure 5, which graphs the decomposition data for three temperatures. The divergences from linearity at short times may be due to a difference in behavior between the higher and lower hydrides of FeTi. The linear parts correspond to compositions below $FeTiH_{1.0}$.

For the hydride $FeTiH_y$ where $y < 1.6$, the decomposition rate in lbs/hr-ft^3 was found (16) to be

$$\text{Rate} = [(P - P_s)/P]\exp(18.9 - 6700/T), \qquad (3)$$

where

P = equilibrium decomposition hydrogen pressure at T and given composition of hydrogen in the hydride;

P_s = system pressure;

T in °R.

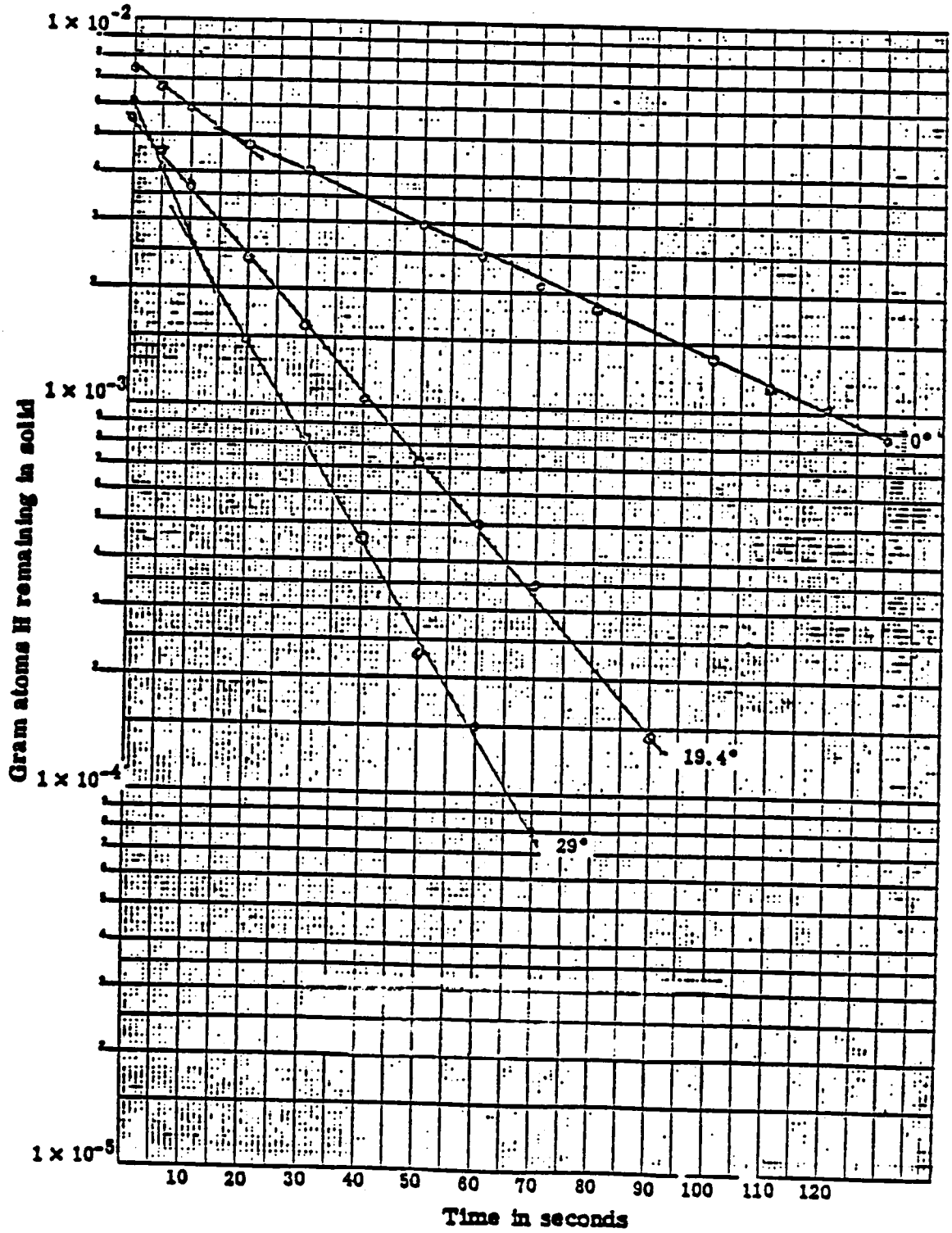

Figure 5. Rate of decomposition of iron titanium hydride at three temperarures.

D. L. Lindner (17) postulated that at any time each hydrogen atom in the hydride has a probability of being lost to the vacuum equal to that of any other hydrogen atom. The decomposition is completed by a series of reactions

$$H\ (\text{interstitial}) \xrightarrow{\text{Diffusion}} H\ (\text{surface}), \tag{4}$$

$$2H\ (\text{surface}) \xrightarrow{k} H_2\ (\text{adsorbed}),$$

$$H_2\ (\text{adsorbed}) \xrightarrow{k'} H_2\ (\text{gas}). \tag{5}$$

The diffusion process in the first step is fast enough to average out the topochemical features which normally dominate the kinetics of decompostion reaction of the type

$$A\ (\text{solid}) \longrightarrow B\ (\text{solid}) + C\ (\text{gas}). \tag{6}$$

In practice, the two reactions expressed by Equation (5) would be difficult to separate, and the diffusion of hydrogen out of the hydride is believed to be the rate determining step.

For a sufficiently long time, an apparent first-order kinetics results

$$1 - \omega \approx (8/\pi^2)\exp(-\pi^2 D_h t/S^2), \tag{7}$$

where ω is the fractional extent of reaction. It is equal to zero for no reaction and one for complete reaction. D_h is the diffusion constant, and S is the characteristic dimensions of hydride fragments. These are on the order of 2-10 μm (18).

1.3 THERMODYNAMICS

(A). Mathematical Expressions For Equilibrium Isotherms

In order to use the thermodynamic relations among temperature, pressure and composition in computer modeling of hydride beds for hydrogen storage, the equilibrium isotherms for hydriding as well as dehydriding have been segmented into several portions, and each portion is fit with an appropriate mathematical expressions.

(1). Hydriding (absorption) isotherms

The hydriding isotherm at 30°C (545.4°R) (Figure 3, page 8) is expressed by the following equations by fitting with the least-equare program (19). Let P represents for the equilibrium absorption pressure in psia, and C = H/M. Then, for the region $C < 0.0178$,

$$P = 1268.2565C. \tag{8}$$

For $0.0178 \leqslant C \leqslant 0.13351$,

$$P = -6388.309C^2 + 2192.365C - 14.42506. \tag{9}$$

For the plateau region $0.13351 < C \leqslant 0.63894$,

$$P = 44.75409C + 158.4295. \tag{10}$$

For $0.63894 < C \leqslant 0.86163$,

$$P = 3156.905C^2 - 3652.196C + 1231.771. \tag{11}$$

For $C > 0.86163$,

$$P = 6111.793C - 4837.469. \tag{12}$$

(2). Dehydriding (dissociation) isotherms

Similarly the dissociation isotherm at 40°C (563.4°R) shown in Figure 6 (19) is also fit with the least-square program, resulting in the following equations. For the region $C < 0.08385904$,

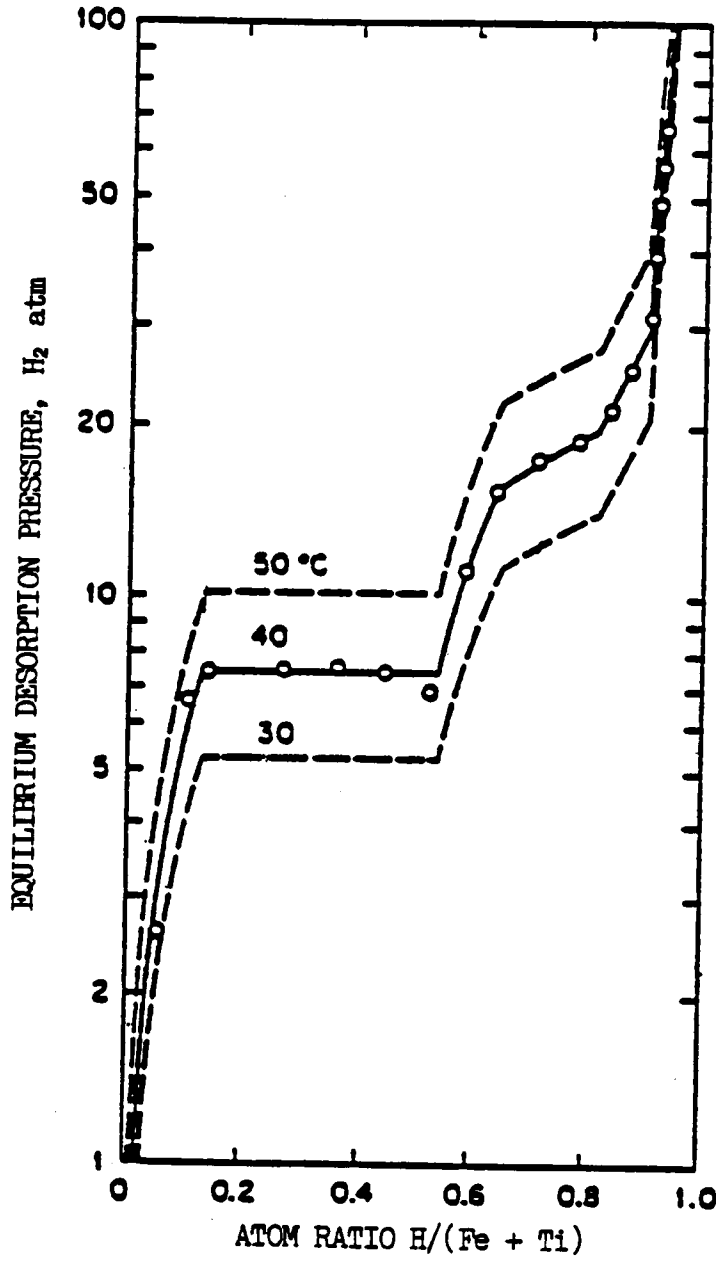

Figure 6. Equilibrium desorption isotherms for the FeTi-H system: points are experimental data, and lines are predictions from the data base.

$$P = g[0.145 - \sqrt{0.16101242^2 - (C + 0.07)^2}]. \quad (13)$$

For $0.083859034 \leqslant C < 0.148282324$,

$$P = g[0.077 + \sqrt{0.0692283695^2 - (C - 0.15)^2}]. \quad (14)$$

For $0.148282324 \leqslant C < 0.51231435$,

$$P = g[0.025C + 0.1425]. \quad (15)$$

For $0.51231435 \leqslant C < 0.72921968$,

$$P = g[0.23028443 - \sqrt{0.075^2 - (C - 0.51043994)^2}]. \quad (16)$$

For $0.72921968 \leqslant C < 0.905$,

$$P = g[0.6 - \sqrt{0.25552989^2 - (C - 0.65)^2}]. \quad (17)$$

$g = 735$.

The equilibrium pressure at other temperatures can be estimated by the van't Hoff equation (3)

$$P_2 = P_1 \exp[A_0(1/T_2 - 1/T_1)] \quad (18)$$

with $T_1 = 30\,^{\circ}C$ for hydriding, $T_1 = 40\,^{\circ}C$ for dehydriding and P_1 the equilibrium pressure corresponding to T_1, where A_0 changes slightly with the composition. An example of the extrapolation to other temperatures is shown in Figure 6. If T in °K, its values are tabulated in Table 1.

Table 1. van't Hoff constant, A_0, for various compositions.

Composition	A_0, °K
$FeTiH_{0.1}$ - $FiTiH_{1.04}$	-3383
$FeTiH_{1.20}$	-3728
$FeTiH_{1.40}$	-4020
$FeTiH_{1.60}$	-4057

(B). Heat Of Reaction

The heat of reaction, ΔH, determined by Reilly and Wiswall (3) were in agreement with those obtained by Pick and Wenzl (20). In Pick and Wenzl's method, the heat of reaction was determined by measuring the temperature change of the sample as small increments of hydrogen were added or withdrawn from the sample.

It has been found that the heat of reaction changes with the atom ratio in the hydride. Again, let $C = H/M$, then for $0.05 \leqslant C \leqslant 0.52$,

$\Delta H = 6058.90$ Btu/lb H_2.

For $0.52 < C \leqslant 0.6$,

$\Delta H = 6669.95$ Btu/lb H_2.

For $0.6 < C \leqslant 0.7$,

$\Delta H = 7164.82$ Btu/lb H_2.

For $C > 0.7$,

$\Delta H = 7250.88$ Btu/lb H_2.

The heats of reaction given here are absolute values. Their signs depend upon the reaction involved. Hydriding is exothermic; thus the heat of reaction is negative according to the convention. The heat of reaction is positive for dehydriding.

(C). Heat Capacity

(1). Iron titanium hydride

The heat capacity of $FeTiH_y$, where $y < 1.46$, was reported to be approximately constant (16);

$C_{ph} = 0.14$ Btu/lb $FeTiH_y$.

(2). Hydrogen

Hydrogen is assumed to behave as an ideal gas, and its heat capacity is a function of temperature only (21).

$$C_{p_{H_2}} = 6.52 + 7.2\times10^{-4}T + 1.2\times10^{4}T^{-2}, \quad (19)$$

where T is in °K and $C_{p_{H_2}}$ is in Btu/lb mole-°R or cal/gmole-°K.

In fact, the heat capacity of hydrogen remains approximately constant over a rather wide range of temperature, i.e., 77-140°F. For two significant digits

$$C_{p_{H_2}} = 3.4 \text{ Btu/lb-°R.}$$

(3). Hydride packing

The heat capacity of the hydride packing and hydrogen gas can be calculated (22) by the following equation.

$$(\rho C_p)_{bulk} = C_p \rho_h (1 - \varepsilon) + C_{p_{H_2}} PM_{H_2}\varepsilon/RT, \quad (20)$$

where

ρ_h = hydride density

$$= 405.5 - 67.5C, \text{ lb/ft}^3, \quad (21)$$

C = H/M

= y/2;

ε = void fraction of the packing;

M_{H_2} = molecular weight of hydrogen, 2.016 lb/lb mole;

R = gas constant, 10.73 psia-ft /lb mole-°R;

C_p is in Btu/lb-°R, P in psia and T in °R.

(D). Thermal Conductivity

The change of the thermal conductivity of the FeTi hydride packing with pressure have been determined twice, as indicated by Line (A) (9) and Line (B) (16) in Figure 7. The discrepancy between the two curves causes difficulty for investigators when accurate thermal conductivity data are needed.

Since thermal conductivity is prabably the most critical property in the modeling study of the hydride bed, it is desirable to obtain more reliable results. We have measured the new values; the experimental procedure and results will be described in the later chapters.

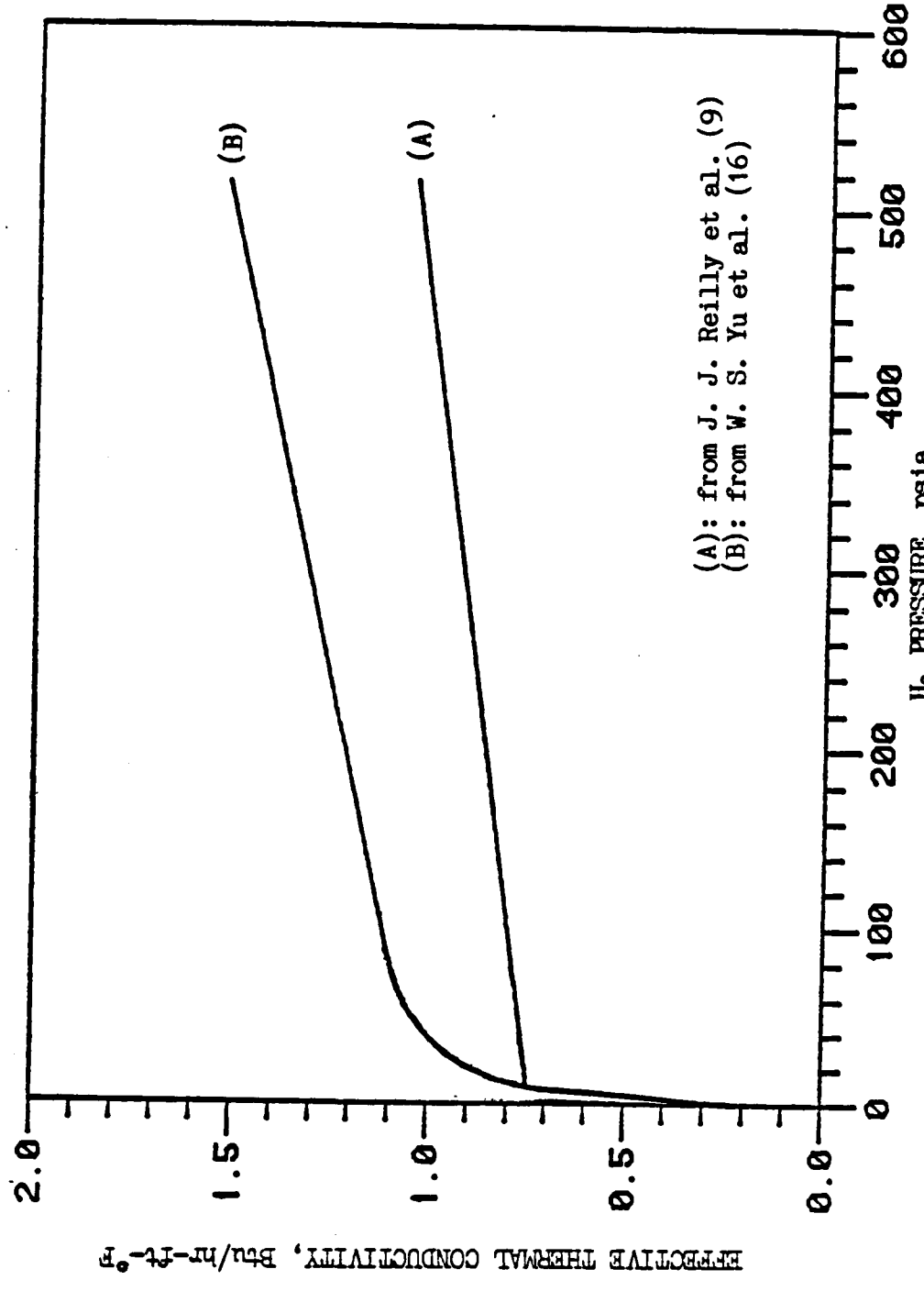

Figure 7. BNL data on the thermal conductivity of FeTi hydride as a function of hydrogen pressure.

CHAPTER 2

HYDRIDE BED DESIGNS

A hydride reservoir consists primarily of a pressure vessel filled with granular hydride and provided with a barrier to hold the particles in place, gas connection(s), and a means for handling the thermal load encountered during hydriding and dehydriding. Various designs of hydride reservoir have been tested or modeled mathematically. Special care must be provided for transporting heat to and from the hydride. The heat of reaction necessary to liberate hydrogen could be supplied by circulating hot hydrogen through a charged hydride bed (16). The hot hydrogen would be heated externally. With hot hydrogen entering one end of the bed, the reaction would travel from the hot end to the cool end. Whether this reaction zone is broad and covers the entire bed or is a narrow band moving from one end to another depends on the relative rates of heat and mass transfer and chemical kinetics within the bed.

The hydride bed itself could be a series of slabs cooled/heated by finned heat transfer surface between the slabs of hydride (23), as shown in Figure 8. During the discharging cycle, a possible heat source is the exhaust heat from a fuel cell or a combustion engine. During the recharging cycle, a coolant would pass through the exchanger to remove the heat of reaction. Hydrogen gets in/out from the top of the bed. In this design, the reaction zones started from both sides of each slab of hydride bed, and then moved toward the center of the slab.

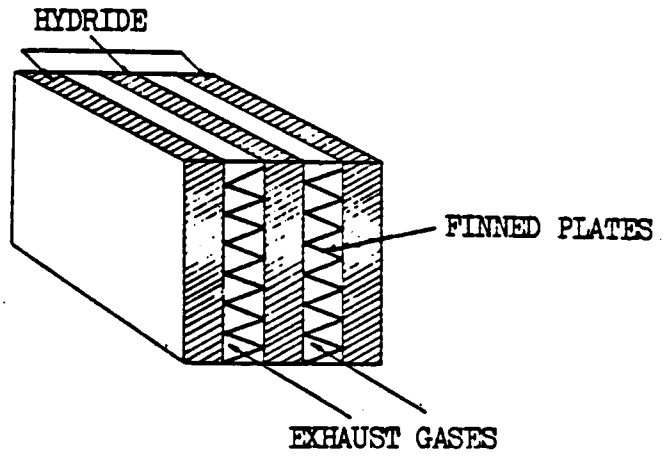

Figure 8. Plate-to-plate heat exchanger for storing hydride.

Another design would use heat exchanger tubes immersed in the bed of hydride (24), as indicated in Figure 9. This is the sectional view of the hydride bed. The porous metal tubes (PMT) through which the gas is distributed to the bed are located near the center of each group of four water cooling/heating tubes.

The heat exchanger could also be in the form of water jacket, as designed by Brookhaven National Laboratory (BNL) (25). The hydride bed they designed was a cylindrical vessel with water jacket and a PMT on its longitudinal axis for hydrogen inlet/outlet. P. W. Fisher and J. S. Watson have made modeling studies to simulate the BNL experimental results (12) (26-27). Their results indicated that thermal conductivity was the only property which had a significant impact on the results, a better data on thermal conductivity, therefore, were needed for more accurate predictions.

Generally hydride beds can be classified as convection and conduction types respectively, and each type, especially the conduction type, rely on the thermal conductivity in the hydride itself to supply and remove the heat of reaction. Since the reaction rate, as indicated previously, is always limited by the rate at which the heat of reaction can be supplied or removed, methods for increasing the heat transfer become some of the most interesting topics in the application of hydrides as energy storage media.

The hydride reservoir we will study is basically similar to that constructed at BNL (25), as shown in Figure 10, except different packing material is used. Between the vessel wall and PMT is the Al-FeTi hydride mesh which is produced by pouring the hydride powder into a

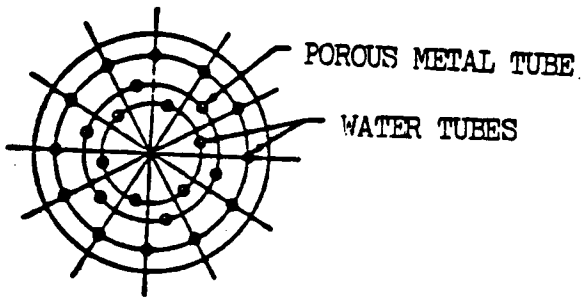

Figure 9. Hydride bed with immersed heat exchanger.

ORNL-DWG 81-36R

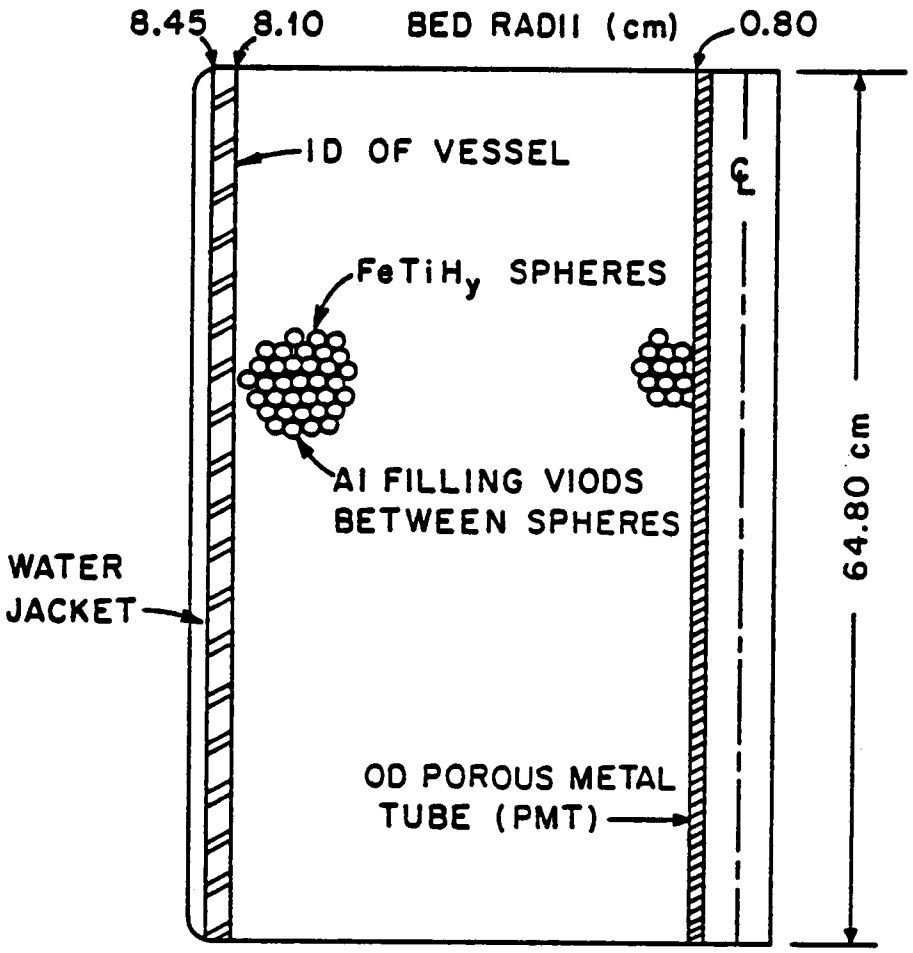

Figure 10. Hydride reservoir used in modeling studies.

porous Al-foam, as illustrated schematically in Figure 11. The channels for hydrogen flow merge to connect to the PMT.

because of its high thermal conductivity, aluminum is used here to enhance the heat transfer. Al-foam, like sponge, is a reticulated open-cell structure (brand named Duocel, produced by Energy Research and Generation Inc., Oakland, California). This structure provides in-situ heat transfer between the poorly conducting hydride powder and the heat transfer fluid. The mean cell size and volume fraction of aluminum can be varied over a wide range of values during the manufacturing.

This research has been focused on two objectives:

1. Obtaining more reliable experimental data on the most critical parameter needed to evaluate these systems, the thermal conductivity of FeTi hydride powder and the FeTi hydride in Al substrates.
2. Development of a mathematical model for the new system, including the effect of the aluminum content, the effect of the size of the aluminum cell, and comparison of the calculation with models and data from studies without heat enhancement by aluminum.

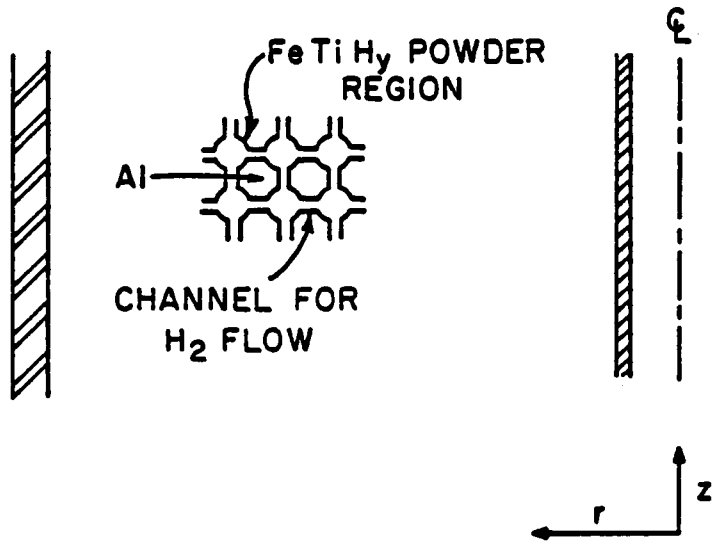

Figure 11. Schematic of the matrix formed by aluminum and FeTi hydride.

CHAPTER 3

EXPERIMENTS

The mathematical model developed in this study will require several physical parameters. Earlier values had been measured at BNL. Their program is continuing, but it has been reduced in scale recently. This study has cooporated with the BNL effort and in some ways supplemented their work. Since the effective thermal conductivities are perhaps the most critical physical property of hydride beds, we concentrated our experimental effort on measurements of this pamameter. Thermal conductivity measurements were made of FeTi hydride powder and FeTi hydride powder in an aluminum substrate. The experiments were performed at the Oak Ridge National Laboratory (ORNL).

3.1 FUNDAMENTAL CONSIDERATIONS

Measurement of the thermal conductivity of a particulate medium is not straightforward. Any porous material with an internal temperature gradient transfers heat by conduction in the particles and their contact surface, by conduction and convection in the gas, and even by radiation in the void space. If conduction, convection, and radiation effects are grouped into a simple entity, Fourier's law can be used to calculate heat fluxes, as long as it is recognized that the effective conductivity so defined is only a composite property rather than a basic property of the solid material.

The method we have used for measuring the effective thermal conductivity of porous material is based on transient heat conduction requiring the meaurement of only time intervals and changes in

temperature at one or more selected points in the sample(28-30). The experiment employs a cylinder initially in thermal equilibrium at temperature T_1 and well insulated at both ends. The cylinder is then suddenly moved to a different environment so the new surface temperature is T_0. The differential equation for this unsteady-state heat conduction is

$$\frac{\partial T}{\partial t} = \frac{\lambda}{r}\frac{\partial}{\partial r}\left(r\frac{\partial T}{\partial r}\right) \tag{22}$$

Subject to the conditions

$$\text{(a).}\quad T = T_1 \qquad 0 < r < a,\ t = 0 \tag{23}$$

$$\text{(b).}\quad T = T_0 \qquad r = a,\ t = t \tag{24}$$

The solution of Equation (22) is given by (30)

$$\frac{T - T_1}{T_0 - T_1} = 1 - 2\sum_{n=1}^{\infty}\frac{\exp(-\lambda\psi_n^2 t)}{Z_n J_1(Z_n)} \tag{25}$$

Where

t = time;

T = temperature on the center line of the cylinder at $t = t$;

$Z_n = a\psi_n$, roots of Bessel function of zero order, i.e.,

$J_0(Z_n) = 0$;

a = radius of cylinder;

λ = thermal diffusivity of the porous material in the cylinder;

$J_1(Z_n)$ = Bessel function of order one.

The derivation of Equation (25) is based on the assumptions that as far as the effective thermal diffusivity is concerned, the material is homogenous (λ is independent of position), isotropic (λ is independent of direction), and independent of temperature over the range involved in the experiment (T_1 to T_0).

The tested powder was randomly packed, and the effects of position and direction could be neglected. The thermal diffusivity of most materials, however, is a definite function of temperature. In principle, it is possible to approximate the assumption of constant thermal diffusivity by limiting the individual meaurement to small temperature ranges.

To solve for the thermal diffusivity, there are three common approaches:

(A). The first approach would be the simplest. Let $c(\theta) = (T - T_1)/(T_0 - T_1)$, and $\theta = \lambda t/a^2$. The values of $c(\theta)$ for given values of have been tabulated (31). That table gives as 0.201 for $c(\theta) = 0.500$. If the time at which $c(\theta) = 0.500$ is designated as $t_{1/2}$, the thermal diffusivity, λ, can be calculated by

$$\lambda = \theta a^2/t_{1/2}$$
$$= 0.201 a^2/t_{1/2} \quad . \tag{26}$$

This approach have been used at BNL. It is very convenient and quick. But the determination of λ is based upon one data point (i.e., $t_{1/2}$), and it is likely to be less accurate than other approaches.

(B). The second approach (32) involves rearranging Equation (25)

$$1 - \frac{T - T_1}{T_0 - T_1} = 2 \sum_{n=1}^{\infty} \frac{\exp(-\lambda \psi_n^2 t)}{Z_n J_1(Z_n)}$$

to give

$$\frac{T_0 - T}{T_0 - T_1} = 2\left[\frac{\exp(-\lambda \psi_1^2 t)}{Z_1 J_1(Z_1)} + \frac{\exp(-\lambda \psi_2^2 t)}{Z_2 J_1(Z_2)} + \cdots + \frac{\exp(-\lambda \psi_n^2 t)}{Z_n J_1(Z_n)}\right] \tag{27}$$

For large t, all terms except the first one on the right-side of Equation (27) can be neglected. Then, if one takes the logarithm of both sides of Equation (27),

$$\ln \frac{T_0 - T}{T_0 - T_1} = -\lambda\psi_1^2 t + \ln \frac{2}{Z_1 J_1(Z_1)} \tag{28}$$

Or

$$\ln \frac{T_0 - T_1}{T_0 - T} = \lambda\psi_1^2 t + \ln \frac{Z_1 J_1(Z_1)}{2}$$

$$= \lambda\psi_1^2 t + \gamma . \tag{29}$$

Where

$$\gamma = \ln[Z_1 J_1(Z_1)/2]$$

$$= \text{constant}$$

$$= -0.48063. \tag{30}$$

The plot of $\ln[(T_0 - T_1)/(T_0 - T)]$ versus t should be a straight line with slope, b, as indicated in Figure 12.

$$b = \lambda\psi_1^2 \tag{31}$$

Therefore,

$$\lambda = K/\rho C_p$$

$$= b/\psi_1^2. \tag{32}$$

Here K is the effective thermal conductivity of the material tested; ρ is the bulk density of the material tested; and C_p is the average specific heat of the material tested.

This approach can combine the results of several data points. However, those data must be the points for longer time.

(C). An ever accurate approach would involve substituting directly a series of values of T and the corresponding t in (25), λ would then be found by an appropriate optimal searching technique. The λ obtained by

ORNL-DWG 81-367

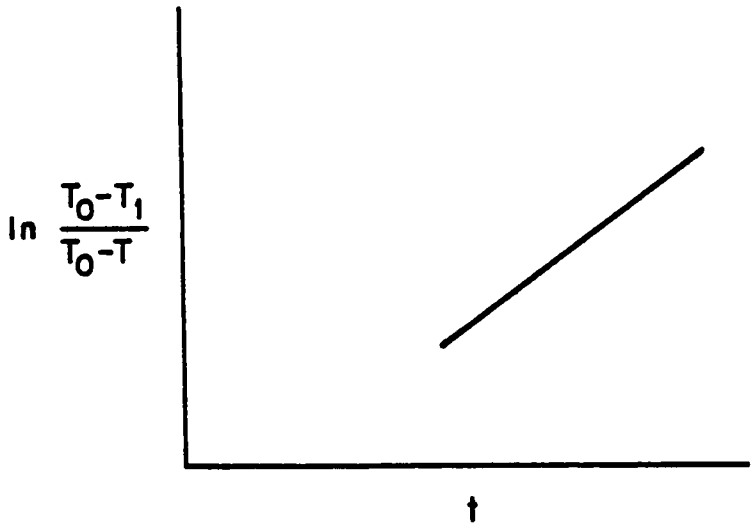

Figure 12. The relation between $\ln[(T_0 - T_1)/(T_0 - T)]$ and time for longer times.

this "curve fitting" method should be more reliable and representative, but it is determined in a more complicated and time consuming way. This approach was adopted in this investigation.

The first few values of Z_n and $J_1(Z_n)$ in Equation (25) can be found from "Mathematical Handbook For Scientists And Engineers," by Korn and Korn, second edition, 1968, P.1038 - 1042. Since $Z_n = a\psi_n$, each ψ_n is thus obtained for a given cylinder radius, a. Values for Z_n, $J_1(Z_n)$ and ψ_n corresponding to a = 0.6875 inch as used in this study are tabulated in Table 2. The experimental apparatus and procedure will be described in detailed later.

Table 2. Numerical values of Z_n, $J_1(Z_n)$ and ψ_n

n	Z_n, dimensionless	$J_1(Z_n)$, dimensionless	ψ_n, in
1	2.4048	0.5143	3.4979
2	5.5201	-0.3403	8.0292
3	8.6537	0.2715	12.5872
4	11.7915	-0.2325	17.1513
5	14.9309	0.2066	21.7177
6	18.0711	0.0195	26.2852
7	24.2116	-0.0146	35.2169

With the values of Z_n, $J_1(Z_n)$ and ψ_n, Equation (25) becomes

$$\frac{T - T_1}{T_0 - T_1} = 1 - 1.61709\exp(-12.2352\lambda t) + 1.06468\exp(-64.4686\lambda t)$$
$$- 0.85125\exp(-158.437\lambda t) + 0.72952\exp(-294.166\lambda t)$$
$$+ 0.64836\exp(-471.657\lambda t) + \cdots \qquad (33)$$

Here t is in minute, and λ is in inch^2/minute

Due to the increasing negative order of the exponential terms, these terms on the right-size of Equation (33) decrease abruptly in absolute value. The error caused by neglecting all the terms after the fifth one is justifiably small.

Once λ is known, the thermal conductivity is then calculated with the following equations

$$K = \lambda(C_p \rho)$$

$$= \lambda[C_{ph}\rho_h(1 - \varepsilon) + C_{pgas}PM_{gas}\varepsilon/RT] \quad (34)$$

With Al-enhancement, the equation becomes

$$= \lambda\{C_p\rho_h[1 - (\varepsilon + V_a)] + V_a C_{pa}\rho_a + C_{pgas}PM_{gas}\varepsilon/R\,T\} \quad (35)$$

Where

P = pressure of gas

M_{gas} = molecular weight of gas

C_{pgas} = specific heat of gas

C_p and ρ are the average specific heat and bulk density of the bed respectively. They are composite values made up of the contributions from the hydride and the gas for nonenhancement cases and from the hydride, gas and aluminum for enhancement cases.

3.2 EXPERIMENTAL APPARATUS AND PROCEDURE

(A). Apparatus

The test vessel was a cylindrical steel tube (1.375" I.D x 0.0675" wall x 16" long) (3.493 cm x 0.1715 cm x 40.64 cm), rated at 5800 psig, and flanged at both ends (with Rotatable Del-Seal Flanges produced by MDC Manufacture Inc. Model No. F275150R). Both ends of the tube were

filled with three inches of asbestos (Marinite Board) which served as an insulating material. Three shielded Chromel Alumel thermocouples with diameter of 0.021" (0.5334 mm) were passed through a small axial hole of the bottom insulation. These were positioned at the center line with longitudinal displacement of 3.5 inches (8.89 cm) between hot junctions. The middle one was at the point midway between the ends of the cylinder; the another two extremes were provided only to insure that end effects were minimal and heat flow was radial.

Two temperature controlled baths were used to provide the constant temperature environment at the outside wall of the test cylinder. The liquid medium in both baths, water, was pumped to circulate to maintance a uniform temperature. The two baths were set at different temperatures. No matter which direction heat flowed, either heating the bed from a low temperature to a new higher temperature or cooling the bed down, either of the baths could be used to provide a uniform initial temperature of the tested material. The heat capacity of the water was sufficient that the change of the water temperature caused by the sudden immersion of the test cylinder from another bath was never greater than 0.5°C.

Assembly of the test cylinder was started by packing one end with six cylindrical pieces of asbestos (1.375" diameter x 0.5" thick) (3.493 cm x 1.27 cm). This end was flanged tightly after the thermocouples were inserted through the small axile hole. Then, the tested material was filled in from the other end. Upon completion of the filling step, the unflanged end was packed with another six pieces of asbestos of the same size, and the second flange was sealed. The cylinder was then

placed on a shaker (Portable Sieve Shaker, Model RX - 24, U. S. Tyler Industrial Products) which vibrated the cylinder up and down a distance of 0.5" (1.27 cm) at the rate of 4 times per second for 30 minutes. Then the cylinder was unflanged, and the material level in the cylinder was examined. If the level dropped, the cylinder was refilled with additional materials, and the shaking was repeated. This procedure was continued until there was no further variation in the bed's void fraction, i.e., the material level was unchanged. The test cylinder was connected to a gas cylinder through a pressure control valve and gauge (0 - 500 psig, Robinair Mfg. Corp. or vacuum gauge, 0 - 30"Hg, Duragauge Ashcroft), and the pressure of the test cylinder was adjusted. The gas (i.g., air) previously occupied the void space of the test cylinder was evacuated to 29" Hg vacuum before connecting to the gas cylinder.

The schematic diagrams of the equipment are shown in Figures 13 and 14.

(B). Procedure

The pressure of the cylinder was set at the desired value. The test cylinder was then immersed into one of the baths, and allowed to equlibrate until the three thermocouples in the apparatus approached the bath temperature, T_1, to within 0.2°C. The test cylinder was then removed and immediately immersed in the another bath with temperature T_0, and the change of temperature with time was recorded. The rate at which the data were taken depended upon the material tested. For the materials with higher thermal diffusivities a minimum of fifteen data points was provided for each run. For the materials with lower thermal

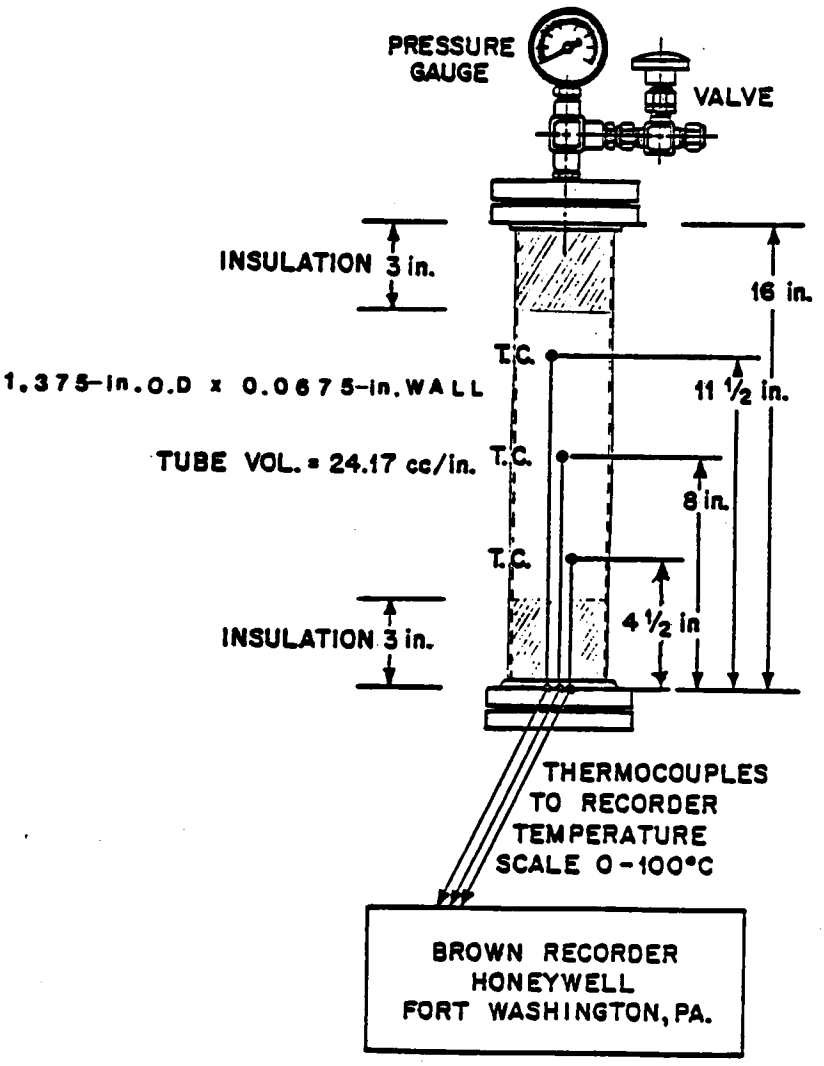

Figure 13. Experimental test cylinder.

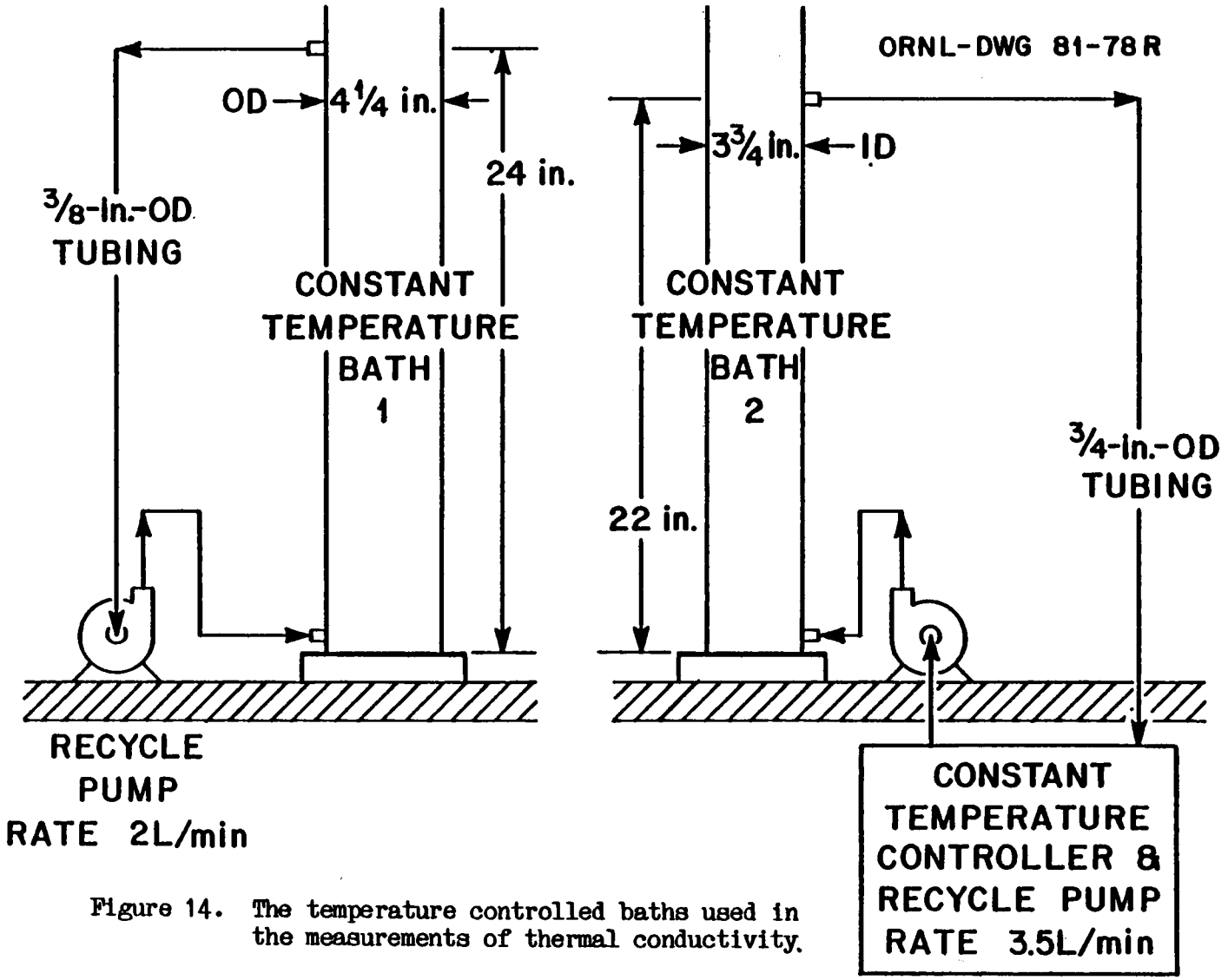

Figure 14. The temperature controlled baths used in the measurements of thermal conductivity.

diffusivities, the data points could be more than thirty. Generally each sample was tested in a temperature range T_1 to T_0 with both heating and cooling runs repeated, the results were reproducible.

3.3 DESCRIPTION OF THE MATERIAL

Two configurations were used : (1) packed bed of deactivated FeTi hydride; and (2) the same bed with 9.2 % volume of aluminum in the form of reticulated foam. The configurations were tested under pressures ranging from -29" Hg to 500 psig with gases of hydrogen, helium, nitrogen and argon.

The size distribution of deactivated FeTi hydride particles was measured, and the results are presented in the Table 3. Most of the material, 95.6 wt.%, was between 12 and 50 mesh.

Table 3. Size distribution of deactivated FeTi hydride (T-82878).

Mesh U. S. standard	Weight gms	Weight Percent wt.%
- 8 + 12	5.05	1.30
- 12 + 16	81.70	20.96
- 16 + 20	74.50	19.12
- 20 + 35	124.50	31.95
- 35 + 50	91.91	23.58
- 50 + 70	8.40	2.16
- 70	3.65	0.94
	389.7	100.01

3.4 DATA PROCESSING AND PRECISION OF RESULTS

The experimental procedure involved two important assumptions : (1) the temperature of the water remained constant, and (2) the surface temperature of the test cylinder changed essentially instantaneously with emersion. Such conditions are, of course, impossible to attain

absolutely because there was a slight change in the bath temperature when the test cylinder was suddenly moved to the bath. Although the change was usually less than 0.5°C, it could be a source of error in those calculations based on the small temperature difference the smallest of which was chosen 10°C. This effect was reduced or eliminated by (a) omitting those reading whose temperature ratio $(T - T_1)/(T_0 - T_1)$ was less than 0.1 and (b) taking as many data points as possible at longer time for fitting to Equation (33). The thermal diffusivity, λ, was then found by the Nelder and Mead searching technique. The upper limit of 0.95 for the temperature ratio was usually reached before data collection was stopped.

The second assumption was approximated by the facts that the major thermal resistance between the outside surface and the center line of the cylinder comes from the poor thermal conductivity of the testing sample, and that the circulation rate of water was high.

Since the thermal diffusivity was assumed to be constant in the temperature range within which an individual set of measurements was made, an equal number of heating and cooling runs were collected for value averaging. The reported temperature is the mean value of the initial temperature of the sample and the temperature of the water bath. The mean temperature for the heating run sometimes differed very slightly from that for the cooling one, but these small differences are negligible.

The calculation search was terminated for $\xi = 0.00001$, where ξ will be defined in Equation (44) (next chapter) as the searching criteria in Nelder and Mead technique. The calculation precision of measurement may

vary for sample of greatly varying magnitudes of diffusivity due to variations in the error involved in the measurement of time. For example, the time interval are much smaller for the samples under hydrogen than those for sample under argon; therefore, the relative accuracy of the time measurement is less for the samples under hydrogen. In general, the longer the time interval, the more data points which could be used for curve fitting and thus the more precise the mesurement result obtained.

CHAPTER 4

DISCUSSION OF EXPERIMENTAL RESULTS

In the following paragraphs, several respects of the current experimental data on thermal conductivity will be presented, (1) temperature dependence, (2) pressure dependence, (3) evidence for no reaction during the experiments, (4) comparisons with the BNL results, (5) implications of the new values in the modeling study and (6) mathematical expressions describing the results.

4.1 DEPENDENCE OF THE THERMAL CONDUCTIVITY ON TEMPERATURE

The change of the thermal conductivity of FeTi hydride, K_h, with temperature have been determined at several pressures, 1 atm, 75 psig, 200 psig, 350 psig and 500 psig of hydrogen. The results are shown in Table 4. It is obviously that in the temperature range of 30 - 50°C, the variation of K_h with temperature is negligibly small.

For a fixed pressure, K_h is found to be inverse related to the temperature and has the form $K_h = A/T + B$, as indicated in the Figure 15. If K_h is in Btu/hr-ft-°F and T is in °R, the parameters A and B found for those pressures have been summarized in Table 5. Note that because of the slopes of the lines in Figure 15, expressed by the negative values of A in Table 5, K_h actually increases with the increase of temperature.

As mentioned previously, K_h is actually a composite value which takes into account the effects of conduction, convection and even radiation in the porous FeTi hydride bed. It would be difficult to tie the results to any one theory. It is thought best to let them stand expressed empirically as other investigators have done (33).

Table 4. The thermal conductivities of the deactivated FeTi hydride bed at pressure of hydrogen

	K_h, Btu/hr-ft-°F				
T, °C	at 1 atm	at 75 psig	at 200 psig	at 350 psig	at 500 psig
9	0.9444242	1.0836675	1.1317909	1.1625802	1.1901454
24	1.0550592	1.1428424	1.1765175	1.2004979	1.2294406
35	1.1114887	1.1807546	1.2064301	1.2361340	1.2571663
45	1.1617991	1.2192724	1.2375381	1.2625030	1.2850528
55	1.2036793	1.2584132	1.2786250	1.3029576	1.3153179
65	1.2484506	1.2712850	1.3043456	1.3245727	1.3375291
75	1.2917994	1.3047414	1.3208356	1.3487570	1.3687416

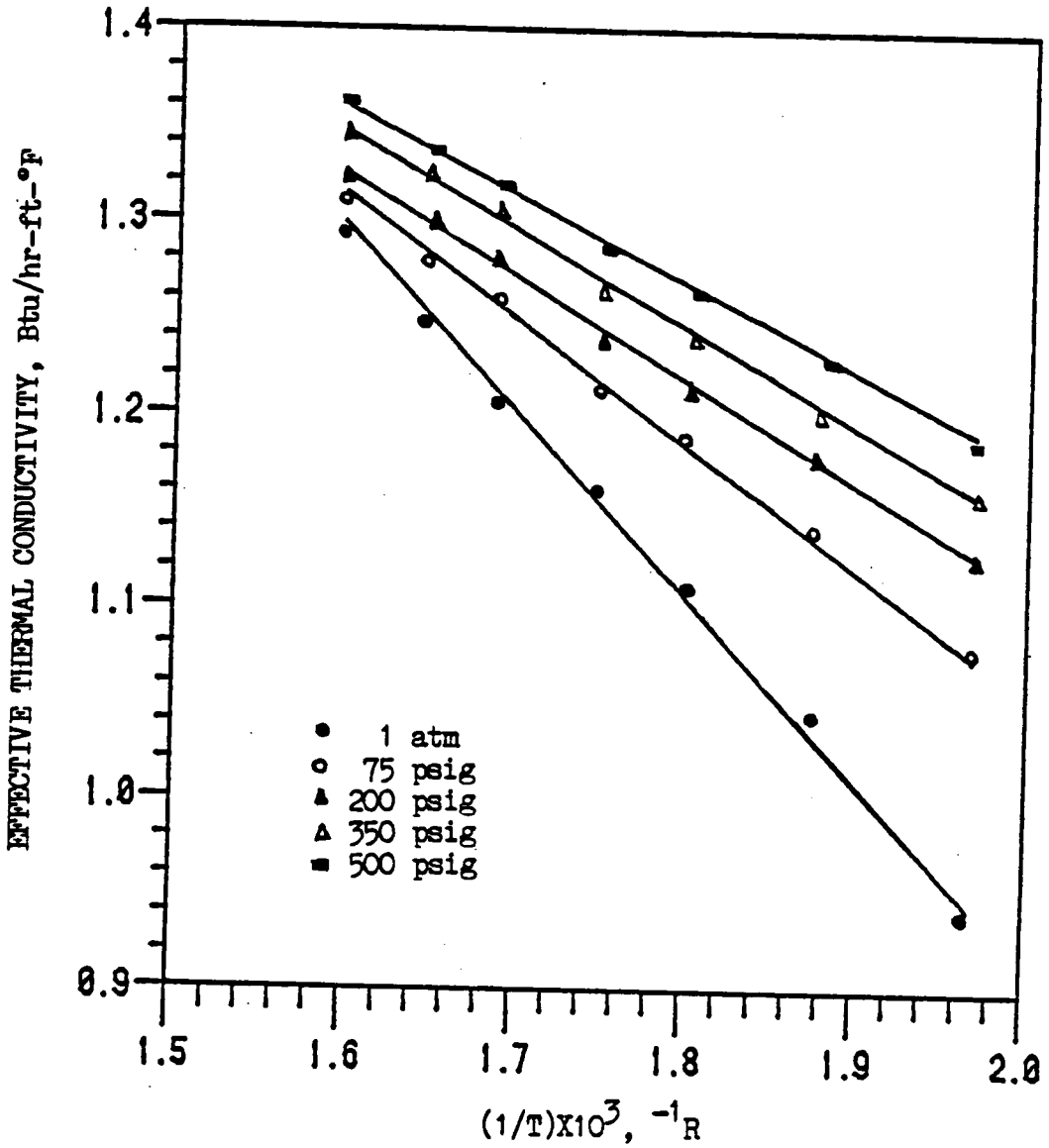

Figure 15. Temperature dependence of the thermal conductivity of the deactivated FeTi hydride bed filled with hydrogen.

Table 5. Parameters A and B in $k_h = A/T + B$ for the thermal conductivity of deactivated FeTi hydride powder filled with hydrogen.

Pressure	A	B
1 atm	-999.90426	2.9066941
75 psig	-599.93709	2.2654154
200 psig	-559.97715	2.2230294
350 psig	-535.96565	2.2069665
500 psig	-459.99784	2.0938527

Like hydrogen, helium has a comparatively high value of thermal conductivity among some common gases. As with hydrogen, the thermal conductivity of FeTi hydride with various pressures of helium, K_{He}, has also been found to be inverse related to the temperature. This is shown in Figure 16. Since helium is inert to the hydride, the similarity between Figure 15 and Figure 16 suggests that no reaction takes place during measurement of K_h even at the highest pressure. The FeTi hydride particles had not been previously activated, so this is not surprising. This is why we made the measurements with helium and determined the dependence of K_{He} with temperature. Since significant reaction between FeTi hydride and hydrogen had occured, the reaction heat should complicate the temperature measurement during experiment.

4.2 DEPENDENCE OF THE THERMAL CONDUCTIVITY ON PRESSURE

The thermal conductivities, K_g, of the FeTi hydride at different pressures of several gases (H_2, He, N_2, A_r) have been measured by setting T_1 and T_0 either 30 or 50°C, depending upon heating or cooling run was performed. Over the small temperature range of 30-50°C, K_g was

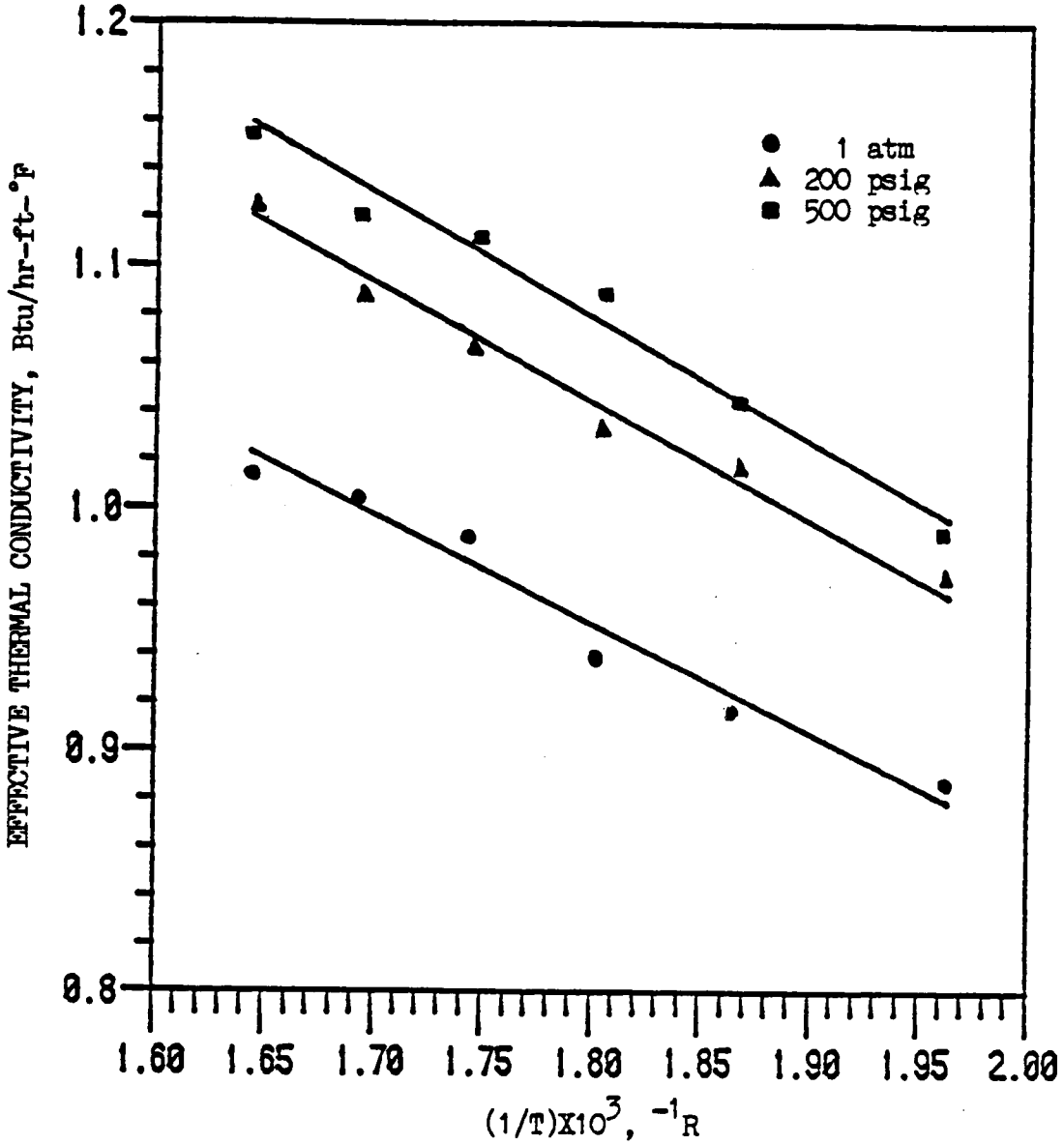

Figure 16. Temperature dependence of the thermal conductivity of the deactivated FeTi hydride bed filled with helium.

assumed independent of temperature. The thermal conductivities of K_g for $g = N_2$ and A_r are shown in Figure 17. They increase with pressure first rapidly at the region near absolute vacuum, and then change more gradually. As seen in Figure 17, K_{N_2} is always greater than K_{A_r}; their difference must come from the gases themselves rather than the porous hydride particles.

To eliminate the gas effect, extrapolating back to zero pressure results in a common point of approximately $K_0 = 0.1145$ Btu/hr-ft-°F. K_0 can be considered as the conductivity of the porous solid; while the difference $K_{g0} = K_g - K_0$ is the contribution of gas to the overall heat transport occuring in the hydride packing. Although K_{g0} is not simply the conductivity of the pure gas, it should be a function of gas pressure, thermal properties of the gas, the pore-size distribution, etc. In the range of very low pressure, the mean-free path of the gas is large enough for free-molecule conduction. But when the pressure of the gas in the void space is increased, the mean-free path becomes substantially less than the pore size, and the gas diffusion changes basically from Knudsen to bulk mode. The effect of pore size on heat diffusion may no longer appear. This could explain why there is a sharp rise in the range of very low pressure, and why K_g changes remarkably little when the pressure is increased still further. This is shown in Figure 18 where data at still higher pressures are presented; additional curves are shown for gases H_2 and H_e as well as N_2 and A_r.

The result of small variation of K_g with pressure for high or even moderate pressures is consistent with the statement of Lenoir, Junk and Comings (34), the effect of pressure on the conductivities of H_2, H_e, N_2 and A_r is small because the conditions are far from the critical point.

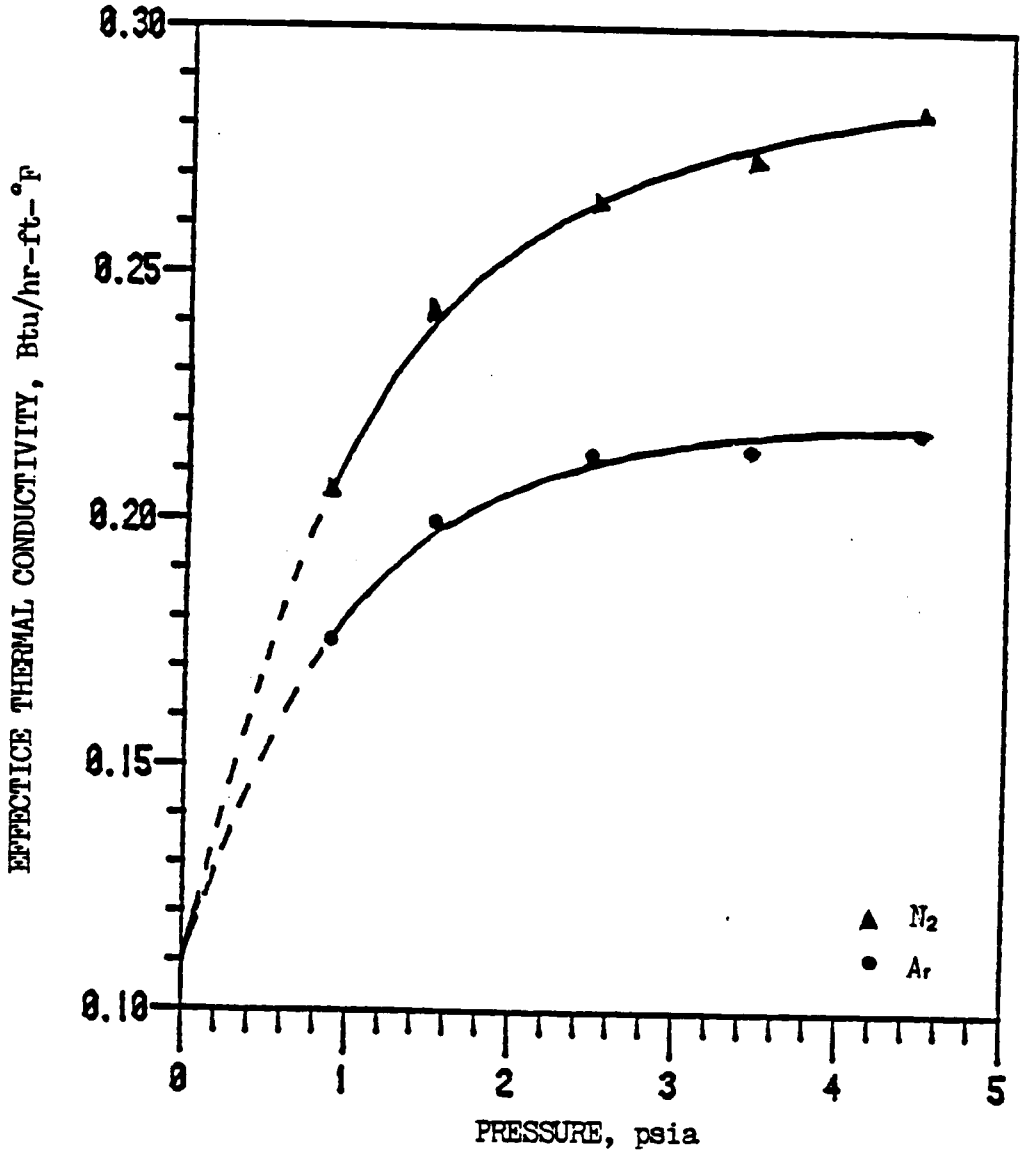

Figure 17. Thermal conductivity of the deactivated FeTi hydride filled with nitrogen and argon. Extrapolation results in K_0 = 0.11 Btu/hr-ft-°F.

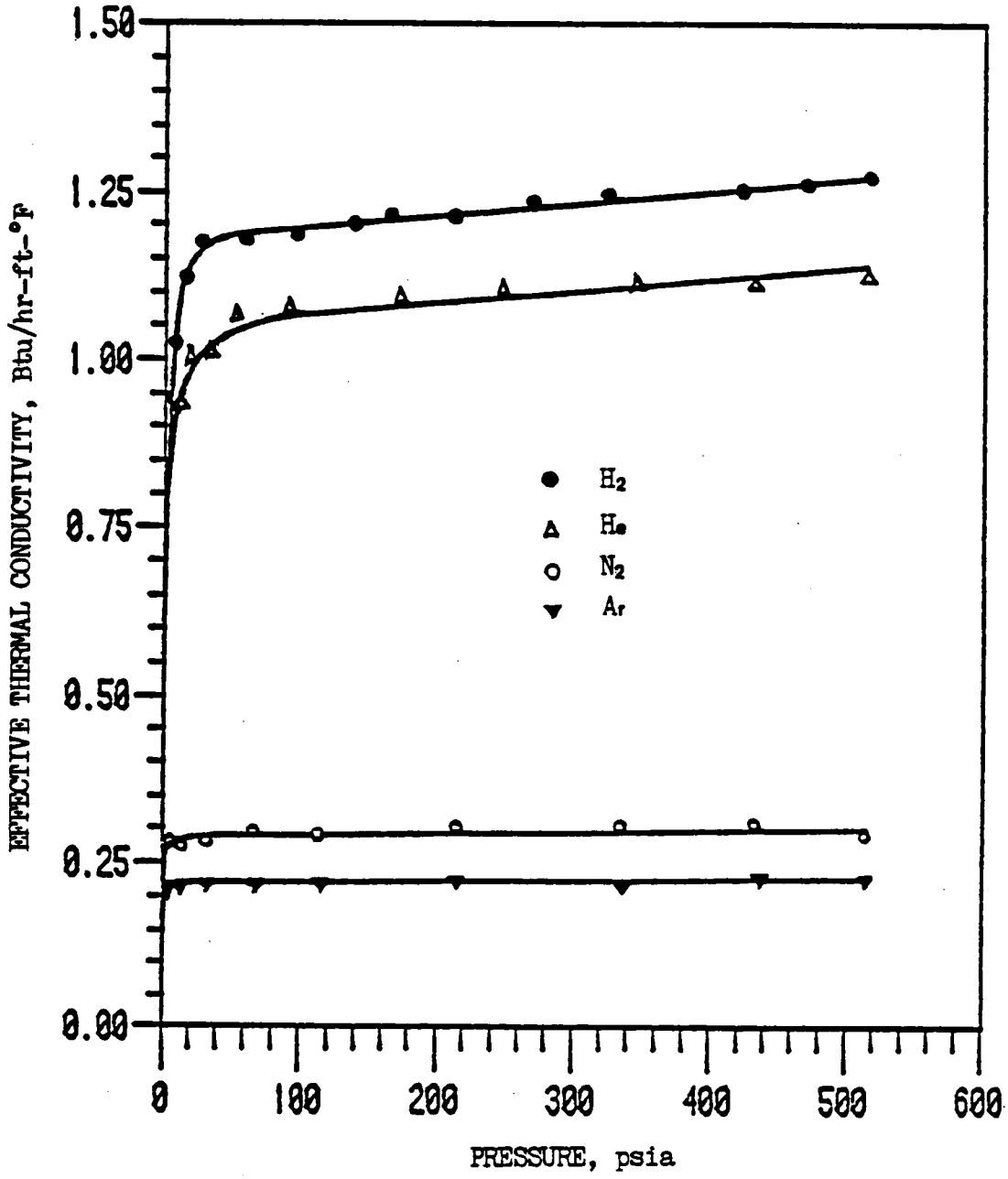

Figure 18. Pressure dependence of the thermal conductivity of the deactivated FeTi hydride filled with hydrogen, helium, nitrogen and argon.

Figure 18 also shows that K_g for H_2 and H_e are much greater than those for N_2 and A_r, and this leads one believe that the greatest contribution to the thermal transport in the presence of H_2 and H_e is made by the gas in the FeTi hydride. The FeTi hydride particles, on the other hand, contribute less to the heat transfer, principally due to the high thermal resistance at the points through which the particles contact each other. On the other hand, K_g for N_2 and A_r are only slightly more than twice the value of K_0. In these cases, the solid conductivity probably is still an important component of the overall conductivity.

One more interesting observation from Figure 18 is the existence of very similar trends in all curves, especially at the region of higher presure. Since H_e, N_2 and A_r do not react with FeTi hydride, their curves correspond to no reaction cases. Therefore, the observation also lends support the assumption that no conversion took place in the measurement of K_h. As mentioned before, the occurrence of reaction during the experiments could not only complicate the measurement of K_h, but the results could even be meaningless.

The dependence of the thermal conductivity, K_h, on pressure is shown in the Figure 19. For purpose of the modeling studies, these empirical data are approximated by several mathematical equations which apply to different regions of pressure. If K_h is in Btu/hr-ft-°F and P in psia, then for $P \leqslant 1.25$,

$$K_h = 0.48040608P + 0.11472394. \qquad (36)$$

For $1.25 < P \leqslant 3.0$,

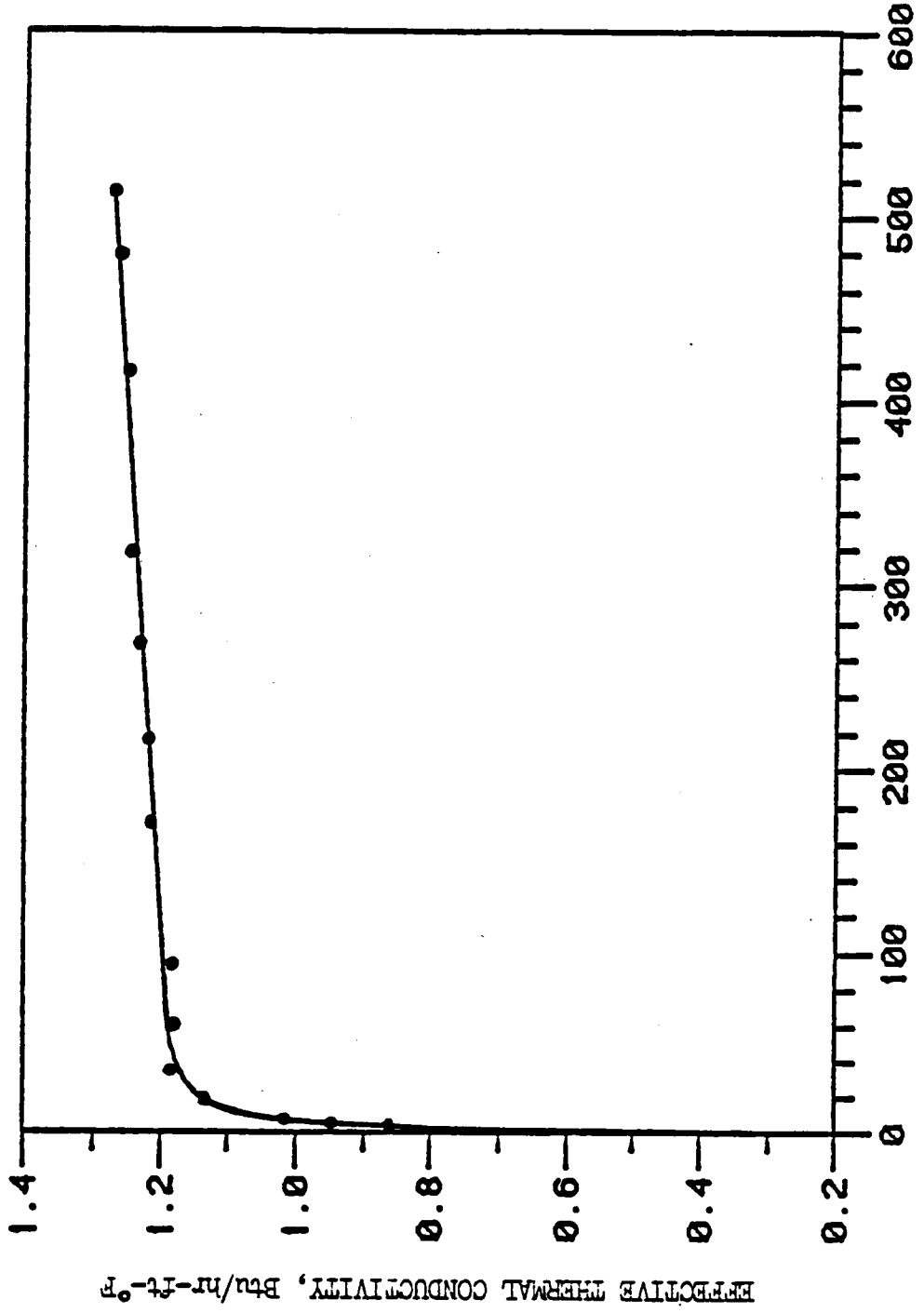

Figure 19. Thermal conductivity of the deactivated FeTi hydride as a function of hydrogen pressure.

$$K_h = -7.2502671\times10^{-2}P^2 + 0.41915179P + 0.3028238. \quad (37)$$

For $3.0 < P \leqslant 11.87$,

$$K_h = 1.8966791\times10^{-2}P + 0.86335858. \quad (38)$$

For $11.87 < P < 59.7$,

$$K_h = -8.3475306\times10^{-5}P + 7.2483123\times10^{-3}P + 1.033451. \quad (39)$$

For $P \geqslant 59.7$,

$$K_h = 1.8380527\times10^{-4}P + 1.178764. \quad (40)$$

These equations have been obtained using a least-square program. Generally

$$(K_h)_{\text{predicted}} = (1 + \Omega)(K_h)_{\text{observed}}. \quad (41)$$

the value of Ω was less than 0.01 for all equations except Equation (37) for that case Ω was less than 0.05. For the predicted K_h, the first three figures after the decimal point are the significant figures.

4.3 COMPARISON WITH PREVIOUS WORK

Figure 20 shows the comparison of the current result with previous work from BNL. Curve (A) (16) and Curve (C) (9) are the BNL results obtained by line-source technique (35-36), and their results were adopted by W. S. Yu et al. (16) and P. W. Fisher and J. S. Watson (26) respectively in their modeling studies. The difference between Curve (A) and (C) could be caused by many factors involved in the experimental measurements, (a) error in the heat supply rate, (b) poor insulation of the heater wire, (c) error in long time data (37), and (d) wall effects (38).

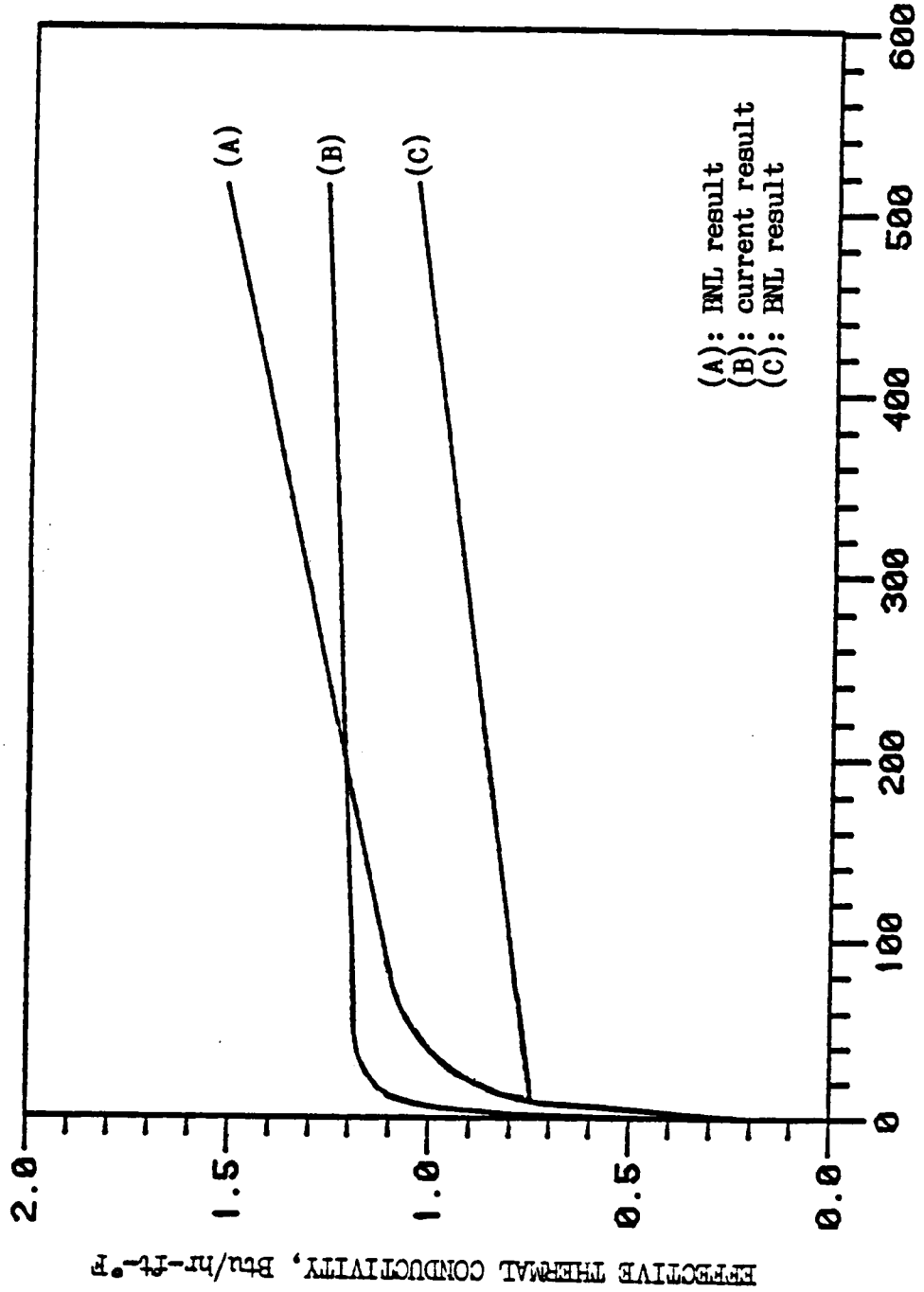

Figure 20. Comparison of the results of the thermal conductivity of the deactivated FeTi hydride as a function of hydrogen pressure.

The line-source technique employed at BNL uses an experimental method of long ideally thin line heat source imbedded in the tested medium of infinite extent, and the thermal conductivity is calculated by the equation

$$K = \frac{q_c}{4\pi(T_2 - T_1)} \ln \frac{t_2}{t_1} \qquad (42)$$

Here q_c is the constant heat supply in the time interval, $t - t$, calculated by the power supplied to the wire. Minor error in the recordings of the electrical current and voltage could cause appreciably different result. Morever, the high electrical conductivity of the deactivated FeTi hydride makes the well insulation assumption especially difficult to achieve.

On the contrary, the method used in our study permits direct measurement of thermal diffusivity without the difficulties involved in measurement of the quantity of heat transferred. By ultilizing transient heat conditions it is necessary to measure only the change in temperature with time. These measurements can be made with greater precision. In addition, multiple data points are picked up for curve fitting, instead of only the two points used in the line-source technique.

As mentioned early in Chapter 2, better data were needed in Fisher and Watson's simulation model for the hydride bed even without Al-enhancement. As shown in Figure 21, for instance, the temperature peak by their code, indicated by the dashed lines, appear at a delayed time. If the current result of pressure dependence of K are used in the model, an improvement in the prediction results.

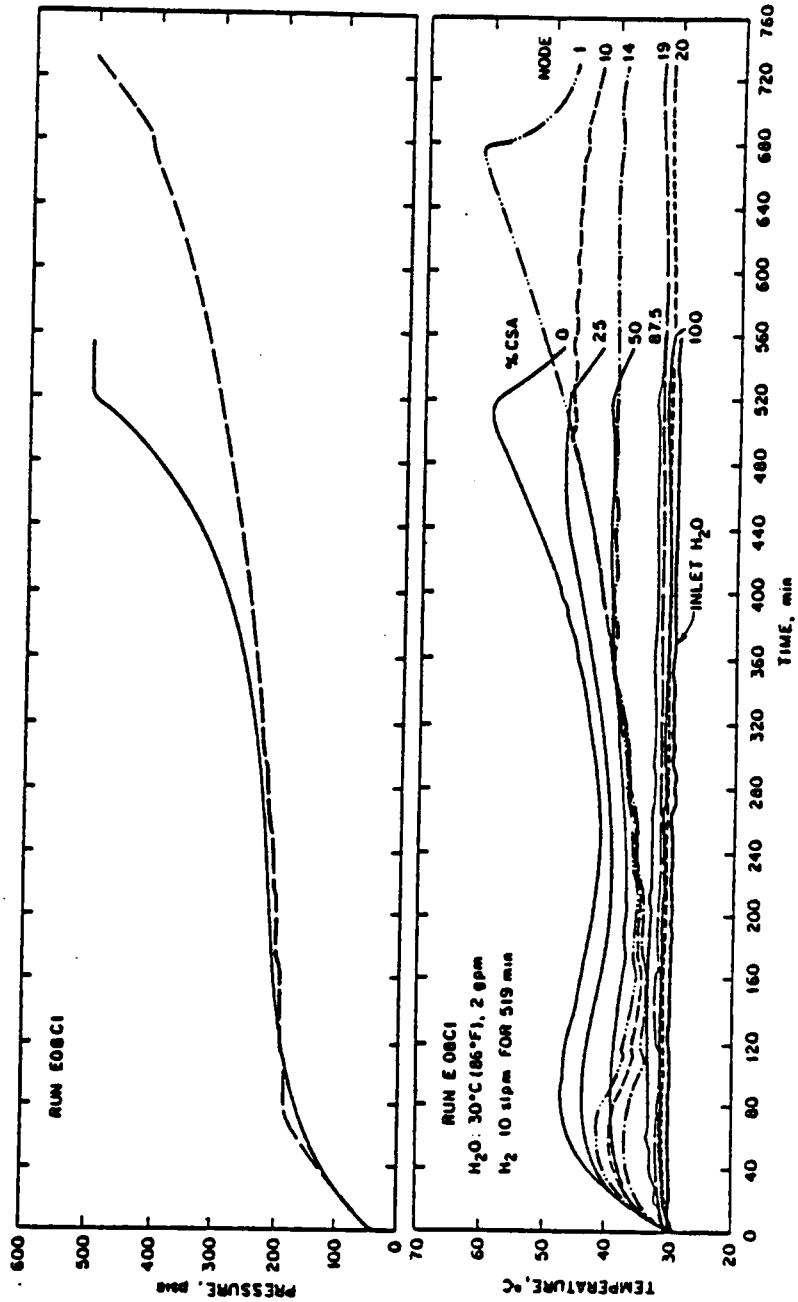

Figure 21. Results of Fisher and Watson's model for a constant hydrogen feed rate of 10 std liters/min. in a hydride bed without Al-enhancement.

4.4 THERMAL CONDUCTIVITY OF THE DEACTIVATED FeTi HYDRIDE FILLED IN Al-FOAM UNDER HYDROGEN

The change of the thermal conductivity of the deactivated FeTi hydride filled in Al-foam with V_a of 9.2 % and a r_m of 1/20", K_{eh}, have been measured with different hydrogen pressures. V_a is the volume fraction of aluminum, and r_m is the radius of the spherical cell. Again, K_{eh} was assumed to be independent of temperature in the range of 30 - 50°C. The results are shown in Figure 22. The thermal conductivities are 1.38 to 1.45 times those of the packing without Al-enhancement (under the basis of the same pressure) over most of the pressure range covered by the measurement, except 1.6 times in the vacuum. Since the void fractions involved in the two kinds of packing differ very little from each other (ε = 0.40396 with enhancement, ε = 0.4191 nonhancement), the increase in the thermal conductivity must come from the addition of 9.2 % volume aluminum. According to the measurements, the statement made in BNL report (22) that "the addition of 5.6 % Al-foam enhances the effective thermal conductivity of a hydride bed at 200 psia by a factor of 2.6" is questionable.

On the other hand, the simple increase in thermal conductivity with the addition of aluminum may mean little. In fact, K_{eh} has never been used in the modeling calcultion in which K_e is used for aluminum part and K_h for the part of FeTi hydride plus hydrogen. We will show later by modeling results that the addition of aluminum in the form of reticulated open-cell structure does enhance the hydrogen loading/unloading rate considerably if the cells are made small enough (i.e., r_m = 1/20"). In other words, the heat transfer improvement is

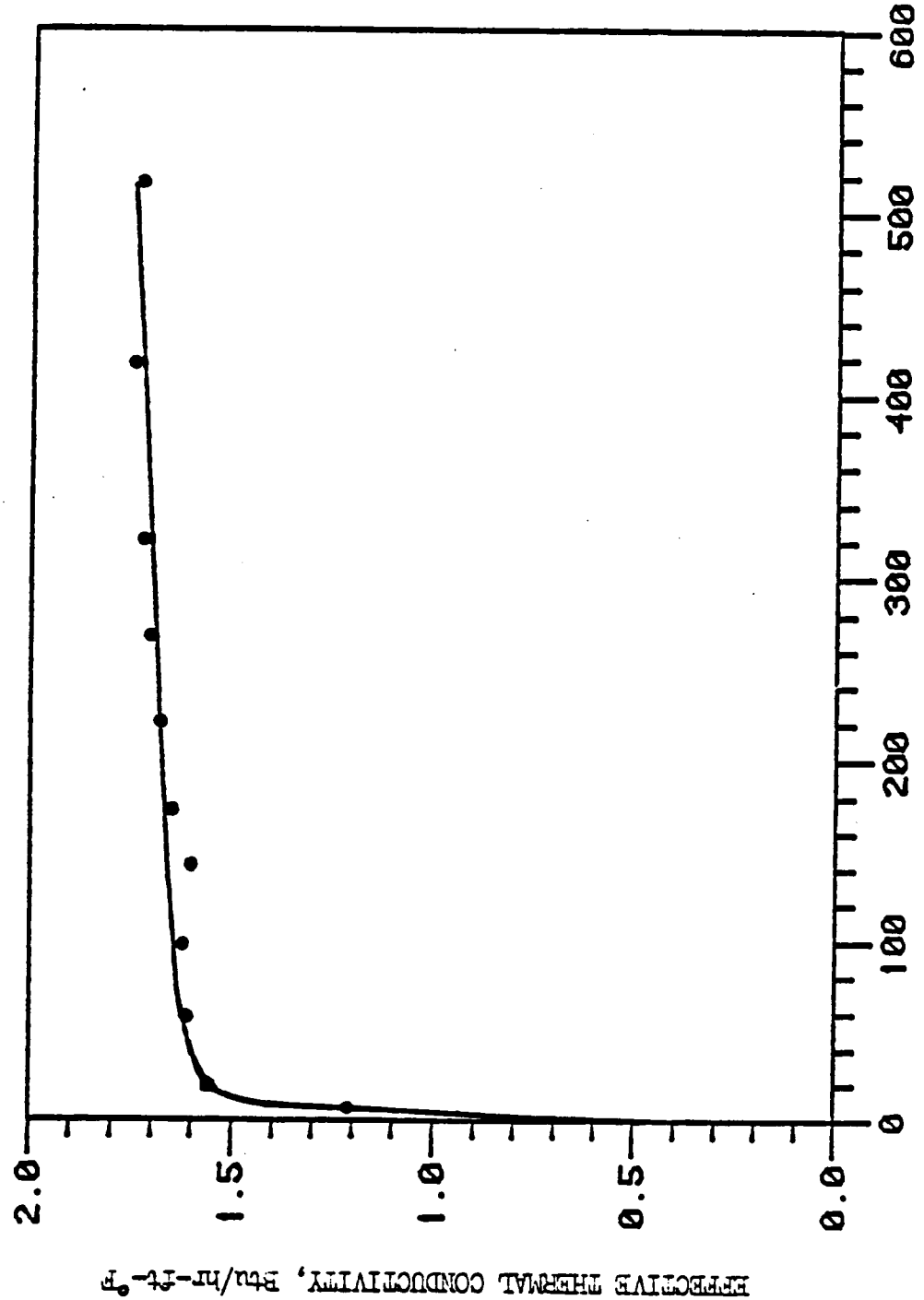

Figure 22. Thermal conductivity of the deactivated FeTi hydride in Al-foam (r_m = 1/20", V_s = 9.2 %) as a function of hydrogen pressure.

achieved by the form of the enhancement material as well as by the increased overall thermal conductivity.

CHAPTER 5

MATHEMATICAL MODELING

Several simplifying assumptions are needed to develop useful models for the systems of interests.

1. The holes in the Al-foam (regions of FeTi hydride powder) are assumed to be spherical, regularly packed, uniform in size. They are assumed to be independent of each other, but, of course, hydrogen must communicate between.
2. The surface temperature of each spherical region is uniform, but the temperature could vary with position in the matrix and with time.
3. There are two kinds of temperature gradients:
   a. within aluminum matrix, variation with cylindrical radial direction.
   b. within the FeTi hydride region, variation in the spherical radial direction.
4. The reaction rate is controlled by heat transfer rates. Hydrogen diffuses through the FeTi hydride fast enough that uniform pressure exists within each FeTi hydride cell and along the vessel radial direction.
5. Hydrogen is always in local equilibrium with the metal hydride.
6. Heat transfer occurs only in the radial direction of the spherical FeTi hydride cells and in the radial direction of the cylindrical vessel.

5.1 MATHEMATICAL MODELING

The mathematical description of the Al-enhanced hydride bed as defined in Figure 10, page 25 is quite complex. The processes occurring involve unsteady state conduction and reaction in the spherical cell, and conduction in the aluminum part of the bed. For the assumptions stated previously, the governing differential equations are, for the hydride in each single spherical cell

$$\frac{1}{r}\frac{d}{dr}\left(K_h r \frac{dT}{dr}\right) - \Delta H(1-\varepsilon)\frac{dC'}{dt} = \rho C_p \frac{dT}{dt} \tag{43}$$

and for the Al part in the cylindrical bed

$$K_a \frac{d}{dR}\left(A_c \frac{dD}{dR}\right) + Q' = \rho_a C_{pa} A_c \frac{dD}{dt} \tag{44}$$

Equations (43) and (44) are solved simultaneously subject to the following boundary conditions

$$\frac{dT}{dr} = 0 \qquad \text{at } r = 0 \tag{45}$$

$$T = D \qquad \text{at } r = r_m \tag{46}$$

$$K_{ss}\frac{dT_s}{dR} = h(T_{ss} - T_w) \qquad \text{at } R = R_{ss}$$

$$K_h A_h \frac{dT}{dr} = q \qquad \text{at } r = r_m \tag{48}$$

and

$$Nq = Q' \tag{49}$$

The initial conditions depend upon the reaction (loading or unloading). And

K_h = effective thermal conductivity of the hydride packing, Btu/hr-ft-°F;

K_a = thermal conductivity of aluminum, Btu/hr-ft-°F;

K_{ss} = thermal conductivity of wall material, Btu/hr-ft-°F;

h = heat transfer coefficient, Btu/hr-ft -°F;

r = radial coordinate on sphere, ft;

R = radial coordinate in cylinder, ft;

r_m = radius of sphere, ft;

R_{ss} = radius of the outside wall of the bed, ft;

ΔH = heat of reaction, Btu/lb H_2;

ε = void fraction in the hydride packing;

ρ = bulk density of the hydride packing, lb/ft^3;

C_p = average specific heat of the hydride packing, Btu/lb-°R;

ρ_a = density of aluminum, lb/ft^3;

C_{pa} = heat capacity of aluminum, Btu/lb-°R;

A_h = surface of sphere, ft^2;

A_c = "effective" surface for conduction via Al

$= 2\pi LRV_a$, ft^2;

L = length of the hydride bed, ft;

V_a = volume fraction of aluminum;

C' = hydrogen composition in hydride packing, lb/ft^3;

T = hydride temperature, °R;

D = aluminum temperature, °R;

T_w = average temperature of water, °R;

T_s = wall temperature, °R;

T_{ss} = outside wall temperature, °R;

N = number of spheres per unit length of cylindrical radius, ft^{-1};

t = time, hr.

The solutions for temperatures and compositions from these equations are sought by the method of finite difference with the aid of the DECsystem-10 computer, UTCC. For this complicated problem, the calculation is very time consuming, even when the space interval is taken reasonably large. The detailed derivation of the difference equations will be found in Appendix A. The resulting equations are listed in the following section for computer implementation.

5.2 COMPUTER IMPLEMENTATION OF THE MODEL

(A). Equations Involved In Spherical System With Node Number = m On Sphere Radius

The following equations are resulted from the approximation of the Equation (43) by "finite difference" approach. In other words, they are from the mass and energy balances for each spherical shell bounded by the appropriate boundaries. The subsript "i" refers to the cylindrical subvolume in which the sphere is located, and "j" the j-th node in the sphere, counting outwards from the sphere center which is assigned as the first node.

Equations	No. of equations

(a). $2 \leqslant j \leqslant m - 3$

$$\delta\frac{3(r_j^2 - \Delta r/2)^2}{3r_j^2 + (\Delta r/2)^2} T_{i,j-1} - \left\{1 + \frac{6\delta[r_j^2 + (\Delta r/2)^2]}{3r_j^2 + (\Delta r/2)^2}\right\}T_{i,j}$$

$$+ \delta\frac{3(r_j + \Delta r/2)^2}{3r_j^2 + (\Delta r/2)^2} T_{i,j+1} - \Phi C_{i,j} + T^*_{i,j} + \Phi C^*_{i,j} = 0 \qquad m - 4$$

(b). $T_{i,1} - T_{i,2} = 0$ 1

(c). $C_{i,1} - C_{i,2} = 0$ 1

(d). $j = m - 2$

$$\delta\frac{3(r_j - \Delta r/2)^2}{3r_j^2 + (\Delta r/2)^2} T_{i,j+1} - \left\{1 + \delta\frac{7r_j^2 + r_j\Delta r + 7(\Delta r/2)^2}{3r_j^2 + (\Delta r/2)^2}\right\}T_{i,j}$$

$$+ \delta\frac{4(r_j + \Delta r/2)^2}{3r_j^2 + (\Delta r/2)^2} T_{i,j+1} - \Phi C_{i,j} + T^*_{i,j} + \Phi C^*_{i,j} = 0 \qquad 1$$

(e). $j = m - 1$

$$\frac{4\delta\Delta r(r_m - \Delta r/2)^2}{r_m^3 - (r_m - \Delta r/2)^3} T_{i,m-2} - \left\{1 + \frac{4\delta\Delta r[4r_m^2 - r_m\Delta r + (\Delta r/2)^2]}{r_m^3 - (r_m - \Delta r/2)^3}\right\}T_{i,m-1}$$

$$+ \frac{12\delta\Delta r r_m D_i}{r_m^3 - (r_m - \Delta r/2)^3} - \Phi C_{i,m-1} + T^*_{i,m-1} + \Phi C^*_{i,m-1} = 0 \qquad \text{†) } \frac{1}{m}$$

where δ and Φ are defined in Appendix A

For convenience of coding the computer, all unknowns are represented by the dimensional variables X(k), i.e.,

$T_{i,j}$	X(k)
$T_{i,1}$	X(1)
$T_{i,2}$	X(2)
⋮	⋮
$T_{i,m-2}$	X(m-2)
$T_{i,m-1}$	X(m-1)

$C_{i,j}$	X(k)
$C_{i,1}$	X(m)
$C_{i,2}$	X(m+1)
⋮	⋮
$C_{i,m-2}$	X(2m-3)
$C_{i,m-1}$	X(2m-2)

Total number of unknowns = 2m - 2

Since there are (m - 2) additional equations which correspond to the equilibrium relationships existing at the second node through to the (m - 1)th node according to the basic assumptions, the total number of equations is thus equal to the number of unknowns. The spherical system is then mathematically consistent.

(B). Equations Involved In The Whole Cylindrical System With Node Number = p On Cylinder Radius

Similarly, the "finite difference" approach to Equation (44) results in the following equations (a)-(c) for the whole cylindrical system, while the equation (d) comes from the boundary condition at vessel wall. The nodes are counted outwards too, with the first node on the outside radius of PMT.

Equations	No. of equations
(a). $n_1 q_1 \Delta t - K_a 2\pi(R_1 + \Delta R/2)LV_a(D_1 - D_1^*)\Delta t/\Delta R - \pi\Delta R(R_1 + \Delta R/4)LV_a\rho_a C_{pa}(D_1 - D_1^*) = 0$	1
(b). $2 \leqslant i \leqslant p - 1$ $n_i q_i \Delta t + K_a 2\pi(R_i - \Delta R/2)V_a L(D_{i-1} - D_i^*)\Delta t/\Delta R - K_a 2\pi(R + \Delta R/2)V_a L(D_i - D_{i+1}^*)\Delta t/\Delta R - 2\pi R\,\Delta R L V_a \rho_a C_{pa}(D_i - D_i^*) = 0$	p - 2
(c). $n_p q_p \Delta t + K_a 2\pi(R_p - \Delta R/2)LV_a(D_{p-1} - D_p^*)\Delta t/\Delta R - 2\pi h R_{ss} L(T_{ss} - T_w)\Delta t - \pi\Delta R(R_p - \Delta R/4)LV_a\rho_a C_{pa}(D_p - D_p^*) = 0$	1
(d). $T_{ss} - \frac{K_{ss} D_p + T_w h R_{ss} \ln(R_{ss}/R_p)}{K_{ss} + h R_{ss} \ln(R_{ss}/R_p)} = 0$	+) 1 p + 1

As is the spherical case, the unknowns are listed in terms of the dimensional variables Y(L)

D_1	D_1	$D_2 \cdots D_{p-1}$	D_p	T_{ss}
Y(L)	Y(1)	Y(2)···Y(p-1)	Y(p)	Y(p+1)

It is obviously that the number of unknowns is the same as the number of equations; the cylindrical system is also mathematical consistent.

(C). Solution Algorithm

All the equations involved in the model are linear except the equilibrium relationships. Their nonlinearity makes the solution of the simultaneous equations difficult and complex. The Nelder and Meed searching technique (39), originally devised by Spendley, Hext and Himsworth (40) in connection with the statistical design of experiments, has been used in the current mathematical system.

The algorithm of this so-called "sequential Simplex method" can be briefly described as follows (41). For a search process involving two variables, three points are selected fairly close together in such a manner that they form the vertices of an equilateral triangle as in the Figure 23.

Let these be points 1, 2, and 3. Following this, three further points (4, 4' and 4") are selected such that each one forms an equilateral triange with any two of the first three points. If the response surface is locally a plane or nearly so, one of the possible

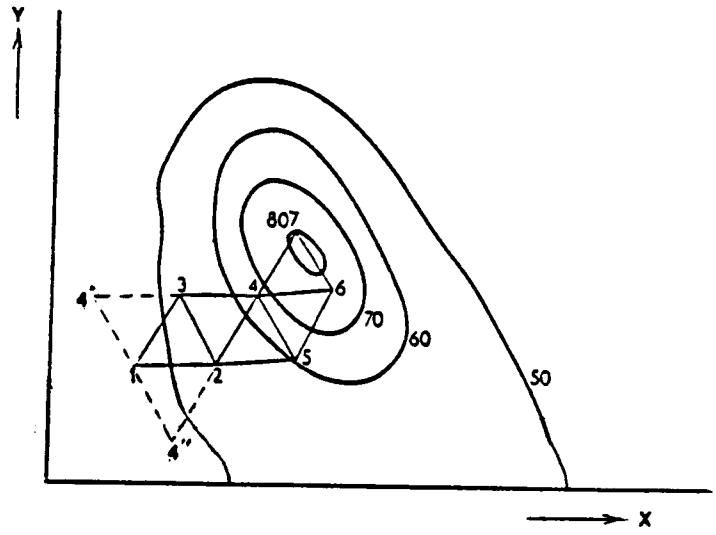

Figure 23. The sequential simplex method of optimization.

new points will give a higher (lower if searching for minimum) result than the other two, and furthermore the point 4 will be a "mirror image" to the lowest point in the first triangle. Hence, after the first three trials the point giving the lowest result is neglected and replaced by the mirror image point forming the second triangle, as shown in Figure 24. This construction process is repeated until the summit is reached. Thus as long as the surface is sloping and approximate plane over the area of a particular triangle, each step in the construction leads to a more favourable region, and the path taken from the starting will zig-zag about the line of steepest assent.

For a system containing more than two variables, the procedure will be similar except that (n + 1) trial points will be made, where n is the number of variables. The most favourable of these points is retained to replace the appropriate member of the original set, thus completing a move towards the optimum. The (n + 1) points correspond to the vertices of a regular simplex in n dimensions. In a modification of the procedure by Nedler and Mead, the simplex is permitted to alter the shape and no longer stays a regular simplex. It is thus called "flexible polyhedron searching technique."

The present mathematical equations can be written in a more condensed form,

$$F(X) = (f_1(X), f_2(X), \cdots f_n(X)) = 0 \qquad (50)$$

where $X = (x_1, x_2, \cdots x_n)$, are the unknowns

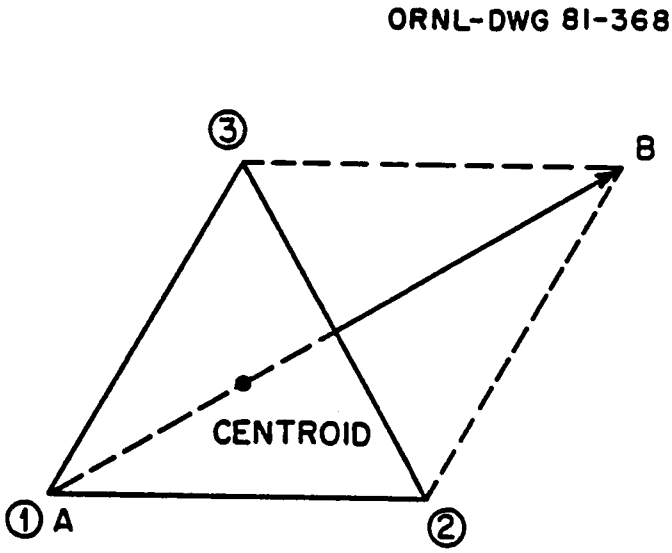

Figure 24. Regular simplex for two variables. The arrow points in the direction of greatest improvement.

The search is terminated when

$$\left\{\frac{1}{n+1}\sum_{i=1}^{n+1}\left[F(X_i) - F(X_{n+2})\right]^2\right\}^{1/2} \leq \xi \qquad (51)$$

where ξ is an arbitrary small number (say 0.005), and $F(X_{n+2})$ is the value of the objective function F(X) at the centroid X_{n+2} (42).

The number of equations, n, depends on how the space interval is chosen. The smaller the space interval selected, the more equations will be produced and thus the more accurate the computation result. However, more equations mean more variables, and, needless to say, the amount of the computer resources (execution time, data transfer time, and memory storage space) used in a single step will be increased.

(D). Calculation Flowsheet

The simplified flow diagram for the computer program used to evaluate model prediction is shown in Figure 25. The detailed computer programs are attached in the Appendix B.

5.3 CALCULATION RESULTS

the mathematical model has been described in the first section of this chapter, and details are given in Appendix A. The model is designed to facilitate solution of the dynamic problem formulated in terms of differential equations. It employs a numerical method with "backward difference" approximation, each variable at time level $t + \Delta t$ is solved from the known values at time t. Since the solution technique involves a large number of events (temperatures and compositions at each node) during the simulated time, fixed time step mode has been used (43), where simulation time is advanced by a fixed increment Δt. T must

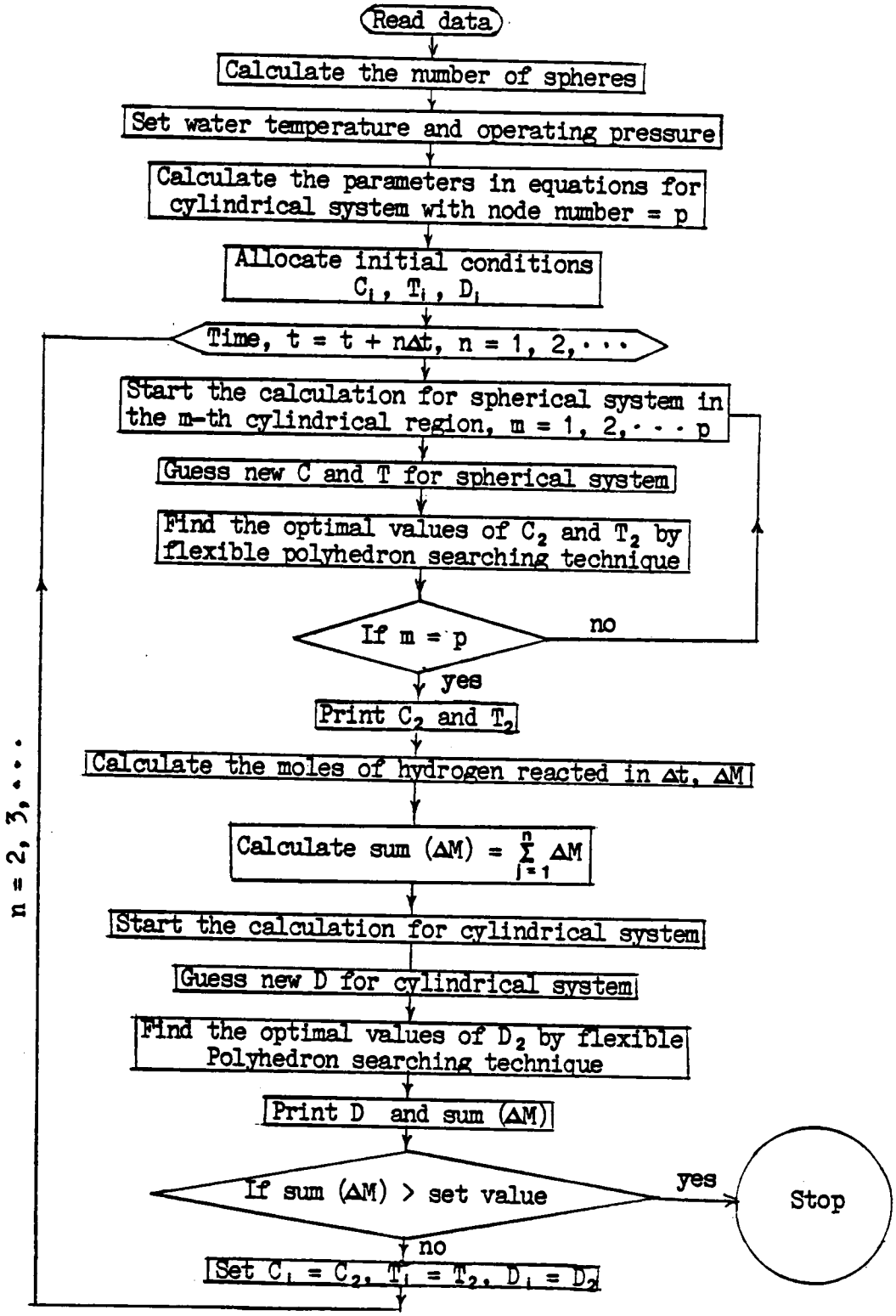

Figure 25. Flowsheet for program used to calculate model prediction.

be selected properly; it must be sufficiently large to save computing time and cost, but not too large to cause the appearance of instabiltity or unacceptable error. The maximum usable time increment is strongly related to Δr, the space interval chosen for the spherical system. For small sized open-cells in the Al-foam, the code could take hours even for calculation of prediction for the early stage of reaction.

As mentioned previouly, the proposed hydride bed is basically similar to that constructed at BNL. The bed dimension, wall material, the circulation rate of water in jacket, etc. can be found from the BNL report (25).

In the following pages some calculation results will be presented. These serve to illustrate use of the model without requiring excessive computer time. For detailed designed purposes, longer computer run time would be acceptable.

(A). Sample Calculations

A sample calculation for a certain reaction is demonstrated here. It is a desorption reaction, the operating conditions are:

Initial Conditions:

$$C_i = (H/M)$$

$$= 0.8$$

$$T_i = 582^\circ R$$

$$P_i = 422.5 \text{ psia}$$

The average temperature of the water flowing in the jacket is

$$T_w = 582^\circ R$$

The constant operating pressure is

$$P_s = 19 \text{ psia}$$

The radius of sphere (spherical cell) is

$$r_m = 1/3"$$

Figure 26 and Figure 27 show the temperature and compostion histories of three outer nodes in the spheres. These spheres are located in the inner, central and outer cylinder regions respectively, and each node is $(1/4)\Delta r$ away from the surface of the sphere. The complicated shape of the temperature curve can be explained by comparing it with the compostion curve. At the very beginning of the reaction, the temperature everywhere drops instantaneously from 582°R to 463°R because the entire bed is releasing hydrogen, and heat is absorbed relatively uniform throughout the bed to supply heat needed for desorption reaction. Then the temperature of the node in the sphere located in the outer cylindrical region (adjacent to the wall), indicated by Line (A) in Figure 26, begins to ascend to a point where the corresponding compostion is C = 0.5. Beyond this point, the temperature of that node remains actually constant for a period of time while the node crosses the plateau region of the equilibrium P-T-C relationship. After passing through the whole plateau region, the temperature of the node ascends again.

As seen in Figure 26, for the first period of 2000 seconds the heat conducted from the wall is nearly consumed in the outer cylindrical region. After that, the node in the sphere which is in the outer cylindrical region approaches complete unloading; and the heat transfer zone, together with the reaction zone, starts to move inwards. This is indicated by the Line (B) in Figure 26 and Figure 27.

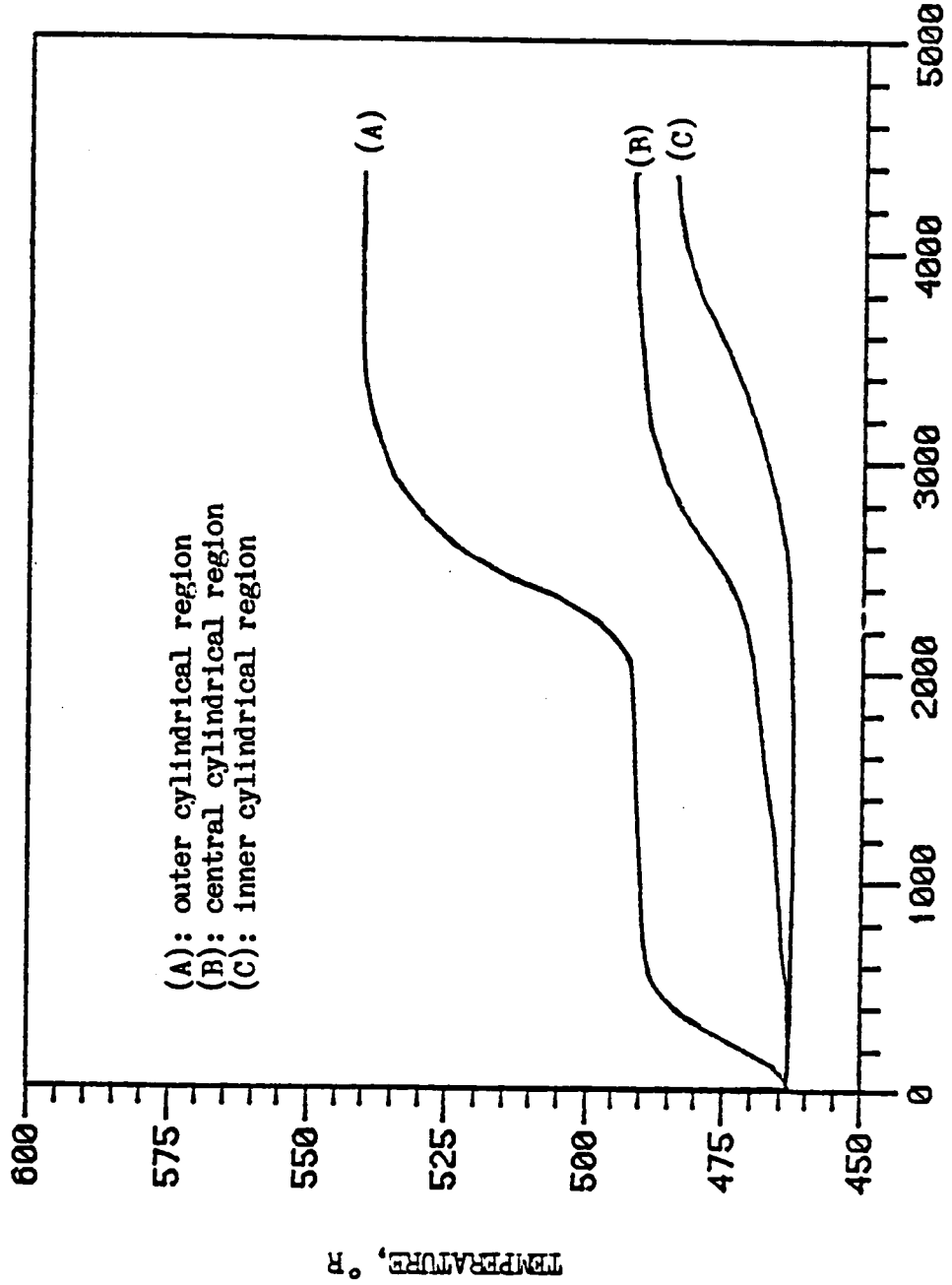

Figure 26. Temperature histories of three outer nodes in the spheres located in the outer, central and inner cylindrical regions respectively during desorption for r_m = 1/3" and V_a = 9.2 %.

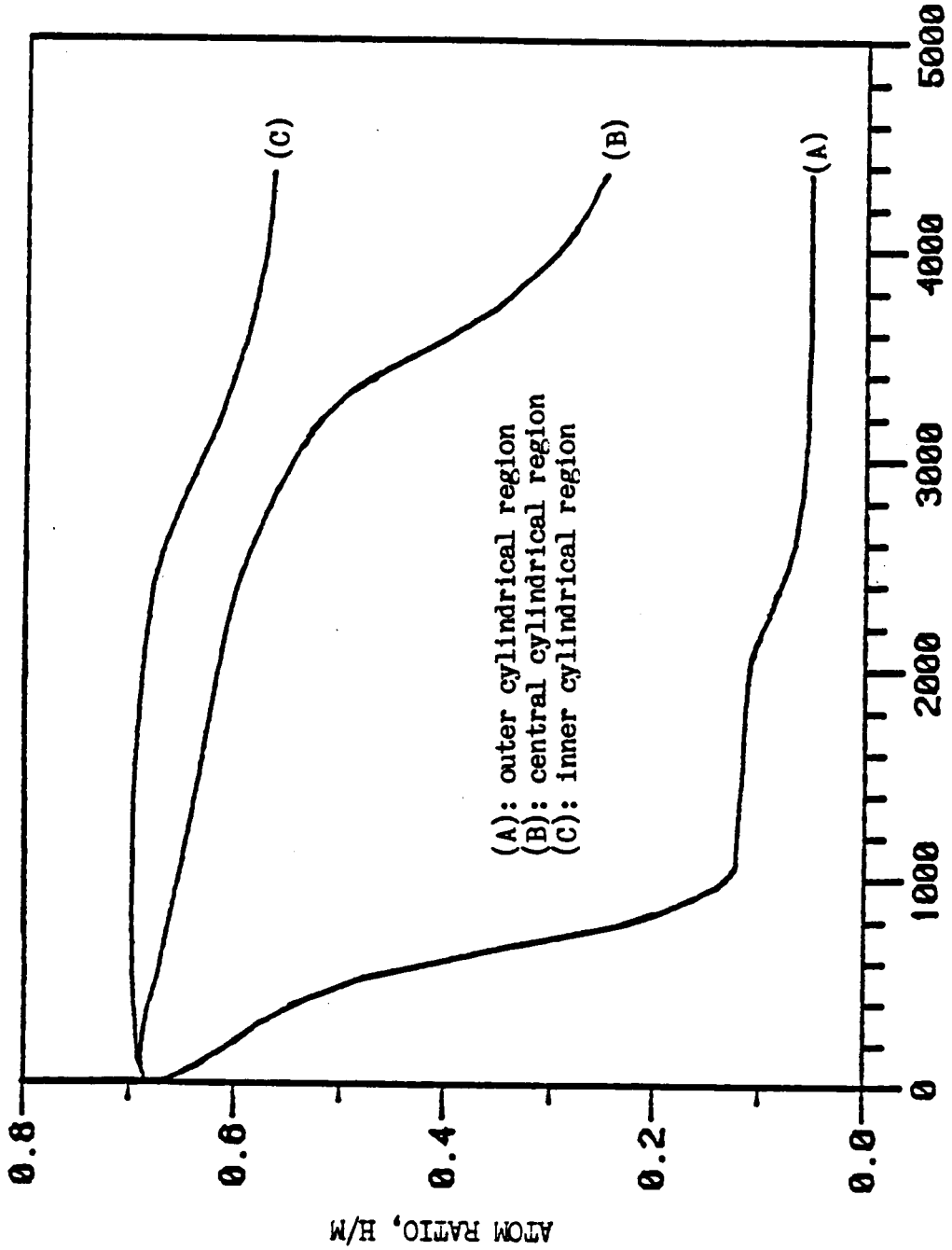

Figure 27. Composition histories of three outer nodes in the spheres located in the outer, central and inner cylindrical regions respectively during desorption for r_m = 1/3" and V_s = 9.2 %.

Figure 28 are also the composition - time curves of two nodes, but these nodes are located in a sphere in the outer cylindrical region. Line (A) represents for the composition change of the center node of the sphere, while Line (B) is for the outer node of that sphere ($\Delta r/4$ away from the surface of the sphere). Corresponding to Figure 28, the temperature histories of those two nodess are shown in Figure 29.

The Figure 28 shows that since the outer node receives more heat from the surrounding aluminum, it experiences a more rapid change of composition. At the moment indicated by the Line p-p the composition potential between the outer node and the central node drives the heat inwards. As a consequence, the desorption rate of the outer node starts to slow. In contrast, that of the center node accelerates.

Since both nodes cross the plateau regions of different isotherms, small temperature differences exist between them until the reactions in both nodes come to the end. Both temperatures then come together as indicated in Figure 29.

However, if the sphere size is much small, i.e., r_m = 1/20", both lines in Figure 28 and 29 are actually very close to each other. In this case, the temperature and composition in a sphere become uniform.

Figure 30 are the temperature histories of four other points. All lines present the changes of the temperature of aluminum in different cylindrical regions, except Line (A) which is for the point on the outside wall. It is easy to understand that Line (B), (C) and (D) are merely the same as those presented in Figure 26, because in the same cylindrical region, the aluminum temperature is same as the temperature on the spherical surface. Since there is little heat transfer

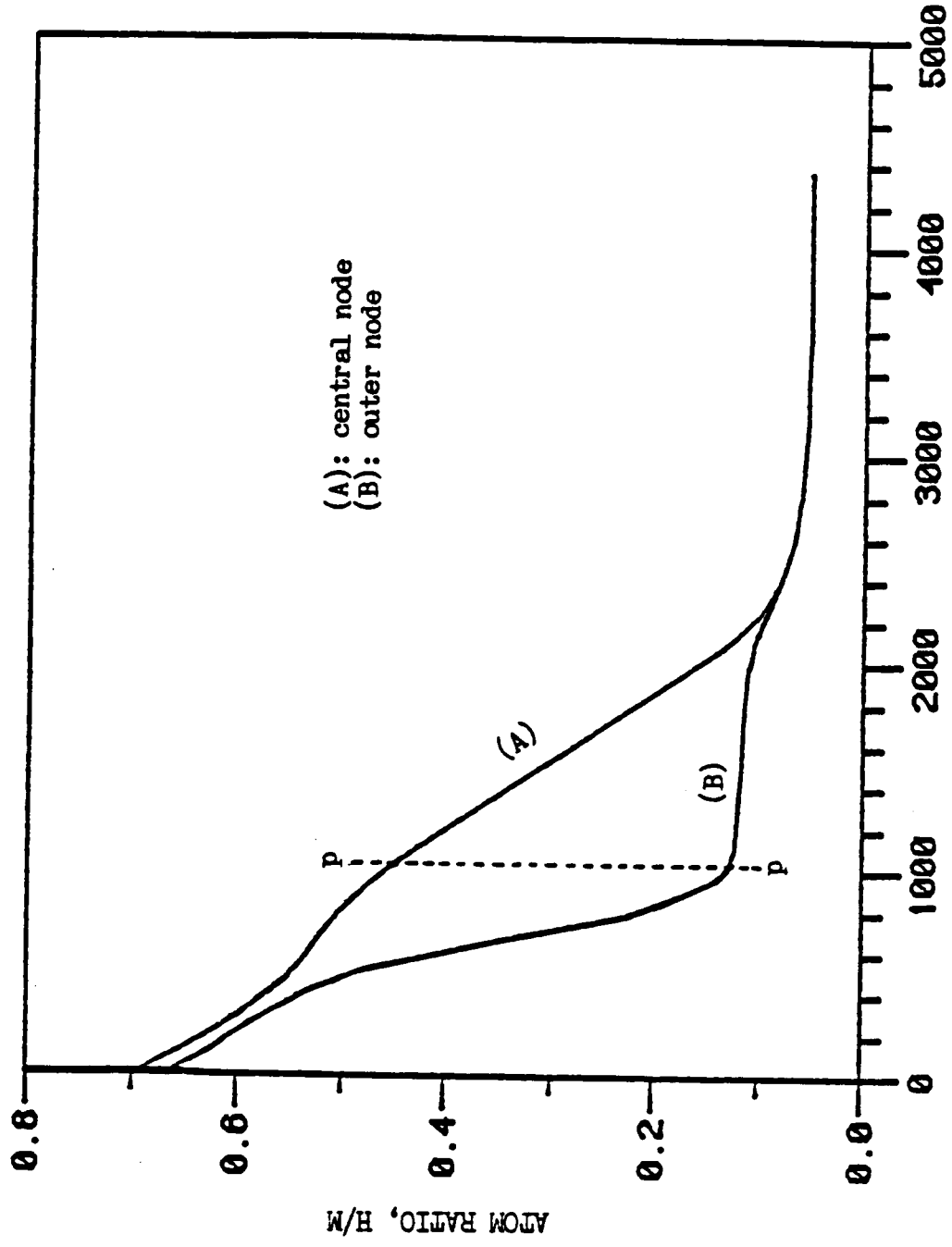

Figure 28. Composition changes with time of two nodes in the sphere located in the outer cylindrical region during desorption for r_m = 1/3" and V_s = 9.2 %.

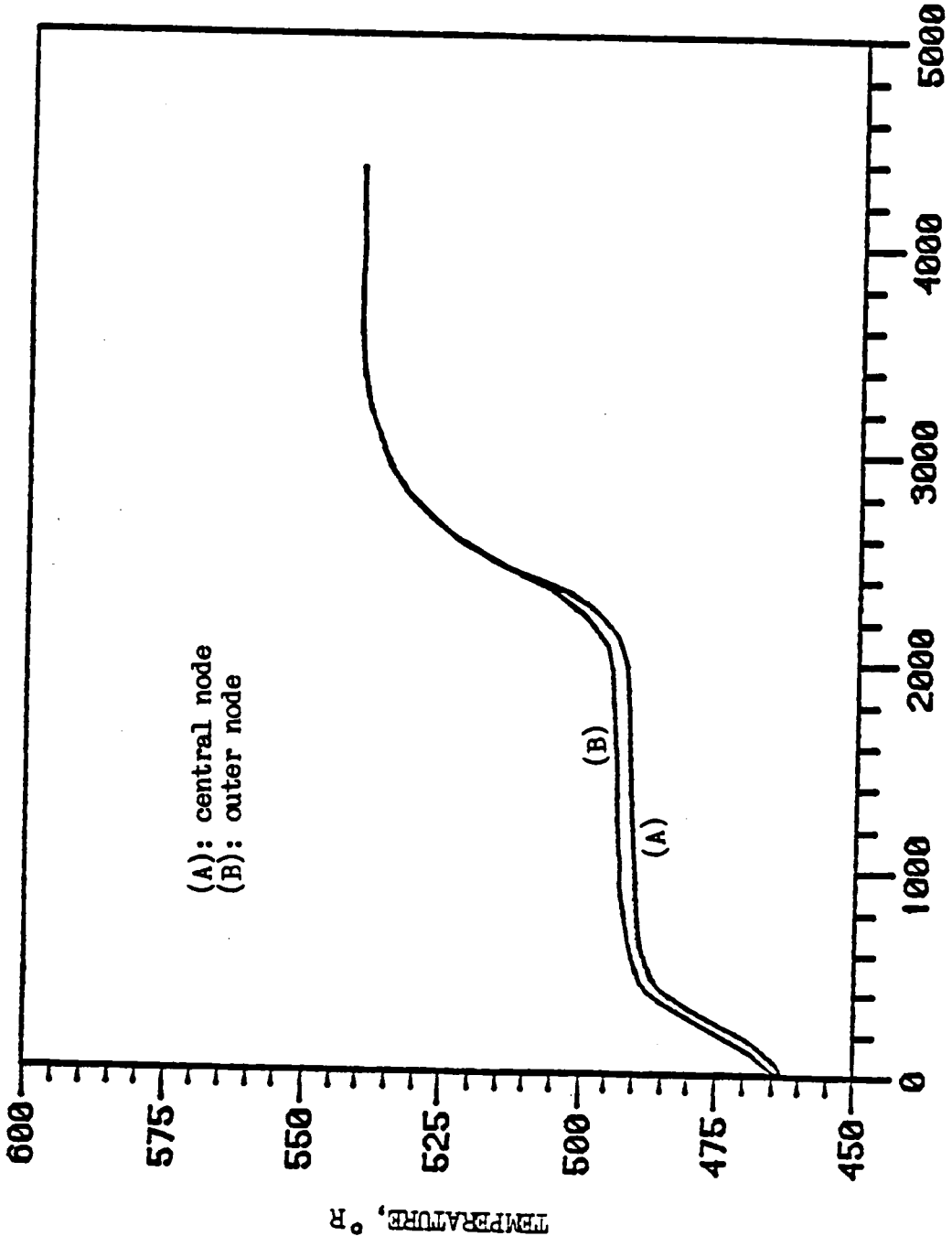

Figure 29. Temperature histories of two nodes in the sphere located in the outer cylindrical region during desorption for r_m = 1/3" and V_s = 9.2 %.

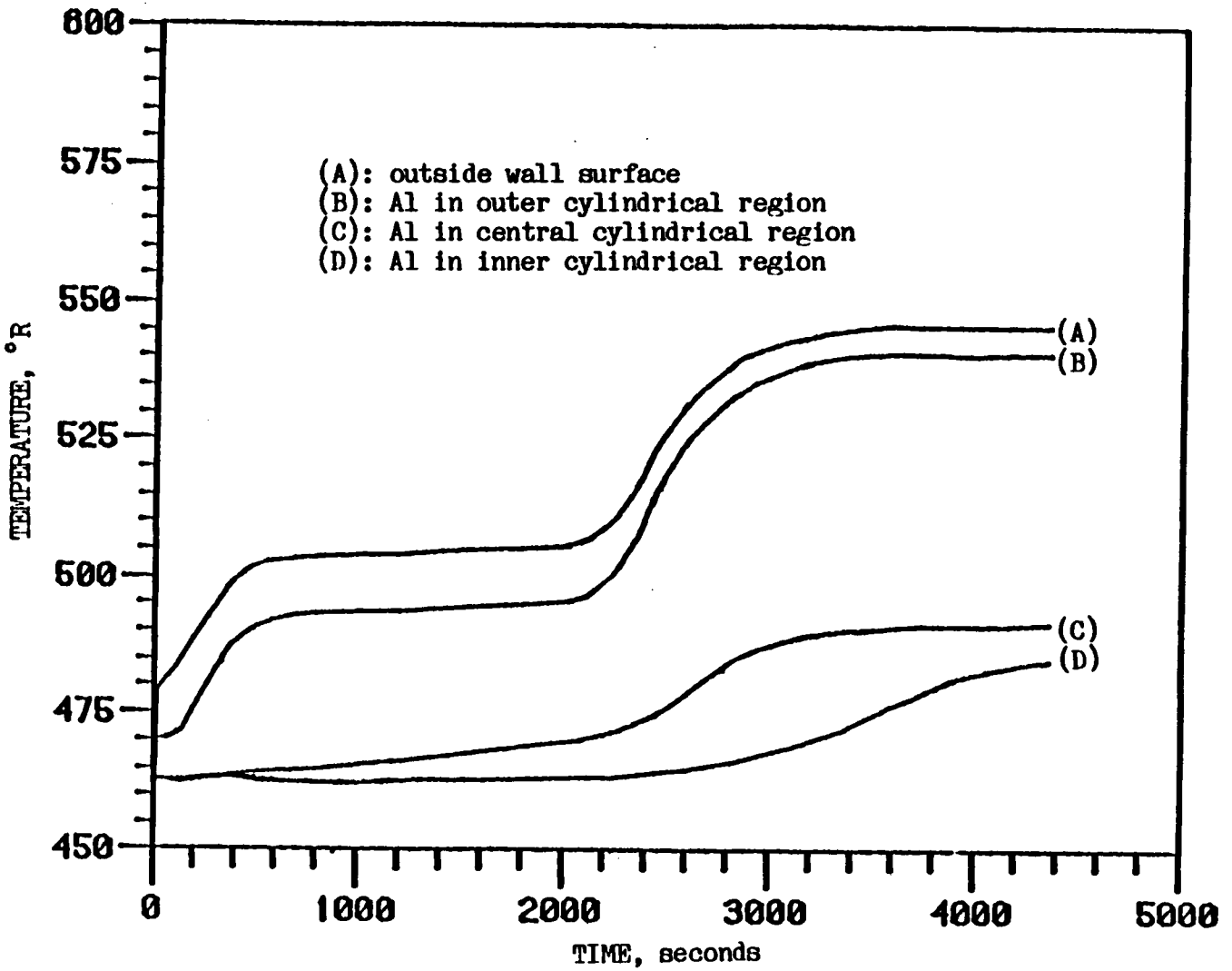

Figure 30. Temperature histories of four points in the cylindrical direction of vessel during desorption for r_m = 1/3" and V_a = 9.2 %.

resistance through the vessel wall, the Line (A) and (B) are similar. Heat of reaction and finite heat transfer resistance between the two points, however, result in the minor variation of their difference with time.

(B). Effect Of The Content Of Aluminum On Reaction

Figure 31 shows the absorptions for sphere of radius 1/10" and the content of aluminum, V_a, of (A) 5.6 % and (B) 9.2 %. During the constant pressure process, the rate of hydrogen absorption is highest at the beginning of the reaction due to the initial "cool" bed. In other words, the initial period is affected more by the heat capacity of the bed than by thermal conductivity. After that, the temperature everywhere in the bed is increased because the reaction heat envolved can not be conducted outwards efficiently. According to the principle of Le Chatlier, the reaction everywhere starts to slow except at the region adjacent to the wall. This is why there is a period of smaller changes after the initial large raise in the Curve (A) in Figure 31. The curve begins to ascend again when the reaction zone starts to move inwards.

Before the time indicated by Line m-m, both beds basically experience a heat capacity-dominated hydrogen absorption process, and the hydrogen absorbed in bed (B) is certainly less than that in bed (A) because the interstitial volume contained in hydride available for loading with hydrogen is less. After that time, however, the aluminum conduction starts to effect the loading rate. The greater aluminum content in bed (B) makes the loading occur with a higher rate than that in bed (A). Until the moment indicated by Line n-n, the hydrogen

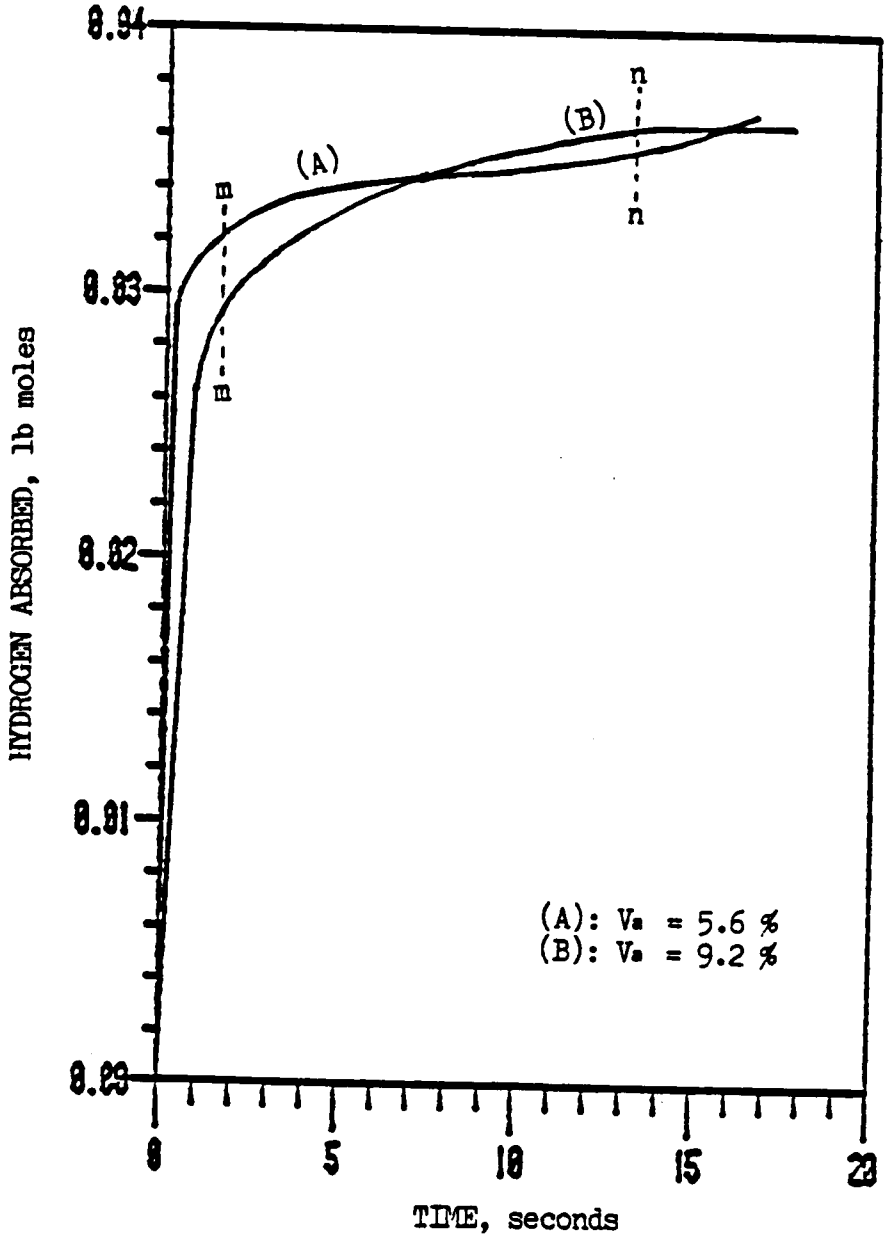

Figure 31. The effect of the content of aluminum on the absorption for r_m = 1/10".

absorbed in bed (B) is even more than in bed (B). After still longer time, the curves become even more complicated. Figure 31 shows the curves crossing again after approximately 16 seconds. This is believed to be an artifact created by the large space size used in the finite difference calculations. For longer periods of time, the higher conductivity of the 9.2 % Al bed should give higher hydrogen loading rate, until the beds are near saturation.

(C). Effect Of The Sphere Size On Reaction

Figure 32 shows the predicted absorption reactions for the content of 9.2 volume % aluminum. The radius of sphere is 1/10" in Curve (A) and 1/3" in Curve (B). Since the thermal conductivity of aluminum is very high (K_a = 137.02 Btu/hr-ft-°F at 27°C), the importance of sphere size is to be expected. As indicated in Figure 32, it is apparently that the smaller the sphere size, the faster the hydrogen loading/or unloading rate expected. In fact, the increase in rate caused by reducing the sphere size is so high, one may believe that for the heat enhanced bed of small spherical cells, the heat transfer resistance may no longer be the controlling factor.

(D). The Performance Comparison

Figure 33 shows the desorptions in two kinds of bed. Curve (A) is the prediction by using the new measured K_h in Fisher and Watson's code, for the bed without Al-foam and the initial bed loading m_i = 1.698 lb. H_2. Curve (B) is for the bed with Al-foam, V_a = 9.2 %, r_m = 1/3" and m_i = 1.429 lb.H_2, simulated by the current model. They are for the same initial and operating conditions. As expected, the bed (A) which has

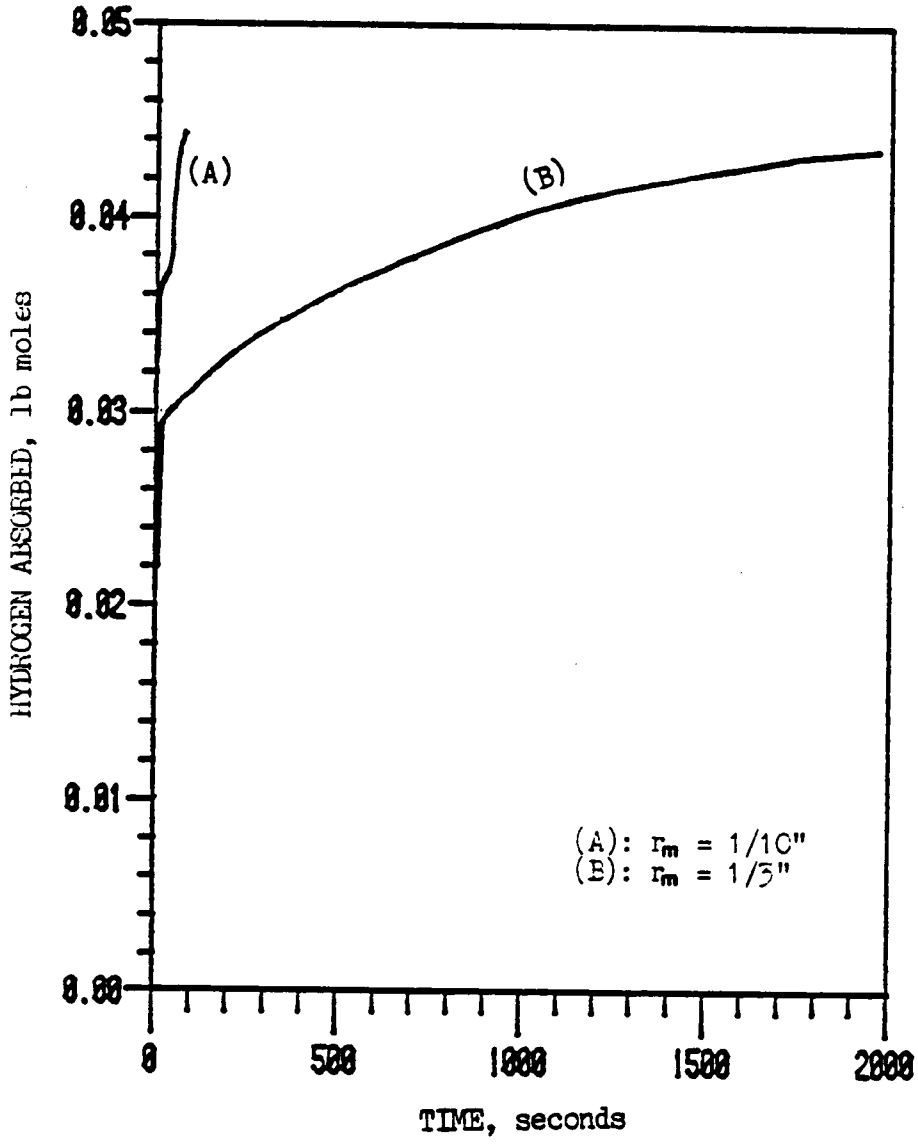

Figure 32. The effect of the sphere size on the absorption for V_a = 9.2 %.

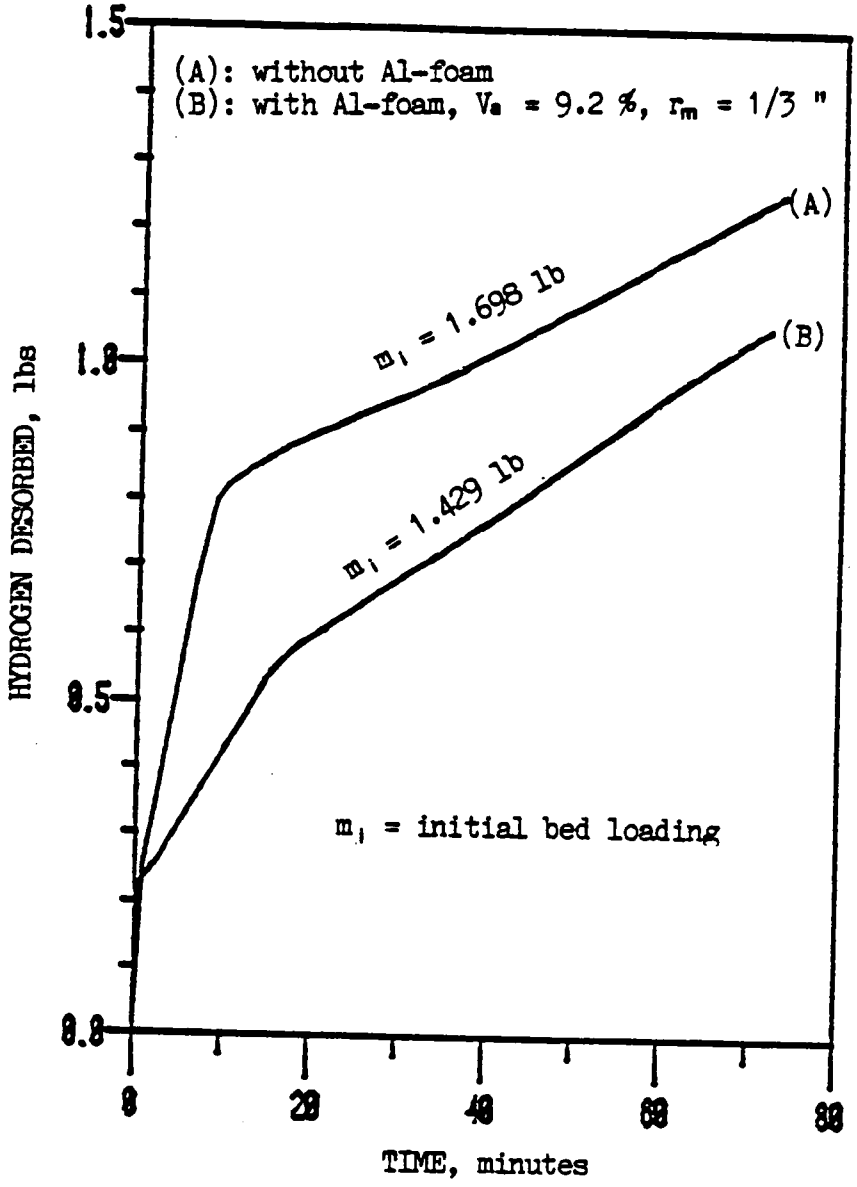

Figure 33. The performance comparison, (A) without Al-foam, predicted by Fisher and Watson's code, (B) with Al-foam, V_a = 9.2 %, r_m = 1/3", predicted by the current code.

more initial loading (i.e., less aluminum and more hydride) also releases more hydrogen at the early step of reaction. The reason has been discussed before. But after that short period of time, the desorption rate, expressed by the slope of the curve, of the bed (B) is always slightly higher than that of the bed (A), even the bed (B) carries less hydride.

Therefore, the addition of Al-foam does benefit the reaction, but not much for this case, r_m = 1/3". In fact, if the sphere size is reduced from r_m = 1/3" to r_m = 1/20", as the sample used in the measurement of the thermal conductivity, K_{eh}, a much greater improvement is expected in the hydrogen loading/or unloading rates.

CHAPTER 6

CONCLUSIONS AND RECOMMENDATIONS

The thermal conductivity of the hydride at the operating pressure of hydrogen is one of the most critical properties for a hydride bed used for hydrogen storage. Earlier data on thermal conductivity of FeTi hydride has been questioned by several investigators. The current experimental results are considered to be more reliable and should be used in model predictions.

Additional experimental studies by using other gases, i.e., helium, nitrogen and argon have not only eliminated the possibility of reaction between hydrogen and FeTi hydride which is not activated in advance; but they also demonstrated that no significant hydriding or dehydriding reaction took place during the experiments. The greatest contribution to the thermal transport is made by the hydrogen gas.

According to the calculation results, the addition of aluminum in the form of reticulated open-cell does benefit the reaction in the hydride bed. The measured thermal conductivity of Al-foam plus FeTi hydride is no more than 1.6 times that of FeTi hydride under same pressure of hydrogen. However the model calculations suggest that the forms of the enhancement material, as well as the increase in the overall thermal conductivity, are important factors. The apparent value of the thermal conductivity of Al-foam plus FeTi hydride under hydrogen gas could actually mean little without also knowing the geometry of the foam-hydride matrix. According to the model study, the smaller the hydride cell size, the faster the hydrogen charging/or discharging rate

expected. However, the amount of the aluminum content will depend upon at least two factors: (1) the expected rate, and (2) the amount of hydrogen to be charged/or discharged. It is recommended that a further study investigate the relation among the above factors and other factors, such as economic considerations for the special application of the hydride.

Our model works and can be used to assess qualitatively the performance of the Al-enhanced hydride bed. In order to predict quantitatively, smaller space interval and thus smaller time step should be used. Of course, that would only involve increasing the overall computing time. The ultimate success of the modeling work now depends upon the accuracy of the knowledge of the kinetics of hydride formaton and decomposition. Since for the Al-enhanced system of small cells, the heat transfer resistance may no longer be the controlling step, the kinetics may need to be considered also.

LIST OF REFERENCES

LIST OF REFERENCES

(1). J. M. Clinch, D. M. Gruen, P. A. Nelson, C. A. Blomquist, J. S. Horowitz, G. J. Lamich and I. Sheft, "The Metal Hydride Chemical Heat Pump,"Proc. Chemical/Hydrogen Energy Systems Contracts Review, Washington, D. C., Nov. 13-14, 1979.

(2). J. J. Reilly and G. D. Sandrock, "Hydrogen Storage in Metal Hydrides,"Scien. Ameri., Vol.242, No.2, 118-129, 1980.

(3). J. J. Reilly and R. H. Wiswall, Jr., "Formation and Properties of Iron Titanium Hydrides,"Inorg. Chem., Vol.13, 218, 1974.

(4). G. D. Sandrock, "A New Family of Hydrogen Storage Alloys Based on the System Nickel - Mischmetal - Calcium," Proc. 12th IECEC, Vol.1, 951, 1977.

(5). K. H. J. Buschow and H. H. Van Mal, "Phase Relations and Hydrogen Absorption in the Lanthanium - Nickel System,"J. Less-Common Metals, Vol.29, 203, 1972.

(6). H. H. Van Mal, K. H. J. Buschow and A. R. Mielema, "Hydrogen Absorption in LaNi and Related Compounds : Experimental Obserations and Their Explanations,"J. Less-Common Metals, Vol.35, 65, 1974.

(7). J. H. N. Van Vucht, F. A. Kuijpers and H. C. A. M. Bruning, "Reversible Room Temperature Absorption of Large Quantities of Hydrogen by Intermetallic Compounds,"Phillips Research Report, 25, 133, 1970.

(8). C. E. Lundin, J. Liu and C. B. Megee, "Development of Hydrogen Storage Material for Application to Energy Needs,"Proc. Chemical/Hydrogen Energy Systems Contracts Review, Washington, D. C., Nov. 27-30, 1978.

(9). J. J. Reilly and R. H. Wiswall, Jr., "Hydrogen Storage and Purification System,"Aug. 1, 1974, BNL 19436.

(10). A. Holt, E. C. Edgar and J. B. Firth, "Z. Physik Chem.,"82, 513, 1913.

(11). C. E. Lundin and F. E. Lynch, "A New Rationale for the Hystersis Effects Observed in Metal Hydrogen Systems,"Proc. International Symposium, 14-19, Geilo, Norway, Aug. 1977.

(12). P. W. Fisher, S. E. Mitchell and J. S. Watson, "Modeling Hydrogen Storage Beds,"Proc. Chemical/Hydrogen Energy Systems Contracts Review, Washington, D. C., Nov. 27-30, 1978.

(13). E. Wicke and K. Otto, "Z. Phys. Chem.,"(Frankfurt am Main), 31, 222, 1962.

(14). P. D. Goodell and G. D. Sandrock, "Metallurgical Studies of Hydrogen Storage Alloy,"Prepared for BNL, Dec. 1979.

(15). P. W. Fisher, Oak Ridge laboratory, private communication, March, 1981.

(16). W. S. Yu, E. Suuberg and C. Waide, "Modeling Studies of Fixed-Bed Metal-Hydride Storage Systems,"Hydrogen Energy Part A, 621-643, T. Nejat Veziroglu, Ed., Plenum Press, 1975.

(17). D. L. Lindner, "Mechanism for the Isothermal Decomposition of Iron Titanium Hydride,"Inorg. Chem., Vol.17, No.12, 1978.

(18). G. D. Sandrock, J. J. Reilly and J. R. Johnson, "Proceedings of the 11-th Intersociety Energy Conversion Engineering Conference AIChE,"Vol.1, 965, 1976.

(19). P. W. Fisher, Oak Ridge Laboratory, private communication, Feb. 1978.

(20). M. A. Pick and H. Wenzl, "Physical Metallurgy of FeTi Hydride and Its Behavior in a Hydorgen Storage Container,"1st World Hydrogen Energy Conference, Miami Beach, Florida, Mar. 1-3, 1976.

(21). R. C. Reid and T. K. Sherwood, "The Properties of Gases and Liquids,"2nd edition, Mcgraw-Hill, New York, Chapter 5, 1966.

(22). M. J. Rosso, Jr. and G. Strickland, "Hydride Beds: Engineering Tests,"Proc. Chemical/Hydrogen Energy System Contracts Review, Washington, D. C., Nov. 13-14, 1979.

(23). D. L. Cummings and G. J. Powers, "The Storage Hydrogen as Metal Hydrides,"Ind. Eng. Chem., Process Des. Develop., Vol.13, No.2, 182-192, 1974.

(24). G. Strickland, J. J. Reilly and R. H. Wiswall, Jr., "An Engineering-Scale Energy Storage Reservoir of Iron Titanium Hydride,"Hydrogen Energy Part A, 611-620, T. Nejat Veziroglu, Ed., Plenum Press, 1975

(25). G. Strickland and W. S. Yu, "Some Rate and Modeling Studies on the Use of Iron-Titanium Hydride as An Energy Medium for Electrical Utility Companies,"Apr. 26, 1977, BNL 50667.

(26). P. W. Fisher and J. S. Watson, "Modeling Solid Hydrogen Beds, July 1979 Progress Report,"submitted to M. J. Rosso , Jr., Brookhaven National Laboratory, Aug. 13, 1979.

(27). P. W. Fisher and J. S. Watson, "Modeling Solid Hydrogen Storage Beds,"Proc. Chemical/Hydrogen Energy System Contracts Review, Washington, D. C., Nov. 13-14, 1979.

(28). A. B. Newman, "Applying Diffusion Calculations to Drying Porous Solids, Chemical and Metallurgical Engineering," Vol.38, No.12, 710, 1931.

(29). E. S. Fitzsimmons, "Thermal Diffusivity of Refractory Oxides,"J. Ameri. Cera. Society, Vol.33, No.11, 327, 1950.

(30). H. S. Carslaw and J. C. Jaeger, "Conduction of Heat in Solids,"Oxford Uni. Press, London, 2nd edition, 199 and 328, 1959.

(31). F. C. W. Olson and O. T. Schultz, "Temperature in Solids During Heating and Cooling. Tables for the Numerical Solution of the Heating Equation,"Ind. Eng. Chem., 34[7], 847-77, 1942; Ceram. Abstracts, 21[9], 196, 1942.

(32). P. W. Fisher, Oak Ridge National Laboratory, private communication, Sept. 1979.

(33). Malcolm Mcguarrie, "Thermal Conductivity: V , Analysis of Variation of Conductivity With Temperature for Al_2O_3, BeO and MgO,"J. Ameri. Cera. Society, 37, 91-95, 1954.

(34). Lenoir, Junk and Comings, Chem. Eng. Progr., 49, 539, 1953.

(35). H. S. Carslaw and J. C. Jaeger, "Conduction of Heat in Solids,"Oxford Uni. Press, 2nd edition, 338, 1959.

(36). H. W. Godbee, "Thermal Conductivity of Magnesia, Alumina and Zirconia Powders in Air at Atomopheric Pressure from 200 F to 1500 F,"Apr. 1966, 166, ORNL 3510.

(37). J. H. Blackwell, "The Axial-Flow Error in The Thermal Conductivity Probe,"Canad. J. Phys. 34, 412, 1956.

(38). J. H. Blackwell, "Radial-Axial Heat Flow in Regions Bounded Internally by Circular Cylinders,"Canad. J. Phys. 31, 472, 1953.

(39). J. A. Nelder and R. Mead, Computer J., 7:308, 1964.

(40). W. Spendly, G. R. Hext and F. R. Himsworth, Technometrics, 4:441,1962.

(41). F. R. Himsworth, Trans. Inst. Chem. Eng., 40., 435, 1962.

(42). D. M. Himmelblau, "Applied Nonlinear Programming,"McGraw-Hill Book Co., 148, 1972.

(43). R. E. Shannon, "System Simulation, The Art and Science,"Englewood Cliffs, N. J. : Prentice-Hall, 1975.

APPENDIXES

APPENDIX A

DERIVATION OF THE DIFFERENCE EQUATIONS

To avoid undesirable restrictions on the size of the time increment, "backward difference" approximation were used in spherical as well as cylindrical systems. Such approximation leads to the so-called "implicit formulation," each variable is evaluated at the advanced point of time $t + \Delta t$ instead of at t.

1. ENERGY AND MASS BALANCES FOR A SINGLE SPHERICAL FeTi HYDRIDE REGION

As shown in Figure 34, the radius of a single spherical FeTi hydride region is equally divided into $(m - 2)$ parts of length Δr. Let node 1 be the center point, node 2 be the first point a distance Δr away from the center, and so on till node $(m - 2)$. The next node is $(m - 1)$ with $(3/4)\Delta r$ from node $(m - 2)$. The point on the surface is node m which is a distance $(1/4)\Delta r$ from node $(m - 1)$. If r_j is the distance of j-th node from the center, then

$$\left.\begin{aligned} r_1 &= 0, \\ r_j &= (j - 1)\Delta r, \quad 2 \leqslant j \leqslant m - 2, \\ r_{m-1} &= r_m - (1/4)\Delta r. \end{aligned}\right\} \tag{52}$$

Here r_m is the radius of the sphere.

Material within each spherical shell extending $(1/2)\Delta r$ is assumed to be uniform in temperature and composition and homogeneous (having physical properties that are volume-weight averages of the properties for the metal hydride and the hydrogen gas).

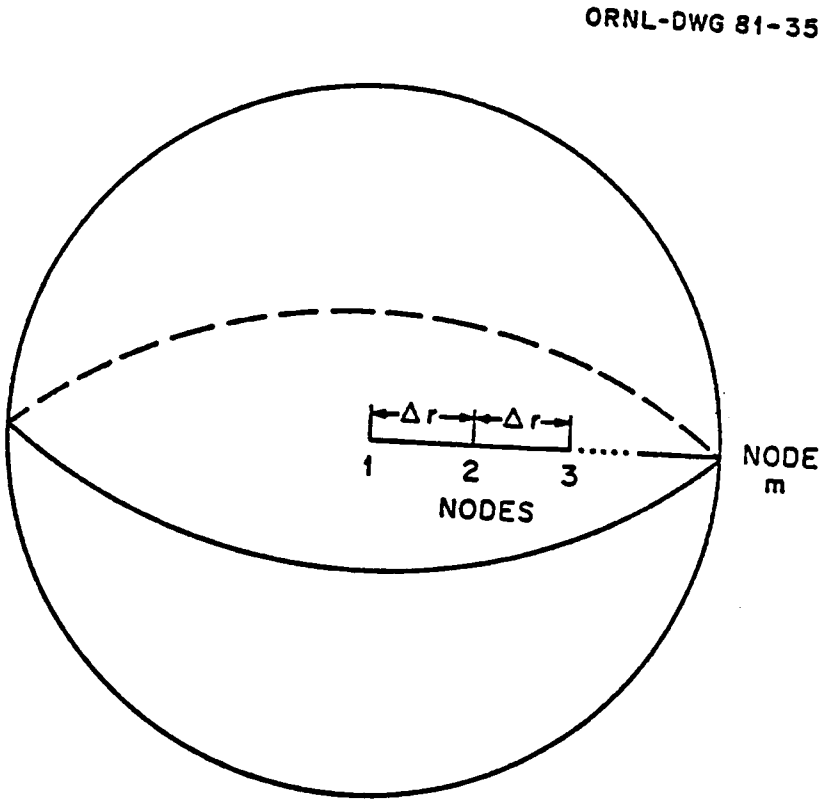

Figure 34. Dividing the spherical radius.

For a time interval Δt, the energy balance can be expressed sematically as

Increase in internal energy of material associated with node j during the last time interval, Δt

= Net heat flow from all neighboring nodes towards node j at time $t + \Delta t$ + Energy generation due to reaction

(A). For Node 1:

Figure 35 shows the node 1 and 2 in the spherical system. For node 1,

$$T_{i,1} - T_{i,2} = 0, \tag{53}$$

$$C_{i,1} - C_{i,2} = 0, \tag{54}$$

due to symmetry.

T = temperature.

C = composition.

$T_{i,j}$ ($C_{i,j}$) = property at time $t + \Delta t$, "i" refers to the i-th cylindrical shell in which the sphere is located, "j" the j-th node in sphere.

The spherical volume bounded by r = 0 and $r = \Delta r/2$ is

$$\Delta V_1 = (4/3)\pi(\Delta r/2)^3. \tag{55}$$

The change in mass within ΔV_1 during the time interval, Δt, is

$$\Delta m_1 = \Delta V_1 (C_{i,1} - C^{\bullet}_{i,1}), \tag{56}$$

where the superscript "$\bullet$" refers to the property at the original time level, t.

The energy change within ΔV_1 during Δt is

$$\Delta h_1 = \Delta V_1 \rho C_p (T_{i,1} - T^{\bullet}_{i,1}). \tag{57}$$

Here ρC_p is the bulk Heat capacity of the hydride packing, defined by Equation (20).

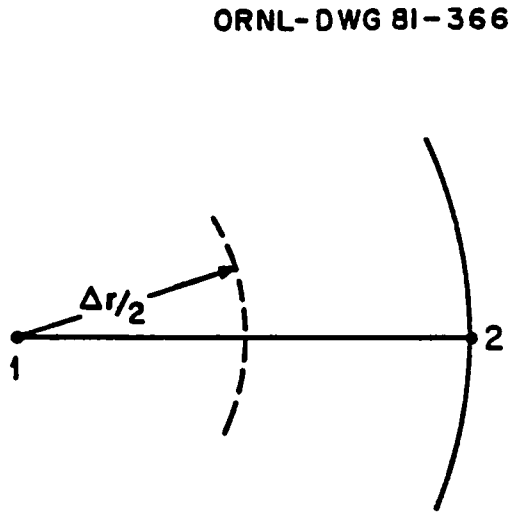

Figure 35. Node 1 and 2 in the spherical system.

(B). For Any Internal Node j ($2 \leqslant j \leqslant m - 2$):

For any internal spherical volume bounded by $r_j \pm \Delta r/2$, as indicated in Figure 36, the energy accumulation is

$$\text{Accumulation} = \Delta V_j \rho C_p (T_{i,j} - T^{\bullet}_{i,j}), \tag{58}$$

the energy input is

$$\text{Input} = K_h 4\pi (r_j - \Delta r/2)^2 (T_{i,j-1} - T_{i,j}) \Delta t/\Delta r, \tag{59}$$

the energy output is

$$\text{Output} = K_h 4\pi (r_j + \Delta r/2)^2 (T_{i,j} - T_{i,j+1}) \Delta t/\Delta r, \tag{60}$$

and the heat generation is

$$\text{Generation} = -\Delta H' \Delta V_j (C_{i,j} - C^{\bullet}_{i,j}), \tag{61}$$

where

ΔV_j = the spherical volume bounded by $(r_j - \Delta r/2)$ and $(r_j + \Delta r/2)$

$$= (4/3)\pi[(r_j + \Delta r/2)^3 - (r_j - \Delta r/2)^3]$$

$$= (4/3)\pi\Delta r[3r_j^2 + (\Delta r/2)^2]; \tag{62}$$

K_h = effective thermal conductivity of the hydride packing;

$\Delta H'$ = heat of reaction multiplied by volume fraction of hydride. Conventional use of sign, i.e., positive for endothermic, negative for exothermic, is applied here.

The law of energy conservation requires that

Accumulation = Input - Output + Generation

This relation leads to the expression

$$T_{i,j} - T^{\bullet}_{i,j}$$

$$= \frac{K_h}{\rho C_p} \frac{3(r_j - \Delta r/2)^2}{3r_j^2 + (\Delta r/2)^2} \frac{(T_{i,j-1} - T_{i,j})\Delta t}{\Delta r^2}$$

$$- \frac{K_h}{\rho C_p} \frac{3(r_j + \Delta r/2)^2}{3r_j^2 + (\Delta r/2)^2} \frac{(T_{i,j} - T_{i,j+1})\Delta t}{\Delta r^2}$$

$$- \Delta H'(C_{i,j} - C^{\bullet}_{i,j})/\rho C_p. \tag{63}$$

ORNL-DWG 81-365

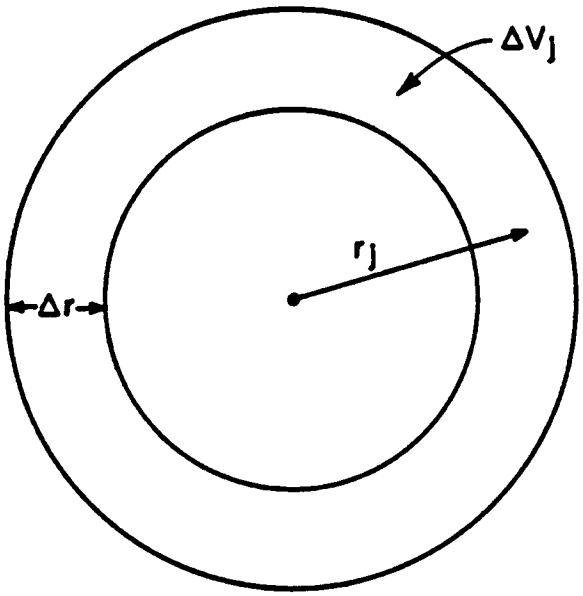

Figure 36. Internal spherical nodes.

Let

$$\delta = \frac{K_h}{\rho C_p}\frac{\Delta t}{\Delta r^2} \tag{64}$$

$$\phi = \Delta H'/\rho C_p. \tag{65}$$

Rearranging Equation (63), we have

$$\delta\frac{3(r_j - \Delta r/2)^2}{3r_j^2 + (\Delta r/2)^2} T_{i,\,j-1} - \left\{1 + \frac{6\delta[r_j + (\Delta r/2)^2]}{3r_j^2 + (\Delta r/2)^2}\right\} T_{i,\,j}$$

$$+ \delta\frac{3(r_j + \Delta r/2)^2}{3r_j^2 + (\Delta r/2)^2} T_{i,\,j+1} - \phi C_{i,\,j} + T^{\circ}_{i,\,j} + \phi C^{\circ}_{i,\,j} = 0 \tag{66}$$

The mass change within ΔV_j during Δt is

$$\Delta m_j = \Delta V_j (C_{i,\,j} - C^{\circ}_{i,\,j}). \tag{67}$$

The energy change within ΔV_j during Δt is

$$\Delta h_j = \Delta V_j \rho C_p (T_{i,\,j} - T^{\circ}_{i,\,j}). \tag{68}$$

(C). For Node m - 2:

Similarly, the energy balance results in

$$\Delta V_{m-2}\rho C_p (T_{i,\,m-2} - T^{\circ}_{i,\,m-2})$$

$$= K_h 4\pi (r_{m-2} - \Delta r/2)^2 (T_{i,\,m-2} - T_{i,\,m-2})\Delta t/\Delta r$$

$$- K_h 4\pi (r_{m-2} + \Delta r/2)^2 (T_{i,\,m-2} - T_{i,\,m-2})\Delta t/(3\Delta r/4)$$

$$- \Delta H' \Delta V_{m-2} (C_{i,\,m-2} - C^{\circ}_{i,\,m-2}). \tag{69}$$

Here

ΔV_{m-2} = the spherical volume bounded by $(r_{m-2} - \Delta r/2)$ and $(r_{m-2} + \Delta r/2)$

$$= 4\pi\Delta r[3r_{m-2}^2 + (\Delta r/2)^2]/3. \tag{70}$$

Rearranging and grouping Equation (69), we have

$$\delta\frac{3(r_{m-2} - \Delta r/2)^2}{3r_{m-2}^2 + (\Delta r/2)^2} T_{i,\,m-3} - \left[1 + \delta\frac{7r_{m-2}^2 + r_{m-2}\Delta r + 7(\Delta r/2)^2}{3r_{m-2}^2 + (\Delta r/2)^2}\right] T_{i,\,m-2}$$

$$+ \delta\frac{4(r_{m-2} + \Delta r/2)^2}{3r_{m-2}^2 + (\Delta r/2)^2} T_{i,\,m-1} - \phi C_{i,\,m-2} + T^{\circ}_{i,\,m-2} + \phi C^{\circ}_{i,\,m-2} = 0 \tag{71}$$

The mass change within ΔV_{m-2} during Δt is

$$\Delta m_{m-2} = \Delta V_{m-2}(C_{i,\,m-2} - C^{\bullet}_{i,\,m-2}). \tag{72}$$

The energy change within ΔV_{m-2} during Δt is

$$\Delta h_{m-2} = \Delta V_{m-2}\rho C_p(T_{i,\,m-2} - T^{\bullet}_{i,\,m-2}). \tag{73}$$

(D). For Node m - 1:

The energy balance for the volume bounded by $r_m - r/2$ and r_m, as indicated in Figure 37, requires that

$$\begin{aligned}&\Delta V_{m-1}\rho C_p(T_{i,\,m-1} - T^{\bullet}_{i,\,m-1})\\ &= K_h 4\pi(r_m - \Delta r/2)\,(T_{i,\,m-2} - T_{i,\,m-1})\Delta t/(3\Delta r/4)\\ &\quad - K_h 4\pi r_m(T_{i,\,m-1} - T_{i,\,m})\Delta t/(\Delta r/4) - \Delta H'\Delta V_{m-1}(C_{i,\,m-1} - C^{\bullet}_{i,\,m-1}),\end{aligned} \tag{74}$$

where

ΔV_{m-1} = the spherical volume bounded by $r_m - \Delta r/2$ and r_m

$$= 4\pi[r_m^3 - (r_m - \Delta r/2)^3]/3. \tag{75}$$

It is assumed that the hydride is so intimately contacted with the surrounding aluminum that the temperature at $r = r_m$ is same as that of aluminum. Or

$T_{i,m} = D_i$, the temperature of Al surrounding the FeTi hydride region

Rearranging (74), we get

$$\begin{aligned}&\delta\frac{4\Delta r(r_m - \Delta r/2)^2}{r_m^3 - (r_m - \Delta r/2)^3}T_{i,\,m-2} - \left[1 + \delta\frac{4\Delta r[4r_m^2 - r_m\Delta r + (\Delta r/2)^2]}{r_m^3 - (r_m - \Delta r/2)^3}\right]T_{i,\,m-1}\\ &+ \delta\frac{12\,\Delta r r_m D_i}{r_m^3 - (r_m - \Delta r/2)^3} - \phi C_{i,\,m-1} + T^{\bullet}_{i,\,m-1} + \phi C^{\bullet}_{i,\,m-1} = 0\end{aligned} \tag{76}$$

The mass change within ΔV_{m-1} during Δt is

$$\Delta m_{m-1} = \Delta V_{m-1}(C_{i,\,m-1} - C^{\bullet}_{i,\,m-1}). \tag{77}$$

The energy change within ΔV_{m-1} during Δt is

$$\Delta h_{m-1} = \Delta V_{m-1}\rho C_p(T_{i,\,m-1} - T^{\bullet}_{i,\,m-1}). \tag{78}$$

ORNL-DWG 81-364

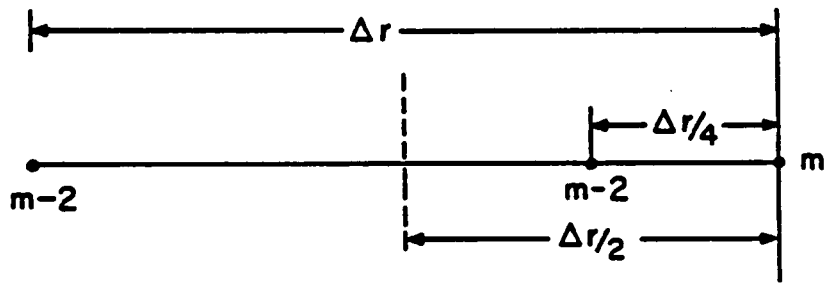

Figure 37. The (m - 1)th node in the spherical system.

The total rate of mass change in a single sphere is obtained by adding Equation(56), (67), (72) and (77)

$$F_i = (\Delta m_1 + \sum_{j=2}^{m-2} \Delta m_j + \Delta m_{m-1})/\Delta t$$

$$= 4\pi\{(\Delta r/2)^3 (C_{i,1} - C^*_{i,1}) + \sum_{j=2}^{m-2} \Delta r[3r^2 + (\Delta r/2)^2](C_{i,j} - C^*_{i,j})$$

$$+ [r_m^3 - (r_m - \Delta r/2)^3](C_{i,m-1} - C^*_{i,m-1})\}/3\Delta t. \qquad (79)$$

The total change of internal energy in a sphere during Δt is obtained similarly by adding Equation (57) (68) (73) and (78)

$$E_i = \Delta h_1 + \sum_{j=2}^{m-2} \Delta h_j + \Delta h_{m-1}$$

$$= (4/3)\pi\rho c_p[(\Delta r/2)^3 (T_{i,1} - T^*_{i,1})$$

$$+ \sum_{j=2}^{m-2} \Delta r[3r^2 + (\Delta r/2)^2](T_{i,j} - T^*_{i,j})$$

$$+ [r_m^3 - (r_m - r/2)^3](T_{i,m-1} - T^*_{i,m-1})\}. \qquad (80)$$

2. MASS AND ENERGY BALANCES FOR THE CYLINDRICAL SYSTEM

As with the sphere, the radius of the cylindrical vessel is subdivided into (p - 1) parts of the ΔR. The first node point is assigned on the outer radius of PMT, the second point is ΔR away from the first one, and so on. Control volume for each internal node includes all the material in the annular region extending radially $\Delta R/2$, as indicated by the dotted lines in Figure 38, and the length of the bed, L. Both of the control volumes for the first and the last node have radius interval of $\Delta R/2$ instead.

ORNL-DWG 81-363

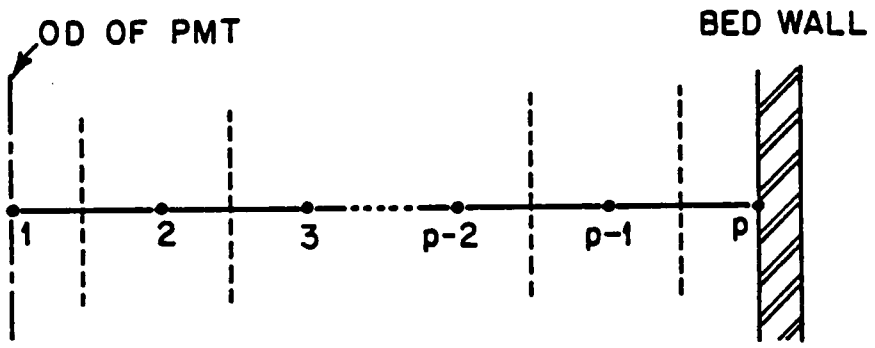

Figure 38. Dividing the cylindrical system.

(A). Number Of Spherical Cells In Each Control Volume

Let n_i be the number of spherical cells in the i-th cylindrical subvolume, and V_a is the volume fraction of aluminum in the whole packing bed. If s is the number of cells in unit volume

$$s = \frac{1 - V_a}{(4/3)\pi r_m^3} \tag{81}$$

Then, the number of cells in the first subvolume is

$$n_1 = \frac{(1 - V_a)}{(4/3)\pi r_m^3}\{\pi L[(R_1 + \Delta R/2)^2 - R_1^2]\}$$
$$= \frac{3}{4}\frac{\Delta R(R_1 + \Delta R/4)L(1 - V_a)}{r_m^3} \tag{82}$$

Here R_1 is the outer radius of the PMT.

Similarly, for the i-th subvolume where $2 \leqslant i \leqslant (p - 1)$

$$n_i = \frac{(1 - V_a)}{(4/3)\pi r_m^3}\{\pi L[R_i + \Delta R/2)^2 - (R_i - \Delta R/2)^2]\}$$
$$= \frac{3}{2}\frac{R_i \Delta R L(1 - V_a)}{r_m^3} \tag{83}$$

For the p-th (last) subvolume

$$n_p = \frac{(1 - V_a)\{\pi L[R_p^2 - (R_p - \Delta R/2)^2]\}}{(4/3)\pi r_m^3}$$
$$= \frac{3}{4}\frac{\Delta R(R_p - \Delta R/4)L(1 - V_a)}{r_m^3} \tag{84}$$

Here R_p is the inner radius of the cylindrical vessel.

(B). Total Rate Of Mass Flow

The changes of the composition and temperature are considered the same for all cells contained in the same cylindrical subvolume. The total flow rate of hydrogen is thus the summation of the reaction rates occuring in all hydride cells. Or

$$F = n_1 F_1 + \sum_{i=2}^{p-1} n_i F_i + n_p F_p. \tag{85}$$

(C). Energy Balance For Each Cylindrical Subvolume

The mass and energy balances for each single hydride cell have already been made. It is assumed that the heat transfer between subvolumes is through the conduction of aluminum, only the energy change in the aluminum part of each cylindrical subvolume will be considered this time.

For each cylindrical subvolume

Accumulation of energy = Energy in - Energy out

Where

Energy in = conduction through the most outer shell of the spherical hydride cells plus conduction through the boundary between two cylindrical subvolumes via aluminum.

Energy out = conduction through the boundary between two cylindrical subvolumes via aluminum.

(1). For the first subvolume

The energy balance for the first cylindrical volume, as indicated in Figure 39, is as follows.

Accmulation

$$= \pi[(R_1 + \Delta R/2)^2 - R_1^2]LV_a\rho_a C_{pa}(D_1 - D_1^\circ)$$

$$= \pi\Delta R(R_1 + \Delta R/4)LV_a\rho_a C_{pa}(D_1 - D_1^\circ), \qquad (86)$$

where

ρ_a = density of aluminum;

C_{pa} = heat capacity of aluminum.

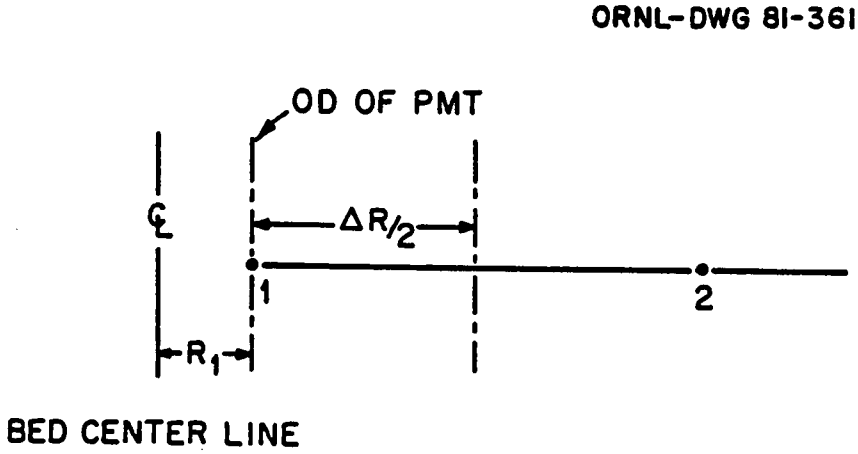

Figure 39. The first subvolume of the cylindrical system.

Note that aluminum temperature is considered uniform everywhere in the subvolume.

Output

$$= K_a A_c (D_1 - D_2)\Delta t/\Delta R$$

$$= K_a 2\pi(R_1 + \Delta R/2)LV_a (D_1 - D_2)\Delta t/\Delta R. \qquad (87)$$

Here

K_h = thermal condictivity of aluminum;

$A_c = 2\pi(R_1 + \Delta R/2)LV_a$, the "effective" surface through which the the heat is conducted.

The heat losses through the wall of the PMT are negligible, while the heat conducted through the most outer shell of each spherical cell in the cylindrical subvolume is $q_1\Delta t$. If Δt is chosen small enough, q_1 can be approximated by Fourier's law,

$$q_1 = - K_h 4\pi r^2 (dT/dr). \qquad (88)$$

Integrating between the points at $r = r_{m-1}$ and at $r = r_m$,

$$\int_{r_{m-1}}^{r_m} \frac{dr}{r} = - \frac{4\pi}{q_1} \int_{T_{m-1}}^{T_m} K_h dT$$

$$\frac{1}{r_{m-1}} - \frac{1}{r_m} = - \frac{4\pi}{q_1} \int_{T_{m-1}}^{T_m} K_h dT$$

$$q_1 = \frac{r_m r_{m-1}}{r_m - r_{m-1}} 4\pi \int_{T_{m-1}}^{T_m} K_h dT \qquad (89)$$

If the dependence of K_h on the temperature is negligibly small

$$q_1 = \frac{r_m r_{m-1}}{r_m - r_{m-1}} 4\pi K_h (T_{m-1} - T_m) \qquad (90)$$

The energy balance for the cylindrical subvolume results in

$$n_1 q_1 \Delta t - K_a 2\pi(R_1 + \Delta R/2) L V_a (D_1 - D_1^*)\Delta t/\Delta R$$
$$= \pi \Delta R (R_1 + \Delta R/4) L V_a \rho_a C_{pa} (D_1 - D_1^*). \quad (91)$$

(2). For the i-th subvolume ($2 \leqslant i \leqslant p - 1$)

The energy balance for any internal cylindrical subvolume bounded by $R_i \pm \Delta R/2$, as shown in Figure 40, is as follows.

Accumulation

$$= \pi[(R_i + \Delta R/2)^2 - (R_i - \Delta R/2)^2] L V_a \rho_a C_{pa} (D_i - D_i^*)$$
$$= 2\pi R_i \Delta R L V_a \rho_a C_{pa} (D_i - D_i^*). \quad (92)$$

Input

$$= n_i q_i \Delta t + K\, 2\pi(R_i - \Delta R/2) L V_a (D_{i-1} - D_i)\Delta t/\Delta R, \quad (93)$$

where q_i is like q_1, calculated by Equation (88).

Output

$$= K_a 2\pi(R_i + \Delta R/2) L V_a (D_i - D_{i+1})\Delta t/\Delta R. \quad (94)$$

Then, the energy balance leads to

$$n_i q_i \Delta t + K_a 2\pi(R_i - \Delta R/2) L V_a (D_{i-1} - D_i)\Delta t/\Delta R$$
$$- K_a 2\pi(R_i + \Delta R/2) L V_a (D_i - D_{i+1})\Delta t/\Delta R$$
$$= 2\pi R_i \Delta R L V_a \rho_a C_{pa} (D_i - D_i^*). \quad (95)$$

(3). For the last subvolume

The last cylindrical subvolume and the boundary conditions at the vessel wall are indicated in Figure 41.

Accumulation

$$= \pi[R_p^2 - (R_p - \Delta R/2)^2] L V_a \rho_a C_{pa} (D_p - D_p^*)$$
$$= \Delta R (R_p - \Delta R/4) L V_a \rho_a C_{pa} (D_p - D_p^*). \quad (96)$$

Input

$$= n_p q_p \Delta t + K_a 2\pi(R_p - \Delta R/2) L V_a (D_{p-1} - D_p)\Delta t/\Delta R. \quad (97)$$

ORNL-DWG 81-362

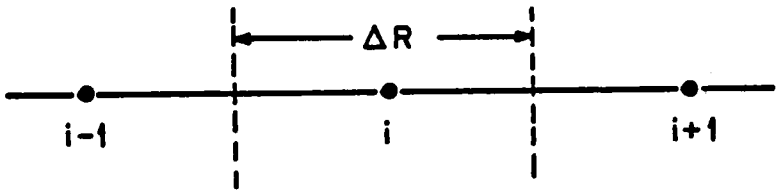

Figure 40. Internal nodes in the cylindrical system.

ORNL-DWG 81-360

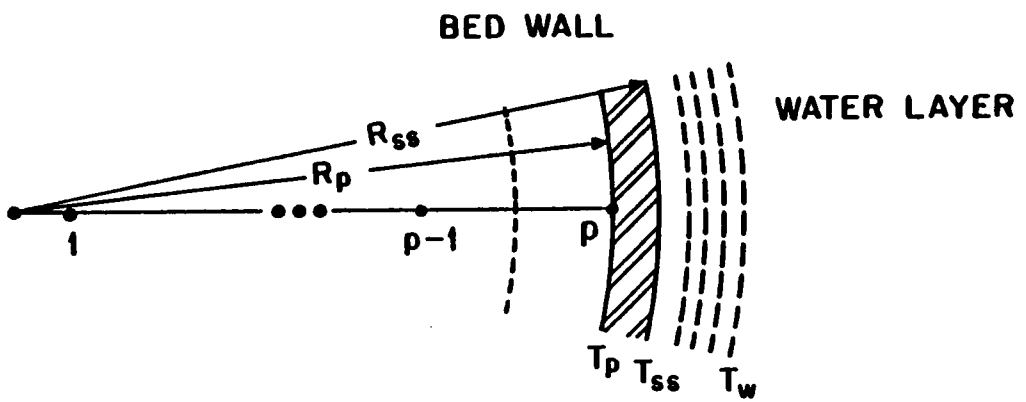

Figure 41. The cylindrical subvolume adjacent to the vessel wall.

The boundary condition at $R = R_{ss}$, the outer radius of the vessel is,

$$K_{ss}\bar{A}\frac{T_p - T_{ss}}{R_{ss} - R_p} = hA_{ss}(T_{ss} - T_w), \tag{98}$$

where

K_{ss} = thermal conductivity of the wall material;

h = heat transfer coefficient of the water flowing in the jacket;

T_p = inside wall temperature;

T_{ss} = outside wall temperature;

T_w = water temperature;

R_{ss} = outer radius of the vessel;

$A_{ss} = 2\pi R_{ss}L$; (99)

$\bar{A}$ = log-mean surface through which the heat is conducted

$$= 2\pi L\frac{R_{ss} - R_p}{\ln(R_{ss}/R_p)} \tag{100}$$

It is assumed that aluminum is so intimately contacted with vessel wall that

$T_p = D_p$. (101)

Rearranging Equation (98) and combining Equations (99) (100) and (101), we have

$$T_{ss} = \frac{K_{ss}D_p + T\,hR_{ss}\ln(R_{ss}/R_p)}{K_{ss} + hR_{ss}\ln(R_{ss}/R_p)} \tag{102}$$

Then, the heat output from the subvolume is

Output $= q_w\Delta t$

$$= 2\pi hR_{ss}L(T_{ss} - T_w)\Delta t, \tag{103}$$

where

q_w = convection heat through the water layer.

The law of energy conservation requires that

$$n_p q_p \Delta t + K_a 2\pi(R_p - \Delta R/2)LV_a(D_{p-1} - D_p)\Delta t/\Delta R$$
$$- 2\pi h R_{ss} L(T_{ss} - T_w)\Delta t$$
$$= \pi \Delta R(R_p - \Delta R/4)LV_a \rho_a C_{pa}(D_p - D_p^*). \qquad (104)$$

APPENDIX B

LISTINGS OF COMPUTER PROGRAMS

The listings of the computer programs are given on the following pages. When possible, the variables names used in the programs duplicate those employed in the report text. Appropriate commemts are given.

Some figures in this report are drawn by the DECsystem-10 Tektronix 4015-1. The subrountines needed for drawing, such as GRAPH, BINITT, etc. are in the IBM storage package.

```
C       THIS PROGRAM MUST BE RUN WITH FOUR SUBROUTINES---
C       VALUE,COST,START AND SUMR,AND FOUR FUNCTIONS-----
C       HEAT,THCON,DENS AND CAPAC TO PREDICT ABSORPTION/
C       OR DESORPTION OCCURRING IN THE AL-ENHANCED BED.
C***** OPTIMIZATION METHOD OF NELDER AND MEAD (SIMPLEX) *****
C------ NS = NODE NO IN A SINGLE SPHERE MINUS ONE,START
C            COUNTING FROM CENTER
C------ NC = NODE NO IN CYLINDER,THE FIRST NODE IS ON THE
C            OUTSIDE RADIUS OF POROUS TUBE
C------ NX = NO. OF INDEPENDENT VARIABLE FOR SPHERE
C------ NY = NO OF INDEPENDENT VARIABLE FOR CYLINDER
C------ NW = NO. OF TIME STEPS
C------ STEP = INITIAL STEP SIZE FOR SPHERE
C------STEPC = INITIAL STEP SIZE FOR CYLINDER
C------ X(I) = INITIAL GUESSES FOR SPHERE
C------ Y(I) = INITIAL GUESSES FOR CYLINDER
C------ AM = 1.0 FOR ADSORPTION, -1.0 FOR DESORPTION
C------ CPA = HEAT CAPACITY OF ALUMINUM,BTU/LB-R
C------ DA = DENSITY OF ALUMINUM,LB/FT**3
C------ EK = THERMAL CONDUCTIVITY OF ALUMINUM,BTU/HR-FT-R
C------ V = VOID FRACTION OF HYDRIDE PACKING IN SPHERE
C------ VA = VOLUME FRACTION OF ALUMINUM
C------ RM = RADIUS OF SPHERE,FT
C------ R1 = OUTER RADIUS OF METAL POROUS TUBE,FT
C------ RC = INNER RADIUS OF VESSEL,FT
C------ RSS = OUTER RADIUS OF VESSEL,FT
C------ SSK = THERMAL CONDUCTIVITY OF VESSEL MATERIAL,
C             BTU/HR-FT-R
C------ AL = LENGTH OF VESSEL,FT
C------ H = HEAT TRANSFER COEFFICIENT FOR THE WATER LAYER,
C           BTU/HR-FT**2-R
C------ TW = WATER TEMPERATURE,R
C------ HK = EFFECTIVE THERMAL CONDUCTIVITY OF HYDRIDE
C            PACKING IN SPHERE,BTU/HR-FT-R
C------ DRS = RADIAL INTERVAL IN SPHERE,FT
C------ DRC = RADIAL INTERVAL IN CYLINDER,FT
      DIMENSION A(6),G(6),FR(6),YN(6),TMASS(500),XO1(10,20)
      COMMON /ONE/ X(30),X1(30,30),NX,STEP,K1,SUM(30),IN
      COMMON /TWO/ TA,XO(30),NS,DRS,R(8),NP,NN,RM
      COMMON /THREE/ Y(30),Y1(30,30),NY,STEPC,M1,SUMY(30),
     1  IM
      COMMON /FOUR/ TW,YO(8),NC,DRC,RO(8),NM,ACC(6)
      COMMON /FIVE/ P(12),AM
      NAMELIST /CYLIN4/CPA,DA,VA,R1,H,V
      NAMELIST /CYLIN/SSK,DELT,TW,EK,RC,AM
      NAMELIST /CYLIN2/RM,AL,DRS,DRC,HK
      AM=-1.0
      NS=3
      NC=3
      NP=NS+1
```

```
      NN=NS-1
      NM=NC-1
      NX=NS+NS
      NY=NC+1
      NW=300
      CPA=0.215
      DA=168.4896
      VA=0.092
      RM=4.1666E-3
      R1=0.0260833
      H=107.37
      V=0.4191
      SSK=9.4
      RC=0.26575
      RSS=0.27733
      AL=2.1258
      EK=137.6531
      DRS=RM/FLOAT(NN)
      DRC=(RC-R1)/FLOAT(NM)
      DELT=5./36000000.
      TW=582.
      HMASS=0.
      IX=1
C---- CALCULATE THE RADII FOR THE NODE POINTS IN SPHERE.
      DO 80 I=1,NN
   80 R(I)=FLOAT(I-1)*DRS
      R(NS)=RM-DRS/4.
C---- FIND THE SUMMATION OF ALL RADII IN SPHERE.
      TOTAR=0.
      DO 83 I=1,NS
   83 TOTAR=TOTAR+R(I)
      WRITE(3,601) (R(I),I=1,NS),TOTAR
  601 FORMAT(1X,'R(I)=',3(F10.6,5X),/1X,'TOTAR=',F10.6)
C---- CALCULATE THE RADII FOR THE NODE POINTS IN CYLINDER.
      DO 106 I=1,NC
  106 RO(I)=R1+FLOAT(I-1)*DRC
C---- FIND THE NUMBER OF SPHERES IN EACH CYLINDRICAL
C     SUBSHELL.
      YN(1)=3.*DRC*(R1+DRC/4.)*AL*(1.-VA)/(4.*RM**3)
      DO 88 I=2,NM
   88 YN(I)=3.*RO(I)*DRC*AL*(1.-VA)/(2.*RM**3)
      YN(NC)=3.*DRC*(RC-DRC/4.)*AL*(1.-VA)/(4.*RM**3)
      WRITE(3,674) (YN(I),I=1,NC)
  674 FORMAT(1X,'YN(I)=',3(F15.4,6X))
C---- CALCULATE THE COEFFIENTS OF THE VARIABLES IN THE
C     RESULTING EQUATIONS,P(1),P(2)...P(12).
      P(3)=19.
      P(4)=SSK/(SSK+H*RSS*ALOG(RSS/RC))
      P(5)=TW*H*RSS*ALOG(RSS/RC)/(SSK+H*RSS*ALOG(RSS/RC))
      P(6)=2.*3.1416*EK*AL*VA*DELT/DRC
```

```
      P(7)=3.1416*DRC*AL*VA*DA*CPA
      P(8)=R1+DRC/2.
      P(9)=R1+DRC/4.
      P(10)=2.*3.1416*H*RSS*AL*DELT
      P(11)=RC-DRC/2.
      P(12)=RC-DRC/4.
C---- INITIALIZE THE REACTION CONDITIONS.
      DO 100 J=1,NC
      DO 100 I=1,NS
  100 XO1(J,I)=582.
      DO 120 J=1,NC
      DO 120 I=NP,NX
  120 XO1(J,I)=0.8
      DO 367 I=1,NY
  367 YO(I)=582.
      HK=THCON(P(3))
      TIME=0.
      WRITE(3,444)
  444 FORMAT(1X,'THIS PROGRAM IS TO PREDICT THE
     1 TEMPERATURE AND COMPOSITION PROFILES FOR THE
     1 SPHERE AND THE TEMPERATURE PROFILE FOR THE
     1 CYLINDER')
      WRITE(3,CYLIN4)
      WRITE(3,CYLIN)
      WRITE(3,CYLIN2)
      JQ=3
      IB=1
      WRITE(3,625) (P(I),I=3,12)
  625 FORMAT(/,1X,'P(3)=',E12.5,5X,'P(4)=',E12.5,5X,
     1 'P(5)=',E12.5,5X,'P(6)=',E12.5,5X,'P(7)=',E12.5,/
     1 ,1X,'P(8)=',E12.5,5X,'P(9)=',E12.5,5X,'P(10)=',
     1 E12.5,4X,'P(11)=',E12.5,4X,'P(12)=',E12.5)
C---- START THE CALCULATION FROM THE FIRST TIME STEP,
C     SECON.D TIME STEP AND SO ON.
      DO 1000 KAPPA=1,NW
      TIME=TIME+DELT
      STIME=TIME*3.6E+3
      IF(IX-30) 271,271,281
  271 NUM=IX/JQ
      GO TO 286
  281 JQ=10
      IF(IX.GT.30.AND.IX.LT.35) IB=1
      NUM=(IX-30)/JQ
C---- CALCULATE THE TEMPERATURE AND COMPOSITION IN SPHERE
C     IN EACH CYLINDRICAL SUBSHELL FIRST. THE TEMPERATURE
C     OF THE SURROUNDING ALUMINUM IS KEPT CONSTANT DURING
C     THE TIME INTERVAL.
  286 DO 64 IW=1,NC
      KAP=KAPPA-1
      IF(KAP-1) 124,128,128
```

```
  124   TA=582.
        GO TO 84
  128   GO TO (111,201,301),IW
  111   TA=YO(1)
        GO TO 84
  201   TA=YO(2)
        GO TO 84
  301   TA=YO(3)
   84   DO 233 LL=1,NX
  233   XO(LL)=XO1(IW,LL)
C------ FIND THE MEAN VALUES OF HEAT OF REACTION AND HEAT
C       CAPACITY OF THE HYDRIDE PACKING IN SPHERE.
        CPD=0.
        RHEAT=0.
        DO 85 I=1,NS
        JU=I+NS
        HDEN=DENS(XO(JU))
        CPD=CPD+CAPAC(P(3),XO(I),V,HDEN)*R(I)
   85   RHEAT=RHEAT+HEAT(XO(JU),V)*R(I)
        CPD=CPD/TOTAR
        RHEAT=RHEAT/TOTAR
        ALPHH=HK/CPD
        P(1)=ALPHH*DELT/DRS**2
        P(2)=RHEAT/CPD
C------ GUESS NEW VALUES FOR THE VARIABLES IN THE SPHERICAL
C       SYSTEM.  TO FACILITATE THE SOLVING OF THE
C       NONLINEAR SIMULTANEOUS EQUATIONS,THE VARIABLES
C       REPRESENTING FOR THE COMPOSITION  ARE MULTIPLIED
C       BY 1000 TO MAKE ALL VARIABLES HAVE SAME ORDER OF
C       MAGNITUDE.
        IF (KAPPA.EQ.1) GO TO 53
        DO 52 I=1,NS
   52   X(I)=XO(I)
        DO 247 I=NP,NX
  247   X(I)=XO(I)*1.E+3
        GO TO 70
   53   CONTINUE
        X(1)=463.
        X(2)=463.
        X(3)=463.
        X(4)=680.
        X(5)=680.
        X(6)=660.
C------ START THE OPTIMIZATION STRATEGY
   70   STEP=3.
        IF (NX) 998,999,998
  998   CONTINUE
C------ ALFA = REFLECTION COEFFICIENT
C------ BETA = CONTRACTION COEFFICIENT
C------ GAMA = EXPENSION COEFFICIENT
```

```
      ALFA=1.0
      BETA=0.5
      GAMA=2.0
      DIFER=0.0
      XNX=NX
      IN=1
      IP=0
      CALL SUMR
C---- K1 = NUMBER OF VERTICES    K2 = INDEX OF CENTROID
C---- K3 = INDEX OF REFLECTION
C---- K4 = INDEX OF EXPENSION OR CONTRACTION
      K1=NX+1
      K2=NX+2
      K3=NX+3
      K4=NX+4
      CALL START
   25 DO 3 I=1,K1
      DO 4 J=1,NX
    4 X(J)=X1(I,J)
      IN=I
      CALL SUMR
    3 CONTINUE
C---- SELECT LARGEST VALUE OF SUM(I) IN SIMPLEX.
   28 SUMH=SUM(1)
      INDEX=1
      DO 7 I=2,K1
      IF (SUM(I).LE.SUMH) GO TO 7
      SUMH=SUM(I)
      INDEX=I
    7 CONTINUE
C---- SELECT MINIMUM VALUE OF SUM(I) IN SIMPLEX.
      SUML=SUM(1)
      KOUNT=1
      DO 8 I=2,K1
      IF (SUML.LE.SUM(I)) GO TO 8
      SUML=SUM(I)
      IF (IP.EQ.0) GO TO 771
      WRITE(3,101) SUML,(X1(KOUNT,J),J=1,NX),DIFER
  771 CONTINUE
      KOUNT=I
    8 CONTINUE
C---- FIND CENTROID OF POINTS WITH I DIFFERENT THAN INDEX.
      DO 9 J=1,NX
      SUM2=0.0
      DO 10 I=1,K1
   10 SUM2=SUM2+X1(I,J)
      X1(K2,J)=1.0/XNX*(SUM2-X1(INDEX,J))
C---- FIND REFLECTION OF HIGH POINT THROUGH CENTROID.
      X1(K3,J)=(1.0+ALFA)*X1(K2,J)-ALFA*X1(INDEX,J)
    9 X(J)=X1(K3,J)
      IN=K3
```

```
      CALL SUMR
      IF (SUM(K3).LT.SUML) GO TO 11
C---- SELECT SECOND LARGEST VALUE IN SIMPLEX.
      IF (INDEX.EQ.1) GO TO 38
      SUMS=SUM(1)
      GO TO 39
   38 SUMS=SUM(2)
   39 DO 12 I=1,K1
      IF ((INDEX-I).EQ.0) GO TO 12
      IF (SUM(I).LE.SUMS) GO TO 12
      SUMS=SUM(I)
   12 CONTINUE
      IF (SUM(K3).GT.SUMS) GO TO 13
      GO TO 14
C---- FORM EXPENSION OF NEW MINIMUM IF REFLECTION HAS
C     PRODUCED ONE MINIMUM.
   11 DO 15 J=1,NX
      X1(K4,J)=(1.0-GAMA)*X1(K2,J)+GAMA*X1(K3,J)
   15 X(J)=X1(K4,J)
      IN=K4
      CALL SUMR
      IF (SUM(K4).LT.SUML) GO TO 16
      GO TO 14
C---- FORM CONTRACTION.
   13 IF (SUM(K3).GT.SUMH) GO TO 17
      DO 18 J=1,NX
   18 X1(INDEX,J)=X1(K3,J)
   17 DO 19 J=1,NX
      X1(K4,J)=BETA*X1(INDEX,J)+(1.0-BETA)*X1(K2,J)
   19 X(J)=X1(K4,J)
      IN=K4
      CALL SUMR
      IF (SUMH.GT.SUM(K4)) GO TO 16
C---- REDUCE SIMPLEX BY HALF IF REFLECTION HAPPENS TO
C     PRODUCE A LARGER VALUE THAN THE MAXIMUM.
      DO 20 J=1,NX
      DO 20 I=1,K1
   20 X1(I,J)=0.5*(X1(I,J)+X1(KOUNT,J))
      DO 29 I=1,K1
      DO 30 J=1,NX
   30 X(J)=X1(I,J)
      IN=I
      CALL SUMR
   29 CONTINUE
      GO TO 26
   16 DO 21 J=1,NX
      X1(INDEX,J)=X1(K4,J)
   21 X(J)=X1(INDEX,J)
      IN=INDEX
      CALL SUMR
      GO TO 26
   14 DO 22 J=1,NX
```

```
      X1(INDEX,J)=X1(K3,J)
   22 X(J)=X1(INDEX,J)
      IN=INDEX
      CALL SUMR
   26 DO 23 J=1,NX
   23 X(J)=X1(K2,J)
      IN=K2
      CALL SUMR
      DIFER=0.0
      DO 24 I=1,K1
   24 DIFER=DIFER+(SUM(I)-SUM1(K2))**2
      DIFER=1.0/XNX*SQRT(DIFER)
      IF (DIFER.GE.0.01) GO TO 28
  999 CONTINUE
      IF(SUML.GT.50.) GO TO 273
      IF(NUM.NE.IB) GO TO 2001
      WRITE(3,101) SUML,DIFER,CPD,RHEAT,P(1),P(2)
  101 FORMAT(/,10X,6H SUML=,E16.6,10X,7H DIFER=,E16.6,/,1X,
     1 'CPD=',E12.5,2X,'BTU/FT**3.R',4X,'HEAT=',E14.4,2X,
     1 'BTU/HOM*FT**3',4X,'P(1)=',E12.4,4X,'P(2)=',E13.5)
 2001 CONTINUE
      DO 55 IK=1,NS
   55 XO(IK)=X(IK)
      DO 58 J=NP,NX
   58 XO(J)=X(J)*1.E-3
C---- FIND THE TOTAL FLOW RATE OF H2 IN THE SPHERE,
C     FT**3-HOM/HR
      FL=0.
      DO 171 I=2,NN
  171 FL=FL+DRS*(3.*R(I)**2+(DRS/2.)**2)*(XO(I+NS)-XO1(IW,
     1 I+NS))
      FL=4.*3.1416*(FL+(DRS/2.)**3*(XO(NP)-XO1(IW,NP))
     1 +(3.*RM*(DRS/2.)*(RM-DRS/2.)+(DRS/2.)**3)*(XO(NX)-
     1 XO1(IW,NX)))/(3.*DELT)
      FR(IW)=AM*FL
C---- CALCULATE THE HEAT TRANSFER RATE CONDUCTED THROUGH THE
C     OUTEST SHELL OF THE SPHERE IN THE TIME INTERVAL,BTU/HR
      G(IW)=4.*3.1416*HK*RC*R(NN)*(XO(NN)-TA)/DRS
C---- FIND THE TOTAL AMOUNT OF HEAT CONDUCTED THROUGH THE
C     SPHERICAL SHELL INTO THE SURROUNDING ALUMINUM IN
C     THE TIME INTERVAL FOR EACH CYLINDRICAL SUBSHELL,BTU
      ACC(IW)=YN(IW)*G(IW)*DELT
      DO 97 J=1,NX
   97 XO1(IW,J)=XO(J)
   64 CONTINUE
C---- FIND THE TOTAL AMOUNT OF H2 REACTED,LB MOLE,IN THE
C     TIME INTERVAL. THE CONVERSION FACTOR,3.91123*(1.-V)
C     COMES FROM (LB MOLE FETI/103.75 LB)*(405.79 LB/FT
C     **3 FETI)*((1.-V)FT**3 FETI/FT**3 TOTAL VOLUME)*(LB
C     MOLE H2/2 LB MOLE H)*(2*(MOLE FE+MOLE TI)/MOLE FETI)
      ZMASS=0.
```

```
      DO 842 I=1,NC
  842 ZMASS=ZMASS+FR(I)*YN(I)
      ZMASS=3.91123*(1.-V)*DELT*ZMASS
      TMASS(KAPPA)=ZMASS
      HMASS=HMASS+TMASS(KAPPA)
      IF(NUM.NE.IB) GO TO 3001
      WRITE(3,117) IX
  117 FORMAT(/,25X,'TIMES OF CALCULATION =',I4)
      WRITE(3,47) STIME
   47 FORMAT(/,25X,'TIME=',F10.4,3X,'SECONDS')
      WRITE(3,333) ((XO1(I,J),J=1,NX),I=1,NC)
  333 FORMAT(//,1X,'T(1,1)=',F10.4,6X,'T(1,2)=',F10.4,6X,
     1 'T(1,3)=',F10.4, /,1X,'C(1,1)=',F10.5,6X,'C(1,2)='
     1 ,F10.5,6X,'C(1,3)=',F10.5,//,1X,'T(2,1)=',F10.4,
     1 6X,'T(2,2)=',F10.4,6X,'T(2,3)=',F10.4,/,1X,
     1 'C(2,1)=',F10.5,6X,'C(2,2)=',F10.5,6X,'C(2,3)=',
     1 F10.5,//,1X,'T(3,1)=',F10.4,6X,'T(3,2)=',F10.4,6X,
     1 'T(3,3)=',F10.4,/,1X,'C(3,1)=',F10.5,6X,'C(3,2)=',
     1  F10.5,6X,'C(3,3)=',F10.5)
      WRITE(3,666)
  666 FORMAT(1X,'--------------------------------------------
     1 ----------------------------------------')
      WRITE(3,78)(G(I),I=1,NC),(FR(I),I=1,NC)
   78 FORMAT(/,1X,'G(1)=',E12.5,6X,'G(2)=',E12.5,6X,'G(3)=',
     1 E12.5,6X,'BTU/HR',/,1X,'F(1)=',E12.5,6X,'F(2)=',
     1 E12.5,6X,'F(3)=',E12.5,6X,'FT**3.HOM/HR')
      WRITE(3,157)(ACC(I),I=1,NC)
  157 FORMAT(1X,'ACC(1)=',F10.5,6X,'ACC(2)=',F10.5,6X,
     1 'ACC(3)=',F10.5,5X,'BTU')
 7000 CONTINUE
      WRITE(3,762) ZMASS
  762 FORMAT(/,10X,'HYDROGEN REACTED=',F12.8,5X,
     1 'LB MOLE H2')
 3001 CONTINUE
C---- START THE CALCULATION FOR THE CYLINDRICAL SYSTEM WITH
C     THE SAME STRATEGY AS THAT USED FOR THE SPHERICAL SYSTEM.
      IF(KAPPA.EQ.1) GO TO 752
      DO 257 I=1,NY
  257 Y(I)=YO(I)
      GO TO 421
  752 CONTINUE
      Y(1)=550.
      Y(2)=552.
      Y(3)=551.
      Y(4)=555.
  421 STEPC=5.
      IF (NY) 888,889,888
  888 CONTINUE
C---- ALF=REFLECTION COEFFICIENT
C---- BET=CONTRACTION COEFFICIENT
C---- GAM=EXPENSION COEFFICIENT
```

```
      ALF=1.0
      BET=0.5
      GAM=2.0
      DIST=0.0
      YNY=NY
      IM=1
      IO=0
      CALL COST
C---- M1=NUMBER OF VERTICES   M2=INDEX OF CENTROID
C---- M3 = INDEX OF REFLECTION
C---- M4 = INDEX OF EXPENSION OR CONTRACTION
      M1=NY+1
      M2=NY+2
      M3=NY+3
      M4=NY+4
      CALL VALUE
 27   DO 5 I=1,M1
      DO 6 J=1,NY
 6    Y(J)=Y1(I,J)
      GO TO 613
      WRITE(3,43) (Y(JJ),JJ=1,NY)
 43   FORMAT(/,1X,3H P=,4F15.5)
 613  CONTINUE
      IM=I
      CALL COST
 5    CONTINUE
C---- SELECT LARGEST VALUE OF SUMY(I) IN SIMPLEX.
 82   SUMQ=SUMY(1)
      INDEY=1
      DO 133 I=2,M1
      IF (SUMY(I).LE.SUMQ) GO TO 133
      SUMQ=SUMY(I)
      INDEY=I
 133   CONTINUE
C---- SELECT MINIMUN VALUE OF SUMY(I) IN SIMPEX.
      SUMP=SUMY(1)
      MOUNT=1
      DO 81  I=2,M1
      IF (SUMP.LE.SUMY(I)) GO TO 81
      SUMP=SUMY(I)
      IF (IO.EQ.0) GO TO 772
      WRITE(3,102) SUMP,DIST
 772  CONTINUE
      MOUNT=I
 81   CONTINUE
C---- FIND CENTROID OF POINTS WITH I DIFFERENT THAN INDEX.
      DO 91 J=1,NY
      SUM1=0.0
      DO 103 I=1,M1
 103  SUM1=SUM1+Y1(I,J)
```

```
      Y1(M2,J)=1.0/YNY*(SUM1-Y1(INDEY,J))
C---- FIND REFLECTION OF HIGH POINT THROUGH CENTROID.
      Y1(M3,J)=(1.0+ALF)*Y1(M2,J)-ALF*Y1(INDEY,J)
 91   Y(J)=Y1(M3,J)
      IM=M3
      CALL COST
      IF (SUMY(M3).LT.SUMP) GO TO 61
C---- SELECT SECOND LARGEST VALUE IN SIMPLEX.
      IF (INDEY.EQ.1) GO TO 48
      SUMT=SUMY(1)
      GO TO 49
 48   SUMT=SUMY(2)
 49   DO 62 I=1,M1
      IF ((INDEY-I).EQ.0) GO TO 62
      IF (SUMY(I).LE.SUMT) GO TO 62
      SUMT=SUMY(I)
 62   CONTINUE
      IF (SUMY(M3).GT.SUMT) GO TO 63
      GO TO 65
C---- FORM EXPENSION OF NEW MINIMUN IF REFLECTION HAS
C     PRODUCED ONE MINIMUM.
 61   DO 66 J=1,NY
      Y1(M4,J)=(1.0-GAM)*Y1(M2,J)+GAM*Y1(M3,J)
 66   Y(J)=Y1(M4,J)
      IM=M4
      CALL COST
      IF (SUMY(M4).LT.SUMP) GO TO 67
      GO TO 65
C---- FORM CONTRACTION.
 63   IF (SUMY(M3).GT.SUMQ) GO TO 68
      DO 69 J=1,NY
 69   Y1(INDEY,J)=Y1(M3,J)
 68   DO 59 J=1,NY
      Y1(M4,J)=BET*Y1(INDEY,J)+(1.0-BET)*Y1(M2,J)
 59   Y(J)=Y1(M4,J)
      IM=M4
      CALL COST
      IF (SUMQ.GT.SUMY(M4)) GO TO 67
C---- REDUCE SIMPLEX BY HALF IF REFLECTION HAPPENS TO
C     PRODUCE A LARGER VALUE THAN THE MAXIMUM.
      DO 40 J=1,NY
      DO 40 I=1,M1
 40   Y1(I,J)=0.5*(Y1(I,J)+Y1(MOUNT,J))
      DO 79 I=1,M1
      DO 90 J=1,NY
 90   Y(J)=Y1(I,J)
      IM=I
      CALL COST
 79   CONTINUE
      GO TO 76
```

```
   67    DO 71 J=1,NY
         Y1(INDEY,J)=Y1(M4,J)
   71    Y(J)=Y1(INDEY,J)
         IM=INDEY
         CALL COST
         GO TO 76
   65    DO 72 J=1,NY
         Y1(INDEY,J)=Y1(M3,J)
   72    Y(J)=Y1(INDEY,J)
         IM=INDEY
         CALL COST
   76    DO 73 J=1,NY
   73    Y(J)=Y1(M2,J)
         IM=M2
         CALL COST
         DIST=0.0
         DO 74 I=1,M1
   74    DIST=DIST+(SUMY(I)-SUMY(M2))**2
         DIST=1.0/YNY*SQRT(DIST)
         IF (DIST.GE.0.005) GO TO 82
  889    CONTINUE
         IF(SUMP.GT.50.) GO TO 273
         IF(NUM.NE.IB) GO TO 4001
         WRITE(3,102) SUMP,DIST
  102    FORMAT(/,10X,6H SUMP=,E16.6,/10X,6H DIST=,E16.6)
         WRITE(3,334) (Y(I),I=1,NY)
  334    FORMAT(//,1X,'TA(1)=',F12.4,5X,'TA(2)=',F12.4,5X,
     1   'TA(3)=',F12.4,5X,'TSS=',F12.4)
C------ FIND THE ENERGY ACCUMULATED IN ALUMINUM FOR EACH
C       CYLINDRICAL SUBSHELL AND HEAT CONVECTED THROUGH
C       THE WATER LAYER IN THE TIME INTERVAL,BTU
         A(1)=P(7)*P(9)*(YO(1)-Y(1))
         A(2)=2.*P(7)*(R1+DRC)*(YO(2)-Y(2))
         A(3)=P(7)*P(12)*(YO(3)-Y(3))
         Q=P(10)*(TW-Y(4))
         WRITE(3,60) (A(I),I=1,3),Q
   60    FORMAT(/,1X,'A1=',E12.5,3X,'A2=',E12.5,3X,'A3=',
     1   E12.5,3X,'Q=',E12.5,4X,'ALL IN "BTU"')
C------ FIND THE TOTAL AMOUNT OF H2 REACTED UP TO THIS
C       POINT,LB MOLE
         WRITE(3,248) HMASS
  248    FORMAT(/,1X,'TOTAL HYDROGON REACTED=',F10.6,5X,
     1   'LB MOLE H2')
         WRITE(3,452)
  452    FORMAT(1X,'**********************************
     1   ****************************************')
         IB=IB+1
 4001    CONTINUE
         DO 502 IK=1,NY
  502    YO(IK)=Y(IK)
         IX=IX+1
```

```
      IF(IX-11) 1000,815,1000
  815 DELT=2./3600000.
 1000 CONTINUE
      WRITE(24,328) ((XO1(J,I),I=1,NX),J=1,NC),(YO(K),
     1 K=1,NY),HMASS,TIME
  328 FORMAT(18F10.5,4F10.4,F13.8,F14.7)
  273 STOP
      END
```

```
      SUBROUTINE VALUE
      DIMENSION A(30,30)
      COMMON /THREE/ Y(30),Y1(30,30),NY,STEPC,M1,SUMY(30),
     1 IM
      VN=NY
      STEPC1=STEPC/(VN*SQRT(2.))*(SQRT(VN+1.)+VN-1.0)
      STEPC2=STEPC/(VN*SQRT(2.))*(SQRT(VN+1.)-1.)
      I=1
      DO 1 J=1,NY
    1 A(I,J)=0.0
      DO 3 I=2,M1
      DO 2 J=1,NY
      A(I,J)=STEPC2
      L=I-1
      A(I,L)=STEPC1
    2 CONTINUE
    3 CONTINUE
      DO 5 I=1,M1
      DO 4 J=1,NY
    4 Y1(I,J)=Y(J)+A(I,J)
    5 CONTINUE
      RETURN
      END
C=======================
      SUBROUTINE COST
      DIMENSION F(4)
      COMMON /THREE/ Y(30),Y1(30,30),NY,STEPC,M1,SUMY(30),
     1 IM
      COMMON /FOUR/ TW,YO(8),NC,DRC,RO(8),NM,ACC(6)
      COMMON /FIVE/ P(12),AM
      F(1)=P(6)*P(8)*Y(2)-(P(6)*P(8)+P(7)*P(9))*Y(1)+
     1 ACC(1)+P(7)*P(9)*YO(1)
      DO 15 I=2,NM
   15 F(I)=(RO(I)-DRC/2.)*P(6)*Y(I-1)-2.*(P(6)+P(7))*RO
     1 (I)*Y(I)+(RO(I)+DRC/2.)*P(6)*Y(I+1)+2.*RO(I)*P(7)*
     1 YO(I)+ACC(I)
      F(NC)=P(6)*P(11)*Y(NM)-(P(6)*P(11)+P(7)*P(12))*
     1 Y(NC)-P(10)*(Y(NY)-TW)+P(7)*P(12)*YO(NC)+ACC(NC)
      F(NY)=Y(NY)-P(4)*Y(NC)-P(5)
      SUMY(IM)=0.
      DO 200 J=1,NY
  200 SUMY(IM)=SUMY(IM)+F(J)**2
      RETURN
      END
```

```
      SUBROUTINE START
      DIMENSION A(30,30)
      COMMON /ONE/ X(30),X1(30,30),NX,STEP,K1,SUM(30),IN
      VN=NX
      STEP1=STEP/(VN*SQRT(2.))*(SQRT(VN+1.)+VN-1.0)
      STEP2=STEP/(VN*SQRT(2.))*(SQRT(VN+1.)-1.)
      I=1
      DO 1 J=1,NX
    1 A(I,J)=0.0
      DO 3 I=2,K1
      DO 2 J=1,NX
      A(I,J)=STEP2
      L=I-1
      A(I,L)=STEP1
    2 CONTINUE
    3 CONTINUE
      DO 5 I=1,K1
      DO 4 J=1,NX
    4 X1(I,J)=X(J)+A(I,J)
    5 CONTINUE
      RETURN
      END
C=======================
      SUBROUTINE SUMR
      DIMENSION F(8),B(8)
      COMMON /ONE/ X(30),X1(30,30),NX,STEP,K1,SUM(30),IN
      COMMON /TWO/ TA,XO(30),NS,DRS,R(8),NP,NN,RM
      COMMON /FIVE/ P(12),AM
C---- THE EQUATIONS F(1) TO F(NP) RESULT FROM THE ENERGY
C     BALANCE FOR EACH CONTROL VOLUME.
      DO 5 J=2,NN
    5 B(J)=3.*R(J)**2+(DRS/2.)**2
      F(1)=X(1)-X(2)
      ID=NS-2
      DO 10 I=2,ID
      II=I+NS
   10 F(I)=P(1)*X(I-1)*(3.*(R(I)-(DRS/2.))**2)/B(I)-X(I)*
     1 (1.+6.*P(1)*(R(I)**2+(DRS/2.)**2)/B(I))+P(1)*X(I+1)*
     1 3.*(R(I)+(DRS/2.))**2/B(I)-P(2)*X(II)*1.E-3+(XO(I)+
     1 P(2)*XO(II))
      F(NN)=P(1)*X(NN-1)*3.*(R(NN)-DRS/2.)**2/B(NN)-X(NN)*
     1 (1.+P(1)*(7.*R(NN)**2+R(NN)*DRS+7.*(DRS/2.)**2)/B(NN))
     1 +P(1)*X(NS)*4.*(R(NN)+(DRS/2.))**2/B(NN)-P(2)*
     1 X(NX-1)*1.E-3+(XO(NN)+P(2)*XO(NX-1))
      RF=RM**3-(RM-DRS/2.)**3
      F(NS)=4.*P(1)*X(NN)*DRS*(RM-DRS/2.)**2/RF-X(NS)*(1.+
     1 4.*P(1)*DRS*((RM-DRS/2.)**2+3.*RM**2)/RF)+12.*TA*P(1)
     1 *DRS*RM**2/RF-P(2)*X(NX)*1.E-3+(XO(NS)+P(2)*XO(NX))
      IY=NS+2
      F(NP)=X(NP)-X(IY)
      DO 640 J=IY,NX
```

```
      IV=J-NS
      DM=-6698.
C---- THE FOLLOWING ARE THE EQULIBRIUM RELATIONS AMONG
C     TEMPERATURE,COMPOSITION AND PRESSURE FOR ADSORPTION
C     IF AM=1., FOR DESORPTION IF AM=-1.0  THEY ARE
C     OBTAINED BY COMBINATION OF THE ISOTHERMAL RELATION,
C     P=FUNCTION OF COMPOSITION, WITH THE VAN'T HOFF'S
C     EQUATION,LN(P)=A/T+B.
      IF(AM.LT.0.0) GO TO 20
      IF(X(J).LT.17.8) F(J)=(1268.2565*X(J)*1.E-3)*EXP(
     1 DM*(1./X(IV)-1./545.4))-P(3)
      IF(X(J).GE.17.8.AND.X(J).LE.133.51) F(J)=(-6388.3
     1 09*(1.E-3*X(J))**2+2192.365*1.E-3*X(J)-14.42506)*
     1 EXP(DM*(1./X(IV)-1./545.4))-P(3)
      IF(X(J).GT.133.51.AND.X(J).LE.638.94) F(J)=(44.75
     1 409*1.E-3*X(J)+158.4295)*EXP(DM*(1./X(IV)-1./545.4
     1 ))-P(3)
      IF(X(J).LE.861.63.AND.X(J).GT.638.94) F(J)=(3156.9
     1 05*(1.E-3*X(J))**2-3652.196*1.E-3*X(J)+1231.771)
     1 *EXP(DM*(1./X(IV)-1./545.4))-P(3)
      IF(X(J).GT.861.63) F(J)=(6111.793*1.E-3*X(J)-4837.
     1 469)*EXP(DM*(1./X(IV)-1./545.4))-P(3)
      GO TO 640
 20   CONTINUE
      IF(X(J).LT.83.859034) F(J)=735.*(0.145-SQRT(0.161
     1 01242**2-(1.E-3*X(J)+0.07)**2))*EXP(DM*(1./X(IV)
     1 -1./563.4))-P(3)
      IF(X(J).GE.83.859034.AND.X(J).LT.148.282324) F(J)=
     1 735.*(0.077+SQRT(0.0692283695**2-(1.E-3*X(J)-0.15)
     1 **2))*EXP(DM*(1./X(IV)-1./563.4))-P(3)
      IF(X(J).GE.148.282324.AND.X(J).LT.512.31435) F(J)=
     1 735.*(0.025*1.E-3*X(J)+0.1425)*EXP(DM*(1./X(IV)-
     1 1./563.4))-P(3)
      IF(X(J).GE.512.31435.AND.X(J).LT.582.04022) F(J)=
     1 735.*(0.23028443-SQRT(0.075**2-(1.E-3*X(J)-0.5104
     1 3994)**2))*EXP(DM*(1./X(IV)-1./563.4))-P(3)
      IF(X(J).GE.582.04022.AND.X(J).LT.729.21968) F(J)=
     1 735.*(0.14+SQRT(0.22830893**2-(1.E-3*X(J)-0.8)**2
     1 ))*EXP(DM*(1./X(IV)-1./563.4))-P(3)
      IF(X(J).GE.729.21968.AND.X(J).LT.905.) F(J)=735.*
     1 (0.6-SQRT(0.25552989**2-(1.E-3*X(J)-0.65)**2))
     1 *EXP(DM*(1./X(IV)-1./563.4))-P(3)
 640  CONTINUE
      SUM(IN)=0.
      DO 200 J=1,NX
 200  SUM(IN)=SUM(IN)+F(J)**2
      RETURN
      END
```

```
      FUNCTION HEAT(HOM,V)
C     THIS IS A FUNCTION TO DETERMINE THE HEAT OF
C     REACTION OF FETIHY AS A FUNCTION OF THE HYDROGEN
C     TO METAL RATIO.

C     THE VALUES FOR HOM RANGING FROM 0.05 TO 0.8 ARE
C     GIVEN IN "PHYSICAL METALLURGY OF FETI-HYDRIDE AND
C     ITS BEHAVIOR IN A HYDROGEN STORAGE CONTAINER" BY
C     M. A. PICK AND H. WENZL IN 1ST WORLD HYDROGEN
C     ENERGY CONFERENCE,VOL. 2,PG.8B-29. THEY DERIVED
C     USING THE VAN'T HOFF'S EQUATION LN(P)=(A/T)+B.
C     THE HEAT OF REACTION FOR THE FORMATION OF FETIHY,
C     Y=1.10,IS TAKEN FROM THE AVERAGE VALUE OF 30 +OR-
C     1.5 KJ/MOLE H2 GIVEN ON PG.8G-30.  NO TEMPERATURE
C     DEPENDENCE IS GIVEN FOR THESE VALUES.

C     DENSITY OF FETI = 405.79 LB/FT**3
C     TO CONVERT THE DIMENSION OF THE HEAT OF REACTION
C     FROM BTU/LB H2 TO BTU/HOM*FT**3
C     HEAT=HEAT*(1.-V)*DEN OF METAL*1.LB/LB MOLE H*
C     LB MOLE/103.75 LB METAL*2*(1.LB MOLE FE+1.LB
C     MOLE TI)/LB MOLE FETI=HEAT*(1.-V)*7.82

C    VARIABLE NAMES AND UNITS:
C    HEAT = HEAT OF REACTION IN BTU/HOM*FT3
C    HOM = HYDROGEN TO METAL RATIO. FOR FETIHY HOM=Y/2

      IF(HOM.LE.0.52) GO TO 10
      IF(HOM.LE.0.6.AND.HOM.GT.0.52) GO TO 20
      IF(HOM.LE.0.7.AND.HOM.GT.0.6) GO TO 30
      IF(HOM.GT.0.7) GO TO 40
10    HEAT=-6058.90
      GO TO 60
20    HEAT=-6669.95
      GO TO 60
30    HEAT=-7164.82
      GO TO 60
40    HEAT=-7250.88
60    HEAT=HEAT*(1.-V)*7.82
      RETURN
      END
```

```
      FUNCTION THCON(P)
C     THIS FUNCTION CALCULATES THE THERMAL CONDUCTIVITY IN
C     BTU/HR-FT-F FOR THE PACKING BED OF FETIH.

C     THE THERMAL CONDUCTIVITY IS EXPRESSED AS A
C     FUNCTION OF THE HYDROGEN PRESSURE.

C     THE FUNCTION IS A REPRESENTATION OF OUR
C     EXPERIMENTAL RESULTS.

C     VARIABLE NAMES:
C     P=PRESSURE IN PSIA H2
C     THCON=THERMAL CONDUCTIVITY IN BTU/HR-FT-F

      IF(P.GT.1.25.AND.P.LE.3.0) GO TO 3
      IF(P.GT.3.AND.P.LE.11.87) GO TO 5
      IF(P.GT.11.87.AND.P.LT.59.7) GO TO 10
      IF(P.GE.59.7)GO TO 15
    1 THCON=0.48040608*P+0.11472394
      GO TO 20
    3 THCON=-7.2502671E-2*P**2+0.41915179*P+0.30282380
      GO TO 20
    5 THCON=1.8966791E-2*P+0.86335858
      GO TO 20
   10 THCON=-8.3479038E-5*P**2+7.2474839E-3*P+1.0334596
      GO TO 20
   15 THCON=1.8380527E-4*P+1.1787640
   20 RETURN
      END
```

```
      FUNCTION DENS(HCM)
C     THIS FUNCTION CALCULATES THE DENSITY OF FETIHY IN
C     LB/FT**3

C     VALUES FOR THE DENSITY AS A FUNCTION OF THE HYDROGEN
C     TO METAL RATIO WERE FOUND IN REPORTS("FORMATION AND
C     PROPERTIES OF IRON TITANIUM HYDRIDE" BY J.J.REILLY
C     AND R.H. WISWALL,JR.). THESE VALUES WERE GRAPHED AND
C     TAKEN AS A LINEAR FUNCTION:
C        DENS=405.79-67.5*HCM

C     THE HYDROGEN TO METAL RAIO FOR FETIHY IS Y/2.

C     VARIABLE NAMES AND UNITS:
C     DENS = DENSITY OF FETIHY IN LB/FT**3
C     HCM = HYDROGEN TO METAL RATIO

      DENS = 405.79 - 67.5*HCM
      RETURN
      END
```

```
      FUNCTION CAPAC(P,T,E,DENS)
C     THIS FUNCTION CALCULATES THE HEAT CAPACITY OF THE
C     HYDRIDE BED.

C     TABLES AND GRAPHS SHOWING THE SPECIFIC HEAT FOR IRON
C     TITANIUM HYDRIDE WERE FOUND AS FUNCTIONS OF
C     TEMPERATURE.

C     TWO GRAPHS SEEM TO CANCEL EACH OTHER GIVING A
C     CONSTANT CLOSE TO 0.14 BTU/LB-R REPORTED AS AN
C     APPROXIMATION IN "MODELING STUDIES OF FIXED-BED
C     METAL-HYDRIDE STORAGE SYSTEMS" ON PG.624

C     THE HEAT CAPACITY OF HYDROGEN IS A FUNCTION OF
C     PRESSURE AND TEMPERATURE,ASSUMING THAT IT BEHAVES
C     LIKE AN IDEAL GAS,IN THE TEMPERATURE RANGE CONCERNED
C     IT IS ESTIMATED TO BE 3.4 BTU/LB-R.

C     THE HEAT CAPACITY OF THE BED IS FOUND IN THE
C     EQUATION:
C        CPS*DENS*(1-E)+ CPG*(P*M/R*T)*E
C     WHERE
C       R= 10.73 PSIA-FT**3/LB MOLE-R, UNIVERSAL GAS
C          CONSTANT
C       CPS= 0.14 BTU/LB-R, SPECIFIC HEAT OF SOLID
C       CPG= 3.4 BTU/LB-R, SPECIFIC HEAT OF HYDROGEN GAS
C       M = 2.016 LB/LB MOLE,MOLECULAR WEIGHT OF HYDROGEN
C       DENS=DENSITY OF BED IN LB/FT**3
C       E = VOID FRACTION OF BED
C       P = PRESSURE OF HYDROGEN IN PSIA
C       T = TEMPERATURE IN DEGREE R

      CAPAC=0.14*(1.-E)*DENS + 0.634*P*E/T
      RETURN
      END
```

```
C——— THIS PROGRAM IS RUN WITH 'SUBROUTINE BEGIN' AND
C      'SUBROUTINE TOTAL' TO FIND THE THERMAL DIFFUSIVITY.
C***** OPTIMIZATION METHOD OF NELDER AND MEAD (SIMPLEX) *****
C——— NX = NO. OF INDEPENDENT VARIABLE
C——— STEP = INITIAL STEP SIZE
C——— X(I) = INITIAL GUESSES
C——— T1 = INITIAL TEMPERATURE OF THE TESTED MATERIAL
C——— TO = TEMPERATURE ON THE OUTSIDE WALL OF THE  CYLINDER
      DIMENSION  T(50)
      COMMON /ONE/ X(30),X1(30,30),NX,STEP,K1,SUM(30),
     1  IN,Y(50)
      COMMON /TWO/ N,TIM(50)
      NX=2
      X(1)=0.006
      X(2)=0.0000001
C——— X(2) IS A DUMMY PARAMETER.
      T1=30.25
      TO=50.
      N=30
      WRITE(5,444)
 444  FORMAT (1X,'THE FOLLOWING DATA ARE FOR THE COOLING
     1  RUN UNDER 420 PSIG ARGON FROM 30.25 TO 50.C')
      WRITE(5,777)
 777  FORMAT(/,7X,'TIME=,SEC',6X,'TEMPERATURE=, C',/)
      DO 100 I=1,N
      READ(23,*) TIM(I),T(I)
      WRITE(5,888) TIM(I),T(I)
 888  FORMAT (1X,F15.4,5X,F12.4)
 100   Y(I)=(T(I)-T1)/(TO-T1)
      STEP=0.01
      IF (NX) 998,999,998
 998  CONTINUE
C——— ALFA = REFLECTION COEFFICIENT
C——— BETA = CONTRACTION COEFFICIENT
C——— GAMA = EXPENSION COEFFICIENT
      ALFA=1.0
      BETA=0.5
      GAMA=2.0
      DIFER=0.0
      XNX=NX
      IN=1
      IP=0
      CALL TOTAL
C——— K1 = NUMBER OF VERTICES    K2 = INDEX OF CENTROID
C——— K3 = INDEX OF REFLECTION
C——— K4 = INDEX OF EXPENSION OR CONTRACTION
      K1=NX+1
      K2=NX+2
      K3=NX+3
      K4=NX+4
      CALL BEGIN
  25  DO 3 I=1,K1
      DO 4 J=1,NX
```

```
    4   X(J)=X1(I,J)
        WRITE(5,41) (X(JK),JK=1,NX)
   41   FORMAT (1X,3H P=,4F7.3)
        IN=I
        CALL TOTAL
    3   CONTINUE
C------ SELECT LARGEST VALUE OF SUM(I) IN SIMPLEX.
   28   SUMH=SUM(1)
        INDEX=1
        DO 7 I=2,K1
        IF (SUM(I).LE.SUMH) GO TO 7
        SUMH=SUM(I)
        INDEX=I
    7   CONTINUE
C------ SELECT MINIMUM VALUE OF SUM(I) IN SIMPLEX.
        SUML=SUM(1)
        KOUNT=1
        DO 8 I=2,K1
        IF (SUML.LE.SUM(I)) GO TO 8
        SUML=SUM(I)
        IF (IP.EQ.0) GO TO 771
        WRITE(5,101) SUML,(X1(KOUNT,J),J=1,NX),DIFER
  771   CONTINUE
        KOUNT=I
    8   CONTINUE
C------ FIND CENTROID OF POINTS WITH I DIFFERENT THAN INDEX.
        DO 9 J=1,NX
        SUM2=0.0
        DO 10 I=1,K1
   10   SUM2=SUM2+X1(I,J)
        X1(K2,J)=1.0/XNX*(SUM2-X1(INDEX,J))
C------ FIND REFLECTION OF HIGH POINT THROUGH CENTROID.
        X1(K3,J)=(1.0+ALFA)*X1(K2,J)-ALFA*X1(INDEX,J)
    9   X(J)=X1(K3,J)
        IN=K3
        CALL TOTAL
        IF (SUM(K3).LT.SUML) GO TO 11
C------ SELECT SECOND LARGEST VALUE IN SIMPLEX.
        IF (INDEX.EQ.1) GO TO 38
        SUMS=SUM(1)
        GO TO 39
   38   SUMS=SUM(2)
   39   DO 12 I=1,K1
        IF ((INDEX-I).EQ.0) GO TO 12
        IF (SUM(I).LE.SUMS) GO TO 12
        SUMS=SUM(I)
   12   CONTINUE
        IF (SUM(K3).GT.SUMS) GO TO 13
        GO TO 14
C------ FORM EXPENSION OF NEW MINIMUM IF REFLECTION HAS
C       PRODUCED ONE MINIMUM.
   11   DO 15 J=1,NX
```

```
      X1(K4,J)=(1.0-GAMA)*X1(K2,J)+GAMA*X1(K3,J)
   15 X(J)=X1(K4,J)
      IN=K4
      CALL TOTAL
      IF (SUM(K4).LT.SUML) GO TO 16
      GO TO 14
C---- FORM CONTRACTION.
   13 IF (SUM(K3).GT.SUMH) GO TO 17
      DO 18 J=1,NX
   18 X1(INDEX,J)=X1(K3,J)
   17 DO 19 J=1,NX
      X1(K4,J)=BETA*X1(INDEX,J)+(1.0-BETA)*X1(K2,J)
   19 X(J)=X1(K4,J)
      IN=K4
      CALL TOTAL
      IF (SUMH.GT.SUM(K4)) GO TO 16
C---- REDUCE SIMPLEX BY HALF IF REFLECTION HAPPENS TO
C     PRODUCE A LARGER VALUE THAN THE MAXIMUM.
      DO 20 J=1,NX
      DO 20 I=1,K1
   20 X1(I,J)=0.5*(X1(I,J)+X1(KOUNT,J))
      DO 29 I=1,K1
      DO 30 J=1,NX
   30 X(J)=X1(I,J)
      IN=I
      CALL TOTAL
   29 CONTINUE
      GO TO 26
   16 DO 21 J=1,NX
      X1(INDEX,J)=X1(K4,J)
   21 X(J)=X1(INDEX,J)
      IN=INDEX
      CALL TOTAL
      GO TO 26
   14 DO 22 J=1,NX
      X1(INDEX,J)=X1(K3,J)
   22 X(J)=X1(INDEX,J)
      IN=INDEX
      CALL TOTAL
   26 DO 23 J=1,NX
   23 X(J)=X1(K2,J)
      IN=K2
      CALL TOTAL
      DIFER=0.0
      DO 24 I=1,K1
   24 DIFER=DIFER+(SUM(I)-SUM(K2))**2
      DIFER=1.0/XNX*SQRT(DIFER)
      IF (DIFER.GE.0.00001) GO TO 28
      WRITE(5,101) SUML,(X1(KOUNT,J),J=1,NX),DIFER
  101 FORMAT (1X,6H SUML=,E16.6,/1X,6H X(I)=,2E16.6,
     1 /1X,7H DIFER=,E15.6)
C---- CHANGE THE DIMENSION OF X(1) FROM IN**2/MIN
```

```
C       TO FT**2/HR.
        X(1)=0.4166666*X(1)
        WRITE(5,333) X(1)
  333   FORMAT(/,1X,'X(1)=EFFECTIVE THERMAL DIFFUSIVITY'
     1  ,/5X,'=',F8.6,2X,'FT**2/HR')
  999   CONTINUE
        STOP
        END
```

```
      SUBROUTINE BEGIN
      DIMENSION A(30,30)
      COMMON /ONE/ X(30),X1(30,30),NX,STEP,K1,SUM(30),
     1 IN,Y(50)
      COMMON /TWO/ N,TIM(50)
      VN=NX
      STEP1=STEP/(VN*SQRT(2.))*(SQRT(VN+1.)+VN-1.0)
      STEP2=STEP/(VN*SQRT(2.))*(SQRT(VN+1.)-1.)
      I=1
      DO 1 J=1,NX
    1 A(I,J)=0.0
      DO 3 I=2,K1
      DO 2 J=1,NX
      A(I,J)=STEP2
      L=I-1
      A(I,L)=STEP1
    2 CONTINUE
    3 CONTINUE
      DO 5 I=1,K1
      DO 4 J=1,NX
    4 X1(I,J)=X(J)+A(I,J)
    5 CONTINUE
      RETURN
      END
C=======================
      SUBROUTINE TOTAL
      DIMENSION R1(100),R2(100),R3(100),R4(100),R5(100)
      COMMON /ONE/ X(30),X1(30,30),NX,STEP,K1,SUM(30),
     1 IN,Y(50)
      COMMON /TWO/ N,TIM(50)
      SUM(IN)=0.
      DO 200 J=1,N
      TIME=TIM(J)/60.
      R1(J)=1.617*EXP(-12.2352*X(1)*TIME)
      R2(J)=1.06468*EXP(-64.4686*X(1)*TIME)
      R3(J)=0.85126*EXP(-158.437*X(1)*TIME)
      R4(J)=0.7294*EXP(-294.166*X(1)*TIME)
  200 SUM(IN)=SUM(IN)+(Y(J)-1.+(R1(J)-R2(J)+R3(J)
     1 -R4(J)))**2+X(2)**2
      RETURN
      END
```

```
C       THE FOLLOWING PROGRAM IS TO FIND THE EFFECTIVE
C       THERMAL DIFFUSIVITY WITH PATERN SEARCH TECHNIQUE.
        COMMON TT(100),T1(100),TC(100),N
        DIMENSION P(2),STEP(2)
        P(1)=0.12
        P(2)=0.000001
        STEP(1)=0.0001
        STEP(2)=0.1
        N=56
        NP=2
        NPASS=4
        IC=2
        READ(20,*)(TT(I),T1(I),TC(I),I=1,N)
        WRITE (5,200)(TT(I),T1(I),TC(I),I=1,N)
  200   FORMAT (1X,3F15.3)
        CALL PATERN (NP,P,STEP,NPASS,IC,COST)
        WRITE(5,300) P(1),P(2),COST
  300   FORMAT (1X,'THE EFFECTIVE THERMAL DIFFUSIVITY IS',
     1  F8.6,5X,'DUMMY PARAMETER=',F10.7,5X,'COST=',E20.6)
        STOP
        END
```

```
      SUBROUTINE PATERN(NP,P,STEP,NRD,IO,COST)
C-----THE SIZE OF B1,B2,T,AND S NEED ONLY BE EQUAL TO
C     THE NUMBER OF PAR
      DIMENSION P(10),STEP(10),B1(10),B2(10),T(10),S(10)
C-----STARTING POINT
      L=1
      ICK=2
      ITTER=0
      DO 5 I=1,NP
      B1(I)=P(I)
      B2(I)=P(I)
      T(I)=P(I)
 5    S(I)=STEP(I)*10.
C-----INITIAL BOUNDARY CHECK AND COST EVALUATION
      CALL BOUNDS(P,IOUT)
      IF(IOUT.LE.0) GO TO 10
                    IF(IO.LE.0) GO TO 6
                    WRITE(5,1005)
                    WRITE(5,1000)(J,P(J),J=1,NP)
 6    RETURN
 10   CALL PROC(P,C1)
                    IF(IO.LE.0) GO TO 11
                    WRITE(5,1001)ITTER,C1
                    WRITE(5,1000)(J,P(J),J=1,NP)
C-----BEGINNING OF PATTERN SEARCH STRATEGY
 11   DO 99 INRD=1,NRD
      DO 12 I=1,NP
 12   S(I)=S(I)/10.0
                    IF(IO.LE.0) GO TO 20
                    WRITE(5,1003)
                    WRITE(5,1000)(J,S(J),J=1,NP)
      WRITE(5,1000) (J,P(J),J=1,NP)
 20   IFAIL=0.0
C-----PRETURBATION ABOUT T
      DO 30 I=1,NP
        IF (L.GT.3000) GO TO 888
      IC=0
 21   P(I)=T(I)+S(I)
      IC=IC+1
      CALL BOUNDS(P,IOUT)
      IF(IOUT.GT.0) GO TO 23
      CALL PROC(P,C2)
                    L=L+1
                    IF(IO.LT.3) GO TO 22
                    WRITE(5,1002)L,C2
                    WRITE(5,1000)(J,P(J),J=1,NP)
 22   IF(C1-C2)23,23,25
 23   IF(IC.GE.2) GO TO 24
      S(I)=-S(I)
      GO TO 21
 24   IFAIL=IFAIL+1
      P(I)=T(I)
```

```
      GO TO 30
   25 T(I)=P(I)
      C1=C2
   30 CONTINUE
      IF(IFAIL.LT.NP) GO TO 35
      IF(ICK.EQ.2) GO TO 90
      IF(ICK.EQ.1) GO TO 35
      CALL PROC(T,C2)
                    L=L+1
                    IF(IO.LT.2) GO TO 31
                    WRITE(5,1002)L,C2
                    WRITE(5,1000)(J,T(J),J=1,NP)
   31 IF(C1-C2)32,34,34
   32 ICK=1
      DO 33 I=1,NP
      B1(I)=B2(I)
      P(I)=B2(I)
   33 T(I)=B2(I)
      GO TO 20
   34 CONTINUE
        C1=C2
   35 IB1=0
      DO 39 I=1,NP
      B2(I)=T(I)
      IF(ABS(B1(I)-B2(I)).LT.1.0E-20)IB1=IB1+1
   39 CONTINUE
      IF(IB1.EQ.NP) GO TO 90
      ICK=0
                    ITTER=ITTER+1
                    IF(IO.LT.2) GO TO 40
                    WRITE(5,1001)ITTER,C1
                    WRITE(5,1000)(J,T(J),J=1,NP)
C-----ACCELERATION STEP
   40 SJ=1.0
      DO 45 II=1,11
        IF (II.EQ.11) SJ=0.0
      DO 42 I=1,NP
      T(I)=B2(I)+SJ*(B2(I)-B1(I))
   42 P(I)=T(I)
      SJ=SJ-.1
      CALL BOUNDS(T,IOUT)
      IF(IOUT.LT.1) GO TO 46
      IF(II.EQ.11)ICK=1
   45 CONTINUE
   46 DO 47 I=1,NP
   47 B1(I)=B2(I)
      GO TO 20
   90 DO 91 I=1,NP
   91 T(I)=B2(I)
   99 CONTINUE
  888 DO 100 I=1,NP
  100 P(I)=T(I)
```

```
      COST=C1
                    IF(IO.LE.0)RETURN
                    WRITE(5,1004)L,C1
        WRITE(5,1000)(P(J),J=1,NP)
      RETURN
1000  FORMAT(6X,3(4H  P(,I2,2H):,F8.4)/)
1001  FORMAT(//1X14HITTERATION NO.  ,I5/5X,5HCOST= ,
     1    E15.6,20X,10HPARAMETERS)
1002  FORMAT(10X3HNO.,I4, 8X5HCOST=,E15.6)
1003  FORMAT(/1X28HSTEP SIZE FOR EACH PARAMETER   )
1004  FORMAT(1H113HANSWERS AFTER ,I6,2X,23HFUNCTIONAL
     1EVALUATIONS // 5X5HCOST=,E15.6,20X,18HOPTIMAL PARAMETERS)
1005  FORMAT(1H135HINITIAL PARAMETERS OUT OF BOUNDS   )
      END
```

```
      SUBROUTINE PROC(P,COST)
      DIMENSION P(2),Y(100),YY(100),R1(100),R2(100),R3(100),
     1  R4(100),R5(100)
      COMMON TT(100),T1(100),TC(100),N
      A=P(1)
      B=P(2)
      SUM=0.
      DELT=0.2
      TIME=-0.2
      DO 10 I=1,N
      TIME=TIME+DELT
      R1(I)=1.617*EXP(-3.85376*A*TIME)
      R2(I)=1.06468*EXP(-20.3058*A*TIME)
      R3(I)=0.85126*EXP(-49.9C292*A*TIME)
      R4(I)=0.7294*EXP(-92.6541*A*TIME)
      R5(I)=0.64836*EXP(-148.55953*A*TIME)
      YY(I)=1.-(R1(I)-R2(I)+R3(I)-R4(I)+R5(I))
      Y(I)=(TT(I)-T1(I))/(TC(I)-T1(I))
10    SUM=SUM+(Y(I)-YY(I))**2+B**2
      COST=SUM
      RETURN
      END
```

```
SUBROUTINE BOUNDS(P,IOUT)
DIMENSION P(2)
IOUT=0.0
IF(P(1).LT.0.0)IOUT=1
RETURN
END
```

```
C---- THIS PROGRAM, TOGETHER WITH THE SUBROUNTINES LEAR
C     AND PAR, IS USED TO CALCULATE THE LINEAR PARAMETERS
C     A AND B IN K=A/T+B, HERE K IS THE THERMAL CONDUCTIVITY
C     AND T THE TEMPERATURE.
C***** OPTIMIZATION METHOD OF NELDER AND MEAD (SIMPLEX) *****
C---- NX = NO. OF INDEPENDENT VARIABLE
C---- STEP = INITIAL STEP SIZE
C---- X(I) = INITIAL GUESSES
      COMMON /ONE/ X(30),X1(30,30),NX,STEP,K1,SUM(30),IN
     1  ,Y(50)
      COMMON /TWO/ N,TIM(50),T(50)
      NX=2
      X(1)=-460.
      X(2)=2.0925
      N=7
      WRITE(3,444)
  444 FORMAT (1X,'THE FOLLOWING DATA ARE FOR THE
     1 RUNS UNDER 1 ATM H2  FROM 9 TO 75C')
      WRITE(3,777)
  777 FORMAT(/,1X,'CONDUCTIVITY,BTU/HR.FT.R',6X,
     1 'TEMPERATURE=,R')
      DO 100 I=1,N
      READ(23,*) TIM(I),T(I)
      WRITE(3,888) TIM(I),T(I)
  888 FORMAT (1X,F15.8,5X,F12.8)
  100  CONTINUE
      STEP=0.3
      IF (NX) 998,999,998
  998 CONTINUE
C---- ALFA = REFLECTION COEFFICIENT
C---- BETA = CONTRACTION COEFFICIENT
C---- GAMA = EXPENSION COEFFICIENT
      ALFA=1.0
      BETA=0.5
      GAMA=2.0
      DIFER=0.0
      XNX=NX
      IN=1
      IP=0
      CALL PAR
C---- K1 = NUMBER OF VERTICES    K2 = INDEX OF CENTROID
C---- K3 = INDEX OF REFECTION
C---- K4 = INDEX OF EXPENSION OR CONTRACTION
      K1=NX+1
      K2=NX+2
      K3=NX+3
      K4=NX+4
      CALL LEAL
   25 DO 3 I=1,K1
      DO 4 J=1,NX
    4 X(J)=X1(I,J)
      WRITE(3,41) (X(JK),JK=1,NX)
   41 FORMAT (1X,3H P=,2F12.5)
```

```
      IN=I
      CALL PAR
    3 CONTINUE
C---- SELECT LARGEST VALUE OF SUM(I) IN SIMPLEX
   28 SUMH=SUM(1)
      INDEX=1
      DO 7 I=2,K1
      IF (SUM(I).LE.SUMH) GO TO 7
      SUMH=SUM(I)
      INDEX=I
    7 CONTINUE
C---- SELECT MINIMUM VALUE OF SUM(I) IN SIMPLEX
      SUML=SUM(1)
      KOUNT=1
      DO 8 I=2,K1
      IF (SUML.LE.SUM(I)) GO TO 8
      SUML=SUM(I)
      IF (IP.EQ.0) GO TO 771
      WRITE(3,101) SUML,(X1(KOUNT,J),J=1,NX),DIFER
  771 CONTINUE
      KOUNT=I
    8 CONTINUE
C---- FIND CENTROID OF POINTS WITH I DIFFERENT THAN INDEX
      DO 9 J=1,NX
      SUM2=0.0
      DO 10 I=1,K1
   10 SUM2=SUM2+X1(I,J)
      X1(K2,J)=1.0/XNX*(SUM2-X1(INDEX,J))
C---- FIND REFLECTION OF HIGH POINT THROUGH CENTROID
      X1(K3,J)=(1.0+ALFA)*X1(K2,J)-ALFA*X1(INDEX,J)
    9 X(J)=X1(K3,J)
      IN=K3
      CALL PAR
      IF (SUM(K3).LT.SUML) GO TO 11
C---- SELECT SECOND LARGEST VALUE IN SIMPLEX
      IF (INDEX.EQ.1) GO TO 38
      SUMS=SUM(1)
      GO TO 39
   38 SUMS=SUM(2)
   39 DO 12 I=1,K1
      IF ((INDEX-I).EQ.0) GO TO 12
      IF (SUM(I).LE.SUMS) GO TO 12
      SUMS=SUM(I)
   12 CONTINUE
      IF (SUM(K3).GT.SUMS) GO TO 13
      GO TO 14
C---- FORM EXPENSION OF NEW MINIMUM IF REFLECTION HAS
C     PRODUCED ONE MIN.
   11 DO 15 J=1,NX
      X1(K4,J)=(1.0-GAMA)*X1(K2,J)+GAMA*X1(K3,J)
   15 X(J)=X1(K4,J)
      IN=K4
      CALL PAR
      IF (SUM(K4).LT.SUML) GO TO 16
```

```
      GO TO 14
C---- FORM CONTRACTION
   13 IF (SUM(K3).GT.SUMH) GO TO 17
      DO 18 J=1,NX
   18 X1(INDEX,J)=X1(K3,J)
   17 DO 19 J=1,NX
      X1(K4,J)=BETA*X1(INDEX,J)+(1.C-BETA)*X1(K2,J)
   19 X(J)=X1(K4,J)
      IN=K4
      CALL PAR
      IF (SUMH.GT.SUM(K4)) GO TO 16
C---- REDUCE SIMPLEX BY HALF IF REFLECTION HAPPENS
C     TO PRODUCE A LARGER VALUE THAN THE MAX.
      DO 20 J=1,NX
      DO 20 I=1,K1
   20 X1(I,J)=0.5*(X1(I,J)+X1(KOUNT,J))
      DO 29 I=1,K1
      DO 30 J=1,NX
   30 X(J)=X1(I,J)
      IN=I
      CALL PAR
   29 CONTINUE
      GO TO 26
   16 DO 21 J=1,NX
      X1(INDEX,J)=X1(K4,J)
   21 X(J)=X1(INDEX,J)
      IN=INDEX
      CALL PAR
      GO TO 26
   14 DO 22 J=1,NX
      X1(INDEX,J)=X1(K3,J)
   22 X(J)=X1(INDEX,J)
      IN=INDEX
      CALL PAR
   26 DO 23 J=1,NX
   23 X(J)=X1(K2,J)
      IN=K2
      CALL PAR
      DIFER=0.C
      DO 24 I=1,K1
   24 DIFER=DIFER+(SUM(I)-SUM(K2))**2
      DIFER=1.0/XNX*SQRT(DIFER)
      IF (DIFER.GE.0.0000001) GO TO 28
  999 CONTINUE
      WRITE(3,101) SUML,(X1(KOUNT,J),J=1,NX),DIFER
  101 FORMAT (1X,6H SUML=,E16.6,/1X,6H X(I)=,2E16.6,/1X,
     1 7H DIFER=,E15.6)
      WRITE(3,333) X(1),X(2)
  333 FORMAT(/,2F15.8)
      STOP
      END
```

```
      SUBROUTINE LEAL
      DIMENSION A(30,30)
      COMMON /ONE/ X(30),X1(30,30),NX,STEP,K1,SUM(30),IN,Y(50)
      COMMON /TWO/ N,TIM(50)
      VN=NX
      STEP1=STEP/(VN*SQRT(2.))*(SQRT(VN+1.)+VN-1.0)
      STEP2=STEP/(VN*SQRT(2.))*(SQRT(VN+1.)-1.)
      I=1
      DO 1 J=1,NX
    1 A(I,J)=0.0
      DO 3 I=2,K1
      DO 2 J=1,NX
      A(I,J)=STEP2
      L=I-1
      A(I,L)=STEP1
    2 CONTINUE
    3 CONTINUE
      DO 5 I=1,K1
      DO 4 J=1,NX
    4 X1(I,J)=X(J)+A(I,J)
    5 CONTINUE
      RETURN
      END
C=======================
      SUBROUTINE PAR
      DIMENSION R(10)
      COMMON /ONE/ X(30),X1(30,30),NX,STEP,K1,SUM(30),IN,Y(50)
      COMMON /TWO/ N,TIM(50),T(50)
      SUM(IN)=0.
      DO 200 J=1,N
      R(J)=X(1)/T(J)+X(2)
  200 SUM(IN)=SUM(IN)+(TIM(J)-R(J))**2
      RETURN
      END
```

```
C---- THIS PROGRAM IS TO GENERATE A SET OF DATA WITH
C     KNOWN THERMAL DIFFUSIVITY,AND THEN TO DRAW A PLOT.
      DIMENSION Y(200),X(200),R1(200),R2(200),R3(200)
     1  ,R4(200),R5(200),Z(200)
      ALPHA = 0.00026444
C---- ALPHA IS THE THERMAL DIFFUSIVITY IN IN**2/SEC.
      T1=30.25
      TO=50.
      TIME = 0.0
      NOBS=90
      DO 100 I=1,NOBS
      TIME = TIME+10.
      X(I)=TIME
      R1(I)=1.617*EXP(-12.2352*ALPHA*TIME)
      R2(I)=1.06468*EXP(-64.4686*ALPHA*TIME)
      R3(I)=0.85126*EXP(-158.437*ALPHA*TIME)
      R4(I)=0.7294*EXP(-294.166*ALPHA*TIME)
      R5(I)=0.64836*EXP(-471.657*ALPHA*TIME)
      Y(I)=1.-(R1(I)-R2(I)+R3(I)-R4(I)-R5(I))
  100 Z(I)=T1+Y(I)*(TO-T1)
      WRITE (20,200) (X(I),Z(I),I=1,NOBS)
  200 FORMAT (1X,2F15.5)
      CALL PLTR (X,Y,NOBS)
      STOP
      END
```

```
      SUBROUTINE PLTR(X,Y,NN)
      REAL XX(6),X(NN),Y(NN)
C
C     ON BYTE MACHINES (IBM-360/370) MAKE LOGICAL*1
C     TO SAVE SPACE
      LOGICAL LXY(51,31),IBLANK,ISTAR
      DATA LXY/ 1581*' '/,IBLANK/' '/,ISTAR/'*'/
      NXL=51
      NYL=21
      NOBS=NN
      YMIN=Y(1)
      YMAX=YMIN
      XMAX=X(1)
      XMIN=XMAX
      DO 10 I=2,NOBS
        IF(YMAX.LT.Y(I)) YMAX=Y(I)
        IF(YMIN.GT.Y(I)) YMIN=Y(I)
        IF(XMAX.LT.X(I)) XMAX=X(I)
10      IF(XMIN.GT.X(I)) XMIN=X(I)
      IF (XMAX.NE.XMIN) GOTO 12
        XMAX=1.05*XMAX+0.5
        XMIN=1.05*XMIN-0.5
12    IF(YMAX.NE.YMIN) GOTO 15
        YMAX=1.05*YMAX+0.5
        YMIN=1.05*YMIN-0.5
15    XINC=(NXL-1)/(XMAX-XMIN)
      YINC=(NYL-1)/(YMAX-YMIN)
      DO 20   I=1,NOBS
      NX=(X(I)-XMIN)*XINC+1
      NY=(YMAX-Y(I))*YINC+1
C     IF(NX.GT.NXL.OR.NX.LT.1.OR.NY.GT.NYL.OR.NY.LT.1)
C     GO TO 20
      LXY(NX,NY)=ISTAR
 20   CONTINUE
      XX(1)=XMIN
      XX(2)=XMIN+20./XINC
      XX(3)=XMIN+40./XINC
      XX(4)=XMIN+10./XINC
      XX(5)=XMIN+30./XINC
      XX(6)=XMAX
            WRITE(3,6000)
6000  FORMAT(//)
6010  FORMAT(10X,3G20.6/20X,3G20.6)
6020  FORMAT(20X,'*',5(10H+....'....),'+')
6030  FORMAT(5X,G15.7,'-',51A1)
            WRITE(3,6020)
      DO 40 I=1,NYL
      YY=(1-I)/YINC+YMAX
 40           WRITE(3,6030)YY,(LXY(J,I),J=1,NXL)
              WRITE(3,6020)
              WRITE(3,6010)XX
      DO 50 I=1,NOBS
```

```
      NX=(X(I)-XMIN)*XINC+1
      NY=(YMAX-Y(I))*YINC+1
C     IF(NX.GT.NXL.OR.NX.LT.1.OR.NY.GT.NYL.OR.NY.LT.1)
C     GO TO 50
      LXY(NX,NY)=LBLANK
   50 CONTINUE
      RETURN
      END
```

```
C---- THE DIP WHICH APPEARS ON THE DESORTION ISOTHERM HAS
C     BEEN SMOOTHED OUT BY THE APPROPRIATE EQUATION. THE
C     VERIFICATION IS CARRIED OUT BY EXPRESSING THAT
C     EQUATION IN DIAGRAM.
      DIMENSION X(50),Y(50)
      WRITE(3,60)
   60 FORMAT(/,10X,'X=',10X,'Y=')
      NOBS=30
      X(1)=0.148282324
      DO 10 I=1,NOBS
      Y(I)=(0.025*X(I)+0.1425)*735./14.7
   10 X(I+1)=X(I)+0.012103
      WRITE(3,100) X(I),Y(I)
  100 FORMAT(1X,2F15.5)
      CALL PLTR (X,Y,NOBS)
      STOP
      END
```

```
C---- THIS PROGRAM, TOGETHER WITH THE SUBROUTINES KP1
C     AND KP1S, IS USED TO CALCULATE THE PARAMETERS A,
C     B AND C IN K=A*P**2+B*P+C, HERE K IS THE THERMAL
C     CONDUCTIVITY AND P THE PRESSURE.
C***** OPTIMIZATION METHOD OF NELDER AND MEAD (SIMPLEX) *****
C---- NX = NO. OF INDEPENDENT VARIABLE
C---- STEP = INITIAL STEP SIZE
C---- X(I) = INITIAL GUESSES
      COMMON /ONE/ X(30),X1(30,30),NX,STEP,K1,SUM(30),IN
     1  ,Y(50)
      COMMON /TWO/ N,TIM(50),T(50)
      NX=3
      X(1)=0.0003
      X(2)=0.3
      X(3)=0.0004
      N=18
      WRITE(5,444)
  444 FORMAT (1X,'THE FOLLOWING DATA ARE FOR THE
     1 REGION P.GT.11.87.AND LT.59.7 PSIA')
      WRITE(5,777)
  777 FORMAT(/,1X,'CONDUCTIVITY,BTU/HR.FT.R',6X,'PRESSURE
     1 ,PSIA')
      DO 100 I=1,N
      READ(22,*) T(I),TIM(I)
      WRITE(5,888) TIM(I),T(I)
  888 FORMAT (1X,F15.8,15X,F12.8)
  100  CONTINUE
      STEP=0.0003
      IF (NX) 998,999,998
  998 CONTINUE
C---- ALFA = REFLECTION COEFFICIENT
C---- BETA = CONTRACTION COEFFICIENT
C---- GAMA = EXPENSION COEFFICIENT
      ALFA=1.0
      BETA=0.5
      GAMA=2.0
      DIFER=0.0
      XNX=NX
      IN=1
      IP=0
      CALL KP1S
C---- K1 = NUMBER OF VERTICES    K2 = INDEX OF CENTROID
C---- K3 = INDEX OF REFLECTION
C---- K4 = INDEX OF EXPENSION OR CONTRACTION
      K1=NX+1
      K2=NX+2
      K3=NX+3
      K4=NX+4
      CALL KP1
   25 DO 3 I=1,K1
      DO 4 J=1,NX
    4 X(J)=X1(I,J)
      WRITE(5,41) (X(JK),JK=1,NX)
```

```
   41   FORMAT (1X,3H P=,3F12.5)
        IN=I
        CALL KP1S
    3   CONTINUE
C------ SELECT LARGEST VALUE OF SUM(I) IN SIMPLEX
   28   SUMH=SUM(1)
        INDEX=1
        DO 7 I=2,K1
        IF (SUM(I).LE.SUMH) GO TO 7
        SUMH=SUM(I)
        INDEX=I
    7   CONTINUE
C------ SELECT MINIMUM VALUE OF SUM(I) IN SIMPLEX
        SUML=SUM(1)
        KOUNT=1
        DO 8 I=2,K1
        IF (SUML.LE.SUM(I)) GO TO 8
        SUML=SUM(I)
        IF (IP.EQ.0) GO TO 771
        WRITE(5,101) SUML,(X1(KOUNT,J),J=1,NX),DIFER
  771   CONTINUE
        KOUNT=I
    8   CONTINUE
C------ FIND CENTROID OF POINTS WITH I DIFFERENT THAN INDEX
        DO 9 J=1,NX
        SUM2=0.0
        DO 10 I=1,K1
   10   SUM2=SUM2+X1(I,J)
        X1(K2,J)=1.0/XNX*(SUM2-X1(INDEX,J))
C------ FIND REFLECTION OF HIGH POINT THROUGH CENTROID
        X1(K3,J)=(1.0+ALFA)*X1(K2,J)-ALFA*X1(INDEX,J)
    9   X(J)=X1(K3,J)
        IN=K3
        CALL KP1S
        IF (SUM(K3).LT.SUML) GO TO 11
C------ SELECT SECOND LARGEST VALUE IN SIMPLEX
        IF (INDEX.EQ.1) GO TO 38
        SUMS=SUM(1)
        GO TO 39
   38   SUMS=SUM(2)
   39   DO 12 I=1,K1
        IF ((INDEX-I).EQ.0) GO TO 12
        IF (SUM(I).LE.SUMS) GO TO 12
        SUMS=SUM(I)
   12   CONTINUE
        IF (SUM(K3).GT.SUMS) GO TO 13
        GO TO 14
C------ FORM EXPENSION OF NEW MINIMUM IF REFLECTION HAS
C       PRODUCED ONE MIN.
   11   DO 15 J=1,NX
        X1(K4,J)=(1.0-GAMA)*X1(K2,J)+GAMA*X1(K3,J)
   15   X(J)=X1(K4,J)
```

```
      IN=K4
      CALL KP1S
      IF (SUM(K4).LT.SUML) GO TO 16
      GO TO 14
C---- FORM CONTRACTION
   13 IF (SUM(K3).GT.SUMH) GO TO 17
      DO 18 J=1,NX
   18 X1(INDEX,J)=X1(K3,J)
   17 DO 19 J=1,NX
      X1(K4,J)=BETA*X1(INDEX,J)+(1.0-BETA)*X1(K2,J)
   19 X(J)=X1(K4,J)
      IN=K4
      CALL KP1S
      IF (SUMH.GT.SUM(K4)) GO TO 16
C---- REDUCE SIMPLEX BY HALF IF REFLECTION HAPPENS
C     TO PRODUCE
C     A LARGER VALUE THAN THE MAX.
      DO 20 J=1,NX
      DO 20 I=1,K1
   20 X1(I,J)=0.5*(X1(I,J)+X1(KOUNT,J))
      DO 29 I=1,K1
      DO 30 J=1,NX
   30 X(J)=X1(I,J)
      IN=I
      CALL KP1S
   29 CONTINUE
      GO TO 26
   16 DO 21 J=1,NX
      X1(INDEX,J)=X1(K4,J)
   21 X(J)=X1(INDEX,J)
      IN=INDEX
      CALL KP1S
      GO TO 26
   14 DO 22 J=1,NX
      X1(INDEX,J)=X1(K3,J)
   22 X(J)=X1(INDEX,J)
      IN=INDEX
      CALL KP1S
   26 DO 23 J=1,NX
   23 X(J)=X1(K2,J)
      IN=K2
      CALL KP1S
      DIFER=0.0
      DO 24 I=1,K1
   24 DIFER=DIFER+(SUM(I)-SUM(K2))**2
      DIFER=1.0/XNX*SQRT(DIFER)
      IF (DIFER.GE.0.0000001) GO TO 28
  999 CONTINUE
      WRITE(5,101) SUML,(X1(KOUNT,J),J=1,NX),DIFER
  101 FORMAT (1X,6H SUML=,E16.6,/1X,6H X(I)=,3E16.8,/1X,
     1 7H DIFER=,E15.6)
      WRITE(5,333) X(1),X(2),X(3)
```

```
333   FORMAT(/,3E20.8)
      STOP
      END
```

```
      SUBROUTINE KP1
      DIMENSION A(30,30)
      COMMON /ONE/ X(30),X1(30,30),NX,STEP,K1,SUM(30),IN,Y(50)
      COMMON /TWO/ N,TIM(50)
      VN=NX
      STEP1=STEP/(VN*SQRT(2.))*(SQRT(VN+1.)+VN-1.0)
      STEP2=STEP/(VN*SQRT(2.))*(SQRT(VN+1.)-1.)
      I=1
      DO 1 J=1,NX
    1 A(I,J)=0.0
      DO 3 I=2,K1
      DO 2 J=1,NX
      A(I,J)=STEP2
      L=I-1
      A(I,L)=STEP1
    2 CONTINUE
    3 CONTINUE
      DO 5 I=1,K1
      DO 4 J=1,NX
    4 X1(I,J)=X(J)+A(I,J)
    5 CONTINUE
      RETURN
      END
C=======================
      SUBROUTINE KP1S
      DIMENSION R(15)
      COMMON /ONE/ X(30),X1(30,30),NX,STEP,K1,SUM(30),IN,Y(50)
      COMMON /TWO/ N,TIM(50),T(50)
      SUM(IN)=0.
      DO 200 J=1,N
      R(J)=X(1)*T(J)**2+X(2)*T(J)+X(3)
  200 SUM(IN)=SUM(IN)+(TIM(J)-R(J))**2
      RETURN
      END
```

```
C---- THIS PROGRAM IS TO DETERMINE HOW GOOD THE
C     CALCULATED THERMAL DIFFUSIVITY FIT TO THE
C     THEORETICAL EQUATION.
      DIMENSION Y(100),YY(100),R1(100),R2(100),R3(100),
     1 R4(100),R5(100),T(100),T1(100),TC(100)
      N=56
      READ(20,*)(T(I),T1(I),TC(I),I=1,N)
      WRITE(3,300)(T(I),T1(I),TC(I),I=1,N)
300   FORMAT(1X,3F15.3)
      SUM=0.
      A=0.126311
      DELT=0.2
      TIME=-0.2
      DO 10 I=1,N
      TIME=TIME+DELT
      R1(I)=1.617*EXP(-3.85376*A*TIME)
      R2(I)=1.06468*EXP(-20.3058*A*TIME)
      R3(I)=0.85126*EXP(-49.90292*A*TIME)
      R4(I)=0.7294*EXP(-92.6541*A*TIME)
      R5(I)=0.64836*EXP(-148.55953*A*TIME)
      YY(I)=1.-(R1(I)-R2(I)+R3(I)-R4(I)+R5(I))
      Y(I)=(T(I)-T1(I))/(TC(I)-T1(I))
      SUM=SUM+(Y(I)-YY(I))**2+B**2
      WRITE(3,240)I,Y(I),YY(I),SUM
240   FORMAT(2X,I2,5X,2(F12.5,6X),E20.7)
 10   CONTINUE
      COST=SUM
      WRITE(3,400) COST
400   FORMAT(15X, E20.7)
      RETURN
      END
```

```
C.      THIS PROGRAM IS USED TO PLOT DATA GENERATED FROM
C.      SIMULATIONS ——— NEW EDITION OF AGII BY JS#3
        DIMENSION XDATA(5001),YDATA(5001)
        LOGICAL IFILE(10),XNAME(10),YNAME(10),POOP(40)
        COMPLEX JFILE
        REAL SY(6),DAY(2), NFILE(2), X1NAME(2), Y1NAME(2)
C       REAL*8 DAT(14)
        REAL DAT(14)
        COMMON/OUTP/IFILE,XNAME,YNAME,POOP
C.
        WRITE(5,120)
 120    FORMAT( 3X,'NAME OF DATA FILE USED: ',$)
        READ(5,130)JFILE
                NFILE(1)=REAL(JFILE)
                NFILE(2)=AIMAG(JFILE)
                CALL DATE(DAY)
                CALL TIME(TIM,SECD)
                SY(1)=NFILE(1)
                SY(2)=NFILE(2)
                SY(3)=DAY(1)
                SY(4)=DAY(2)
                SY(5)=TIM
                SY(6)=SECD
        WRITE(5,1310)SY
 1310   FORMAT(3X,6A5)
        WRITE(5,1305)
 1305   FORMAT( 3X,'TYPE IN YOUR TITLE FOR THESE FIGURES:
     1  '//10X,$)
                CALL TINSTR(40,POOP)
        WRITE(5,125)
 125    FORMAT( 3X,'DATA FILE IS FORMATFREE(0)/FREEFORMAT(1)
     1  ? ',$)
        READ(5,*)IOPT
 130    FORMAT( 2A5)
        WRITE(5,100)
 100    FORMAT( 3X,'INPUT NUMBER OF PLOTS TO BE MADE ON
     1  THIS FIGURE:',$)
        READ(5,*)NPLT
        WRITE(5,200)
  200   FORMAT( 3X, 'FIGURE: PLAIN(0) OR CROSS-HATCH(NON-0)—
     1  ',$)
        READ(5,*)IFIG
C.
        WRITE(5,110)
 110    FORMAT( 3X,'INPUT NUMBER OF DATA POINTS:',$)
        READ(5,*)NPTS
C       WRITE(5,115)
C 115   FORMAT( 3X,'DATA POINT SKIP ?: ',$)
C       READ(5,*)ISKIP
C       JSKIP=0
C.
C.
```

```
      XDATA(1)=NPTS
      YDATA(1)=NPTS
C.
      NPTS=NPTS+1
C.
      WRITE(5,150)
 150  FORMAT( 3X,'TOTAL NUMBER OF VARIABLES: ',$)
      READ(5,*)NVARS
C.
      OPEN(UNIT=1,ACCESS='SEQIN',FILE=jFILE)
C.
 4392 CONTINUE
      WRITE(5,9001)
 9001 FORMAT( 3X, 'LABEL FOR X-AXIS: ',$)
           CALL TINSTR(10,XNAME)
      WRITE(5,9002)
 9002 FORMAT( 3X, 'LABEL FOR Y-AXIS: ',$)
           CALL TINSTR(10,YNAME)
      DO 10 K=1,NPLT
C.
C.
      WRITE(5,160)
 160  FORMAT( 3X,'NAME VARIABLES TO BE PLOTTED: X VS Y -->
     1  ',$)
      READ(5,*,END=4393)KX,KY
      REWIND 1
C.
      DO 20 I=2,NPTS
C.
  30  CONTINUE
C     JSKIP=JSKIP+1
      IF(IOPT.EQ.0)READ(1)(DAT(J),J=1,NVARS)
      IF(IOPT.NE.0)READ(1,*)(DAT(J),J=1,NVARS)
C     IF(JSKIP.LT.ISKIP)GOTO 30
C     JSKIP=0
      XDATA(I)=DAT(KX)
      YDATA(I)=DAT(KY)
  20  CONTINUE
C.
      IPLT=K
C.
      CALL GRAPH(IPLT,XDATA,YDATA,IFIG)
C.
  10  CONTINUE
C.
C.
      GOTO 4392
 4393 STOP
      END
      SUBROUTINE GRAPH(I,XDATA,YDATA,IFIG)
C.
C.    ROUTINE ORIGINALLY SUPPLIED BY RFP....
```

```
C.
      DIMENSION XDATA(1),YDATA(1)
      LOGICAL IFILE(10),XNAME(10),YNAME(10),POOP(40)
      COMMON/OUTP/IFILE,XNAME,YNAME,POOP
      DATA HT/.15/
C.
      IF(I.GT.1)GOTO 10
C.
      CALL INITT(120)
      CALL BINITT
      CALL BELL
      CALL TINPUT(JHES)
C.
 10   CONTINUE
      IF(I.GT.1)GOTO 20
C.
      CALL SLIMX(250,950)
      CALL SLIMY(125,625)
            IF(IFIG.NE.0)GOTO 40
            CALL XFRM(2)
            CALL YFRM(2)
 40         CONTINUE
      CALL CHECK(XDATA,YDATA)
      CALL DSPLAY(XDATA,YDATA)
            CALL FRAME
            CALL MOVABS(900,20)
C.....      CALL SYMBOL(900,20,HT,XNAME,0.0,9)
            CALL HLABEL(10,XNAME)
            CALL MOVABS(20,700)
C.....      CALL SYMBOL(20,700,HT,YNAME,90.0,9)
            CALL VLABEL(10,YNAME)
            CALL NOTATE(10,10,40,POOP)
C.....      CALL SYMBOL(HT,HT,HT,SY,0,0,27)
      GOTO 30
C.
 20   CONTINUE
      CALL CPLOT(XDATA,YDATA)
 30   CONTINUE
C.
      CALL BELL
      CALL TINPUT(JHES)
C.
      RETURN
      END
```

```
C---- THIS PROGRAM, TOGETHER WITH THE SUBROUNTINES KP2
C     AND KP2S, IS USED TO ESTIMATE THE LINEAR PARAMETERS
C     A AND B IN K=A*P+B, HERE K IS THE THERMAL CONDUCTIVITY
C     AND P THE PRESSURE.
C***** OPTIMIZATION METHOD OF NELDER AND MEAD (SIMPLEX) *****
C---- NX = NO. OF INDEPENDENT VARIABLE
C---- STEP = INITIAL STEP SIZE
C---- X(I) = INITIAL GUESSES
      COMMON /ONE/ X(30),X1(30,30),NX,STEP,K1,SUM(30),IN
     1  ,Y(50)
      COMMON /TWO/ N,TIM(50),T(50)
      NX=2
      X(1)=-357.647
      X(2)=0.879294
      N=7
      WRITE(5,444)
  444 FORMAT (1X,'THE FOLLOWING DATA ARE FOR THE
     1  AT 500 PSIG')
      WRITE(5,777)
  777 FORMAT(/,1X,'CONDUCTIVITY,BTU/HR.FT.R',6X,'PRESSURE
     1  ,PSIA')
      DO 100 I=1,N
      READ(23,*) TIM(I),T(I)
      WRITE(5,888) TIM(I),T(I)
  888 FORMAT (1X,F15.8,15X,F12.8)
  100  CONTINUE
      STEP=0.03
      IF (NX) 998,999,998
  998 CONTINUE
C---- ALFA = REFLECTION COEFFICIENT
C---- BETA = CONTRACTION COEFFICIENT
C---- GAMA = EXPENSION COEFFICIENT
      ALFA=1.0
      BETA=0.5
      GAMA=2.0
      DIFER=0.0
      XNX=NX
      IN=1
      IP=0
      CALL KP2S
C---- K1 = NUMBER OF VERTICES    K2 = INDEX OF CENTROID
C---- K3 = INDEX OF REFLECTION
C---- K4 = INDEX OF EXPENSION OR CONTRACTION
      K1=NX+1
      K2=NX+2
      K3=NX+3
      K4=NX+4
      CALL KP2
   25 DO 3 I=1,K1
      DO 4 J=1,NX
    4 X(J)=X1(I,J)
      WRITE(5,41) (X(JK),JK=1,NX)
   41 FORMAT (1X,3H P=,2F12.5)
```

```
      IN=I
      CALL KP2S
    3 CONTINUE
C---- SELECT LARGEST VALUE OF SUM(I) IN SIMPLEX
   28 SUMH=SUM(1)
      INDEX=1
      DO 7 I=2,K1
      IF (SUM(I).LE.SUMH) GO TO 7
      SUMH=SUM(I)
      INDEX=I
    7 CONTINUE
C---- SELECT MINIMUM VALUE OF SUM(I) IN SIMPLEX
      SUML=SUM(1)
      KOUNT=1
      DO 8 I=2,K1
      IF (SUML.LE.SUM(I)) GO TO 8
      SUML=SUM(I)
      IF (IP.EQ.0) GO TO 771
      WRITE(5,101) SUML,(X1(KOUNT,J),J=1,NX),DIFER
  771 CONTINUE
      KOUNT=I
    8 CONTINUE
C---- FIND CENTROID OF POINTS WITH I DIFFERENT THAN INDEX
      DO 9 J=1,NX
      SUM2=0.0
      DO 10 I=1,K1
   10 SUM2=SUM2+X1(I,J)
      X1(K2,J)=1.0/XNX*(SUM2-X1(INDEX,J))
C---- FIND REFLECTION OF HIGH POINT THROUGH CENTROID
      X1(K3,J)=(1.0+ALFA)*X1(K2,J)-ALFA*X1(INDEX,J)
    9 X(J)=X1(K3,J)
      IN=K3
      CALL KP2S
      IF (SUM(K3).LT.SUML) GO TO 11
C---- SELECT SECOND LARGEST VALUE IN SIMPLEX
      IF (INDEX.EQ.1) GO TO 38
      SUMS=SUM(1)
      GO TO 39
   38 SUMS=SUM(2)
   39 DO 12 I=1,K1
      IF ((INDEX-I).EQ.0) GO TO 12
      IF (SUM(I).LE.SUMS) GO TO 12
      SUMS=SUM(I)
   12 CONTINUE
      IF (SUM(K3).GT.SUMS) GO TO 13
      GO TO 14
C---- FORM EXPENSION OF NEW MINIMUM IF REFLECTION HAS
C     PRODUCED ONE MIN.
   11 DO 15 J=1,NX
      X1(K4,J)=(1.0-GAMA)*X1(K2,J)+GAMA*X1(K3,J)
   15 X(J)=X1(K4,J)
      IN=K4
      CALL KP2S
```

```
      IF (SUM(K4).LT.SUML) GO TO 16
      GO TO 14
C---- FORM CONTRACTION
   13 IF (SUM(K3).GT.SUMH) GO TO 17
      DO 18 J=1,NX
   18 X1(INDEX,J)=X1(K3,J)
   17 DO 19 J=1,NX
      X1(K4,J)=BETA*X1(INDEX,J)+(1.0-BETA)*X1(K2,J)
   19 X(J)=X1(K4,J)
      IN=K4
      CALL KP2S
      IF (SUMH.GT.SUM(K4)) GO TO 16
C---- REDUCE SIMPLEX BY HALF IF REFLECTION HAPPENS
C     TO PRODUCE A LARGER VALUE THAN THE MAX.
      DO 20 J=1,NX
      DO 20 I=1,K1
   20 X1(I,J)=0.5*(X1(I,J)+X1(KOUNT,J))
      DO 29 I=1,K1
      DO 30 J=1,NX
   30 X(J)=X1(I,J)
      IN=I
      CALL KP2S
   29 CONTINUE
      GO TO 26
   16 DO 21 J=1,NX
      X1(INDEX,J)=X1(K4,J)
   21 X(J)=X1(INDEX,J)
      IN=INDEX
      CALL KP2S
      GO TO 26
   14 DO 22 J=1,NX
      X1(INDEX,J)=X1(K3,J)
   22 X(J)=X1(INDEX,J)
      IN=INDEX
      CALL KP2S
   26 DO 23 J=1,NX
   23 X(J)=X1(K2,J)
      IN=K2
      CALL KP2S
      DIFER=0.0
      DO 24 I=1,K1
   24 DIFER=DIFER+(SUM(I)-SUM(K2))**2
      DIFER=1.0/XNX*SQRT(DIFER)
      IF (DIFER.GE.0.00000001) GO TO 28
  999 CONTINUE
      WRITE(5,101) SUML,(X1(KOUNT,J),J=1,NX),DIFER
  101 FORMAT (1X,6H SUML=,E16.6,/1X,6H X(I)=,2E16.6,/1X,
     1 7H DIFER=,E15.6)
      WRITE(5,333) X(1),X(2)
  333 FORMAT(/,2E20.8)
      STOP
      END
```

```
      SUBROUTINE KP2
      DIMENSION A(30,30)
      COMMON /ONE/ X(30),X1(30,30),NX,STEP,K1,SUM(30),IN,Y(50)
      COMMON /TWO/ N,TIM(50)
      VN=NX
      STEP1=STEP/(VN*SQRT(2.))*(SQRT(VN+1.)+VN-1.0)
      STEP2=STEP/(VN*SQRT(2.))*(SQRT(VN+1.)-1.)
      I=1
      DO 1 J=1,NX
    1 A(I,J)=0.0
      DO 3 I=2,K1
      DO 2 J=1,NX
      A(I,J)=STEP2
      L=I-1
      A(I,L)=STEP1
    2 CONTINUE
    3 CONTINUE
      DO 5 I=1,K1
      DO 4 J=1,NX
    4 X1(I,J)=X(J)+A(I,J)
    5 CONTINUE
      RETURN
      END
C=======================
      SUBROUTINE KP2S
      DIMENSION R(30)
      COMMON /ONE/ X(30),X1(30,30),NX,STEP,K1,SUM(30),IN,Y(50)
      COMMON /TWO/ N,TIM(50),T(50)
      SUM(IN)=0.
      DO 200 J=1,N
      R(J)=X(1)*T(J)+X(2)
  200 SUM(IN)=SUM(IN)+(TIM(J)-R(J))**2
      RETURN
      END
```

APPENDIX C

SAMPLES OF THE EXPERIMENTAL RESULTS

During the experiments of measuring the thermal conductivity, the temperature changes of the tested material with time have been recorded. Attached in the following pages two sample results are selected, as shown in Figures 42 and 44 in which the number are temperature in °C. The paper of the temperature recorder was moved with a speed of 1 cm./minute. Temperature changes with time are read and presented in those figures also.

Figures 43 and 45 show that the prediction created by Equation (33) with the known thermal diffusivity matches very well with the experimental data. As described in Chapter 3, the thermal diffusivity is obtained by the curve-fitting procedure.

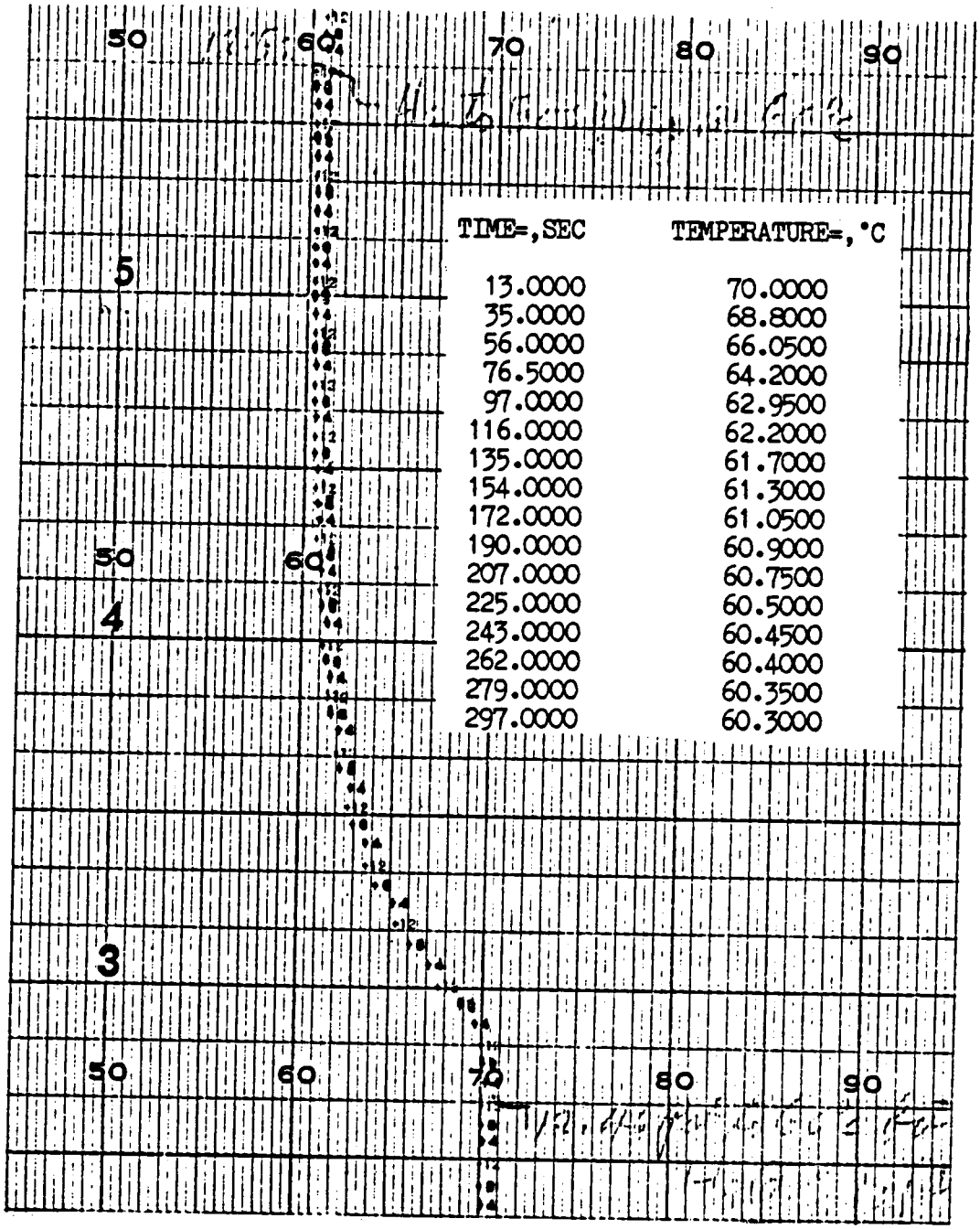

Figure 42. Experimental record on the temperature change of the deactivated FeTi hydride at pressure of 200 psig hydrogen, cooling from 70.05 to 60°C.

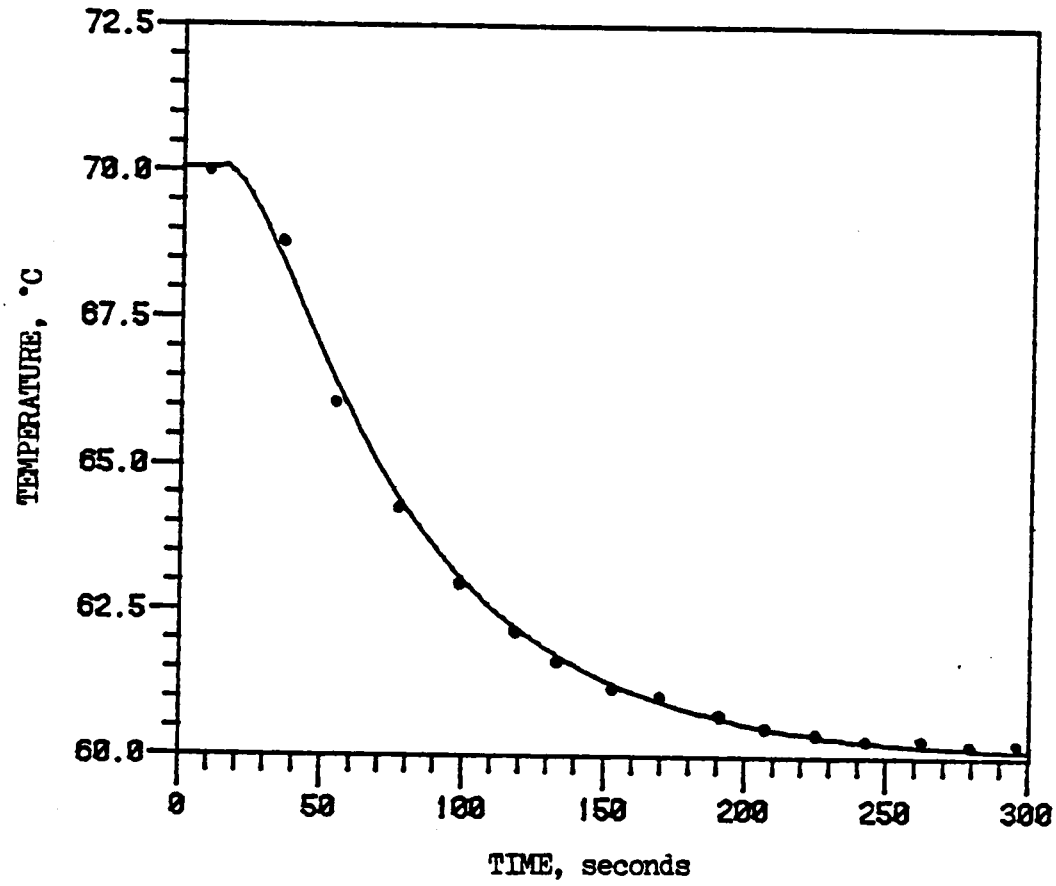

Figure 43. Temperature change of the deactivated FeTi hydride at pressure of 200 psig hydrogen, cooling from 70.05 to 60 °C. Points are the experimental data, and line is the prediction from the known thermal diffusivity.

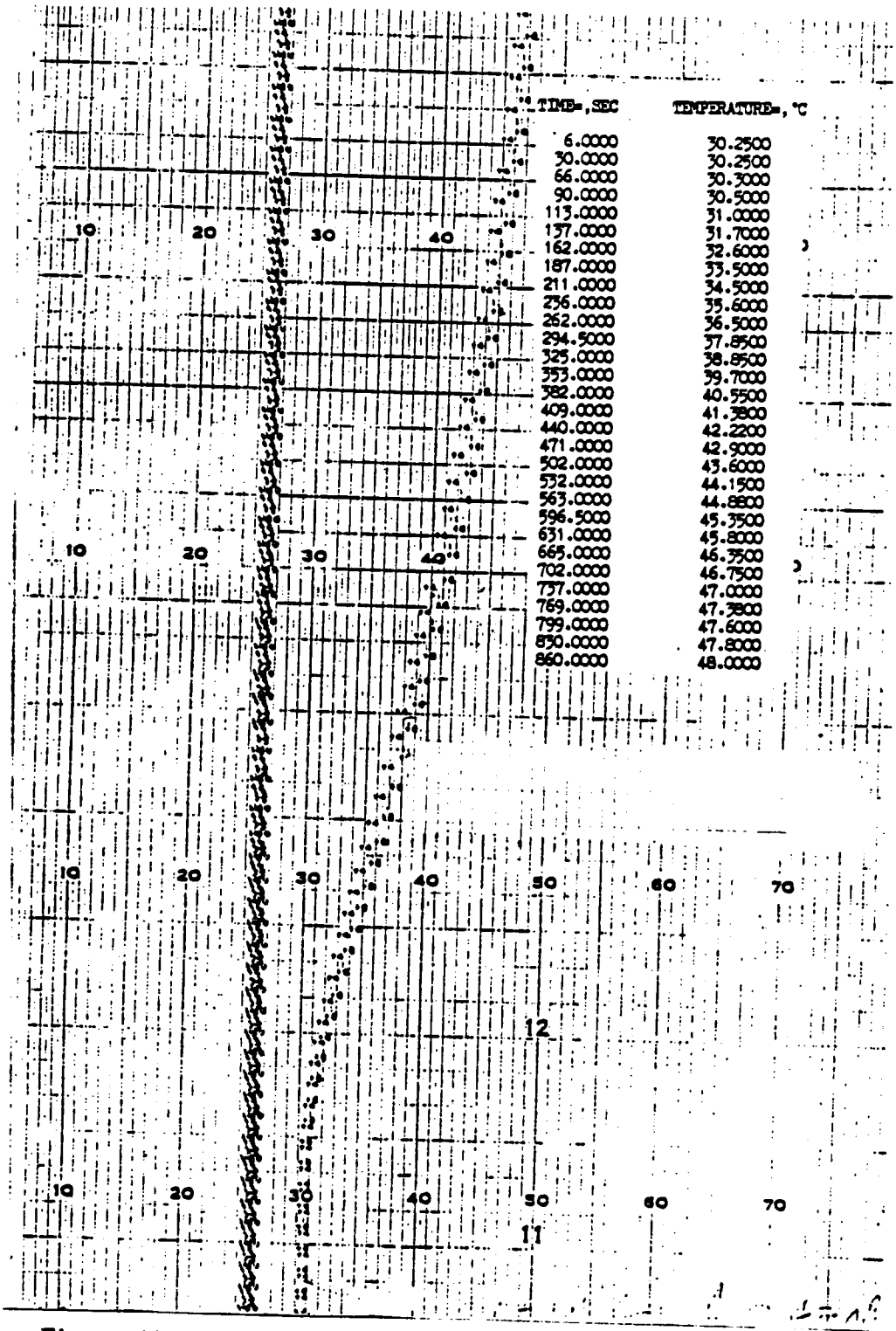

Figure 44. Experimental record on the temperature change of the deactivated FeTi hydride at pressure of 420 psig argon, heating from 30.25 to 50 °C.

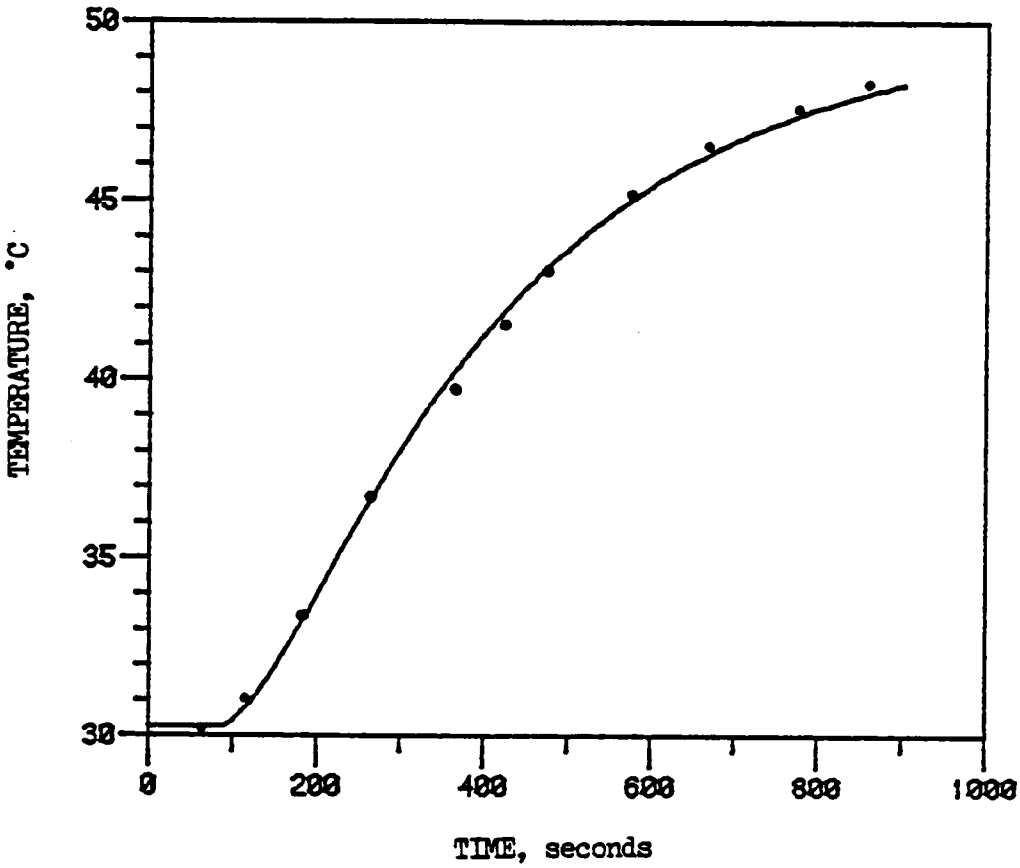

Figure 45. Temperature change of the deactivated FeTi hydride at pressure of 420 psig argon, heating from 30.25 to 50 °C. Points are the experimental data, and line is the prediction from the known thermal diffusivity.

LIST OF SYMBOLS

A_0	van't Hoff constant.
A, B	parameters in the relation between the thermal conductivity and temperature.
A_c	"effective" surface for conduction via aluminum.
A_h	surface of sphere.
a	radius of the test cylinder.
b	defined by Equation (31)
C, C'	hydrogen composition in hydride.
C_p	average specific heat of the hydride packing.
C_{pa}	specific heat of aluminum.
C_{ph}	specific heat of FeTi hydride
C_{pH_2}	specific heat of hydrogen gas.
D	aluminum temperature.
D_h	diffusion constant defined by Equation (7).
g	defined by Equation (13) through Equation (17).
ΔH, $\Delta H'$	heat of reaction.
h	heat transfer coefficient.
k, k'	reaction rate constants defined by Equation (5).
K_a	thermal conductivity of aluminum.
K_{ah}	thermal conductivity of Al-foam filled with FeTi hydride at pressure of hydrogen.
K_g	thermal conductivity of FeTi hydride plus gas.
K_{A_r}	thermal conductivity of FeTi hydride plus argon.
K_{H_e}	thermal conductivity of FeTi hydride plus helium.
K_{N_2}	thermal conductivity of FeTi hydride plus nitrogen.

K_h	thermal conductivity of FeTi hydrie plus hydrogen.
K_0	thermal conductivity of porous FeTi hydride particles.
K_{ss}	thermal conductivity of vessel wall.
L	length of the hydride bed.
m_i	initial hydrogen loading in hydride bed.
n	number of equations.
n_i	number of spherical cells in i-th cylindrical subvolume.
N	number of spheres in the differential cylindrical element, defined by Equation (49).
q	defined by Equation (48)
q_c	constant heat supply, defined by Equation (42).
q_i	conduction heat defined by Equation (88).
Q'	defined by Equation (49).
r	radial coordinate in sphere.
r_m	radius of sphere.
R	radial coordinate in cylinder.
R_1	outside radius of PMT.
R_p	inside radius of vessel.
R_{ss}	outside radius of vessel.
s	characteristic dimensions defined by Equation (7).
t	time.
$t_{½}$	defined in Chapter 3.
T	hydride temperature.
T_s	temperature of vessel wall.
T_p	inside wall temperature.
T_{ss}	outside wall temperature.

T_w average temperature of water.

V_a volume fraction of aluminum.

α hydride phase.

β hydride phase.

γ hydride phase.

ω fractional extent of hydriding reaction.

ρ bulk density of the hydride packing.

ρ_a aluminum density.

ρ_h hydride density.

δ defined by Equation (64).

ϕ defined by Equation (65).

ε void fraction of the hydride packing.

λ thermal diffusivity.

ψ exponential coefficient of Bessel function of order one.

θ defined as $\lambda t/a^2$.

ξ defined by Equation (51).

Ω constant defined by Equation (41).

γ defined by Equation (30).

ΔM moles of hydrogen reacted in Δt.

Δr radial interval in spherical system.

ΔR radial interval in cylindrical system.

Δt time increment.

VITA

Lin Te-Hua was born in China on February 22, 1942. He was graduated from Chungli High School in Taiwan in June 1959. The following September he entered Chung Cheng Institute of Technology (Taiwan), and in February 1964 he received a Bachelor of Science degree in Chemical Engineering.

After a four-year service in the army, he entered the Graduate School of National Cheng Kung University (Taiwan) through an entrance examination. In June 1970 he was awarded a Master of Science degree. Since then, he was employed as assistant professor at Army Academy (September 1970 - February 1972), section deputy chief at Chung Shan Institute of Science and Technology (March 1972 - November 1975) and department chairman at Tower Institute of Technology (December 1975 - August 1976) (all in Taiwan).

In September 1977 he was admitted to The University of Tennessee, Knoxville working for Ph.D degree. This degree was awarded in June 1981.